# The Role of Genetic Background in Bacterial Adaptation

by

**Stepan Ovchinnikov**

September, 2026

*A thesis submitted to the*
*Graduate School*
*of the*
*Institute of Science and Technology Austria*
*in partial fulfillment of the requirements*
*for the degree of*
*Doctor of Philosophy*

Committee in charge:

Johannes Fink, Chair

Calin Guet

Nicholas Barton

Gašper Tkačik

Meriem El Karoui



The thesis of Stepan Ovchinnikov, titled *The Role of Genetic Background in Bacterial Adaptation*, is approved by:

**Supervisor**: Calin Guet, ISTA, Klosterneuburg, Austria

Signature: _____

**Co-supervisor**: Nicholas Barton, ISTA, Klosterneuburg, Austria

Signature: _____

**Committee Member**: Gašper Tkačik, ISTA, Klosterneuburg, Austria

Signature: _____

**Committee Member**: Meriem El Karoui, ENS Paris-Saclay, Gif-sur-Yvette, France

Signature: _____

**Defense Chair:** Johannes Fink, ISTA, Klosterneuburg, Austria

Signature: _____

Signed page is on file

© by Stepan Ovchinnikov, September, 2026
CC BY-NC-SA 4.0 The copyright of this thesis rests with the author. Unless otherwise indicated, its contents are licensed under a Creative Commons Attribution-NonCommercial-ShareAlike 4.0 International License. Under this license, you may copy and redistribute the material in any medium or format. You may also create and distribute modified versions of the work. This is on the condition that you credit the author, do not use it for commercial purposes and share any derivative works under the same license.

ISTA Thesis, ISSN: 2663-337X

I hereby declare that this thesis is my own work and that it does not contain other people's work without this being so stated; this thesis does not contain my previous work without this being stated, and the bibliography contains all the literature that I used in writing the dissertation.

I accept full responsibility for the content and factual accuracy of this work, including the data and their analysis and presentation, and the text and citation of other work.

I declare that this is a true copy of my thesis, including any final revisions, as approved by my thesis committee, and that this thesis has not been submitted for a higher degree to any other university or institution.

I certify that any republication of materials presented in this thesis has been approved by the relevant publishers and co-authors.

Signature: _____

Stepan Ovchinnikov

September, 2026

Signed page is on file

## Abstract

Bacterial adaptation depends not only on the selective environment but also on the genetic background that determines which variants can arise and how they affect fitness. This thesis investigates how genetic background affects bacterial adaptive capacity by experimentally examining the effect of insertion sequence (IS) activity and establishing a strain system for future experiments to reveal the role of natural competence.

The main experimental study compared *Escherichia coli* MG1655 with a derivative lacking all 45 chromosomal IS elements, together with additional strains designed to separate the effects of IS removal from restoration of the IS-disrupted gene *wbbL*. Replicate populations were adapted to increasing concentrations of a five-antibiotic mixture and to each antibiotic individually, and their adaptive responses and evolutionary routes were compared. Under mixture selection, IS-containing and IS-free populations reached similar endpoint resistance and acquired similar numbers of mutations, although their mutation spectra differed significantly. IS-driven mutations were rare, indicating that IS activity contributed little to adaptation under this condition. Adaptation to individual antibiotics produced larger treatment-specific resistance gains and more recurrent mutations in the same loci across independently evolved populations than adaptation to the antibiotic mixture. The contribution of IS-driven mutations varied among antibiotics and was highest under tetracycline selection. Under tetracycline treatment, IS-containing populations adapted faster and reached higher selection concentrations than IS-free populations. Inactivation of *wbbL* partially restored the adaptive capacity of the IS-free strain but did not fully eliminate the difference, while IS-containing populations repeatedly accessed IS-mediated mutations unavailable to the IS-free strains.

Earlier experiments examining adaptation to ethanol, sodium chloride, and butanol did not provide reliable evidence for differences between the IS backgrounds. Growth observed at high sodium chloride and butanol concentrations during selection was not retained after stress-free recovery, whereas turbidostat-based ethanol experiments revealed technical limitations of using the device for parallel long-term evolution. These results motivated the more robust antibiotic-selection design. Finally, an experimental framework was developed to test whether natural competence contributes to the adaptive capacity of *Bacillus subtilis*. As a first step toward the proposed experiments, a genotypically verified Δ*comEC* strain and characterized fluorescent strains were constructed, but the evolution experiments remain to be initiated.

Together, these results show that IS elements can expand the repertoire of accessible mutations without conferring a universal adaptive advantage. Whether IS activity improves adaptation depends on the selective environment, the wider genetic background, and whether IS-mediated mutations provide particularly beneficial adaptive routes.

## Acknowledgements

First, I would like to thank my supervisors, Calin Guet and Nick Barton. Nick taught me to build a clear narrative, connecting existing knowledge to the research question, aims, and results. His courses in evolutionary biology helped me see the larger picture. I appreciated Calin's practical approach: starting with what the data show and working towards their broader implications. These approaches complemented each other, and I learned from both. I also thank Calin for providing the environment and freedom to carry out independent research from start to finish.

I am grateful to my committee members, Gašper Tkačik and Meriem El Karoui, for their time, interest, and valuable feedback. I also thank Johannes Fink for chairing my defense.

I thank my collaborators, Roderich Roemhild and Catalin Rusnac. Roderich and I designed the project presented in Chapter Two, which became a central part of this thesis. I thank him for his advice on microbiological experiments, our discussions about what the results meant, and the insertion sequence-free strains that made this research possible. I thank Catalin for sharing his wonderful turbidostat and teaching me how to use it. I had a lot of fun with the hands-on work and tinkering it involved.

I thank the members of Calin's and Nick's groups for discussions, feedback, and the time we spent together. I am also grateful to the staff of the Life Sciences Facility and the Media Kitchen for their work and assistance.

Finally, I thank my parents for their support and encouragement, and Ksenia and little Varvara for their love and support throughout these years.

## About the Author

Stepan Ovchinnikov completed a BSc in Biochemistry at Lomonosov Moscow State University and an MSc in Life Sciences at the Skolkovo Institute of Science and Technology before joining ISTA in September 2020. He is broadly interested in prokaryotic evolution, both on the population level and over long evolutionary timescales. During his master's studies, he published a first-author paper in *Nucleic Acids Research* on acetyltransferase toxin-antitoxin systems. He subsequently worked as a research assistant in Tim Clausen's laboratory, contributing to the development of bacPROTACs. During his PhD, he studied how mechanisms that generate and recombine genetic variation, specifically activity of insertion sequences and natural transformation, affect the ability of bacteria to adapt.

## List of Collaborators

Chapter 2 is based on work designed and discussed in collaboration with Roderich Roemhild.

Chapter 3 is based on work with Catalin Rusnac, who provided the turbidostat device and helped establish its operation.

Chapters 2 and 3 use bacterial strains constructed by Roderich Roemhild.

All chapters are based on work under the supervision of Calin Guet and Nicholas Barton.

# Table of Contents

**Abstract** ..... i

**Acknowledgements** ..... ii

**About the Author** ..... iii

**List of Collaborators** ..... iv

**Table of Contents** ..... v

**List of Figures** ..... vii

**List of Tables** ..... viii

**List of Abbreviations** ..... viii

**1 Introduction** ..... 1

1.1 Mechanisms influencing bacterial evolutionary potential ..... 1
1.2 The lack of direct comparison across similar genetic backgrounds ..... 2
1.3 Experimental evolution ..... 2
1.4 Scope and aim of the thesis ..... 3

***2* Context-dependent contributions of insertion sequences to antibiotic adaptation in *Escherichia coli*** ..... 4

2.1 Introduction ..... 4
2.2 Results ..... 5
*2.2.1 IS removal did not reduce adaptation to a five-antibiotic mixture* ..... 5
*2.2.2 WT and ΔIS evolved distinct mutation spectra under MIX selection despite minimal involvement of IS elements* ..... 9
*2.2.3 WT populations generally reached higher relative resistance under single-antibiotic selection than under MIX selection* ..... 11
*2.2.4 The contribution of IS-driven mutations varied among antibiotics* ..... 13
*2.2.5 Single-antibiotic selection produced more parallel and treatment-specific genetic adaptation* ..... 14
*2.2.6 Inactivation of wbbL shifts the ΔIS mutation spectrum toward that of WT* ..... 16
*2.2.7 IS background and wbbL status both affected adaptive capacity under TET selection* ..... 18
2.3 Discussion ..... 21
*2.3.1 IS removal did not reduce adaptation under MIX selection* ..... 21
*2.3.2 The contribution of IS elements in adaptation depended on the selection environment* ..... 22
*2.3.3 wbbL status partly explained mutation spectrum differences between WT and ΔIS under MIX selection* ..... 23
*2.3.4 TET selection demonstrated an adaptive advantage of WT over ΔIS not fully explained by wbbL status* ..... 23
*2.3.5 Limitations and implications* ..... 23
2.4 Materials and methods ..... 24
*2.4.1 Bacterial strains and genotypes* ..... 24
*2.4.2 Media, antibiotics, and growth conditions* ..... 24
*2.4.3 Composition and calibration of MIX* ..... 25
*2.4.4 Experimental evolution* ..... 26
*2.4.5 Experimental design and treatment groups* ..... 26
*2.4.6 Analysis of adaptation trajectories* ..... 27
*2.4.7 MIC measurements and dose-response assays* ..... 27
*2.4.8 DNA extraction and whole-genome sequencing* ..... 27
*2.4.9 Mutation identification and annotation* ..... 28
*2.4.10 Mutation-spectrum comparisons* ..... 28

**3 Adaptation of *Escherichia coli* to complex stress environments ..... 30**

3.1 INTRODUCTION ..... 30
3.2 RESULTS AND DISCUSSION ..... 31
*3.2.1 Continuous ethanol exposure in the turbidostat was limited by recurrent cross-contamination ..... 31*
*3.2.2 No detectable adaptation to butanol and NaCl ..... 36*
*3.2.3 Concluding remarks ..... 39*
3.3 MATERIALS AND METHODS ..... 39
*3.3.1 Bacterial strains ..... 39*
*3.3.2 Media and growth conditions ..... 40*
*3.3.3 Turbidostat device and evolution experiments ..... 40*
*3.3.4 Population DNA extraction, sequencing and variant calling ..... 40*
*3.3.5 Pin-replication evolution experiments ..... 41*

**4 Construction of strains to study the role of natural competence in adaptation ..... 42**

4.1 INTRODUCTION ..... 42
*4.1.1 Potential effect of natural transformation on adaptation ..... 43*
*4.1.2 Experimental evidence and open questions ..... 44*
4.2 EXPERIMENTAL FRAMEWORK ..... 45
*4.2.1 Model system and strain design ..... 46*
*4.2.2 Direct detection of recombination ..... 46*
*4.2.3 Fitness trajectories during adaptation ..... 47*
4.3 RESULTS AND DISCUSSION ..... 47
*4.3.1 Construction of the ΔcomEC strain ..... 47*
*4.3.2 Construction and testing of fluorescent strains ..... 47*
*4.3.3 Progress toward the proposed experimental system ..... 49*
4.4 MATERIALS AND METHODS ..... 50
*4.4.1 Bacterial strains, plasmids, and primers ..... 50*
*4.4.2 Growth and culture conditions ..... 51*
*4.4.3 Strain construction ..... 52*
*4.4.4 Transformation of Bacillus subtilis ..... 52*
*4.4.5 Fluorescence characterization ..... 53*

**References ..... 54**

**A. Appendix 1 - Supplementary Figures ..... 60**

**B. Appendix 2 - Declaration of the use of Generative AI and AI tools ..... 63**

## List of Figures

Figure 1. Schematic representation of the genomes of the WT and ΔIS strains used in the evolution experiments. ..... 6
Figure 2. Adaptation of WT and ΔIS *E. coli* populations to increasing MIX concentrations. ..... 8
Figure 3. Minimum inhibitory concentration of MIX in ancestral and MIX-adapted WT and ΔIS isolates. ..... 9
Figure 4. Distribution of mutated loci among WT MIX, ΔIS MIX, WT media, and ΔIS media isolates. ..... 10
Figure 5. Adaptation of WT *E. coli* populations under single-antibiotic and MIX selection. ..... 12
Figure 6. Treatment-specific minimum inhibitory concentrations and fold increases of ancestral and antibiotic-adapted WT *E. coli*. ..... 13
Figure 7. Recurrence of mutated loci across replicate WT isolates adapted to MIX and individual antibiotics. ..... 15
Figure 8. Mutation spectra of WT isolates adapted to MIX and individual antibiotics. ..... 16
Figure 9. Adaptation of WT, ΔIS, ΔIS *wbbL**, and *wbbL+ E. coli* populations under MIX selection. ..... 17
Figure 10. Mutation spectra of MIX-adapted WT, *wbbL+*, ΔIS, and ΔIS *wbbL** isolates under MIX selection. ..... 18
Figure 11. Adaptation of WT, ΔIS, and ΔIS *wbbL** populations under MEC, NIT, and TET selection. ..... 19
Figure 12. Mutation spectra of WT, ΔIS, and ΔIS *wbbL** isolates under TET and NIT selection. ..... 20
Figure 13. Diagram of the Replifactory turbidostat system. ..... 32
Figure 14. Representative OD profiles illustrating culture maintenance, responses to ethanol exposure, and signs of contamination during turbidostat experiments. ..... 35
Figure 15. Cross-contamination repeatedly appeared in turbidostat runs after approximately 6 days and was not affected by tube shaking. ..... 35
Figure 16. Pin-replication experiments with increasing NaCl and butanol concentrations. ..... 37
Figure 17. Validation of growth after selection in butanol and NaCl. ..... 38
Figure 18. Schematic representation of natural transformation in Gram-positive and Gram-negative bacteria. ..... 43
Figure 19. Bacitracin-inducible fluorescent markers produced strong signals in liquid medium but weak signals on solid medium. ..... 48
Figure 20. Fluorescent marker expression on agar plates. ..... 49

Supplementary Figure 1. Preliminary dose-response curves of ancestral WT and ΔIS strains to individual antibiotics and MIX. ..... 60
Supplementary Figure 2. Adaptation of original WT, repeated WT, and original ΔIS *E. coli* populations under MIX selection. ..... 60
Supplementary Figure 3. Dose-response curves of ancestral and evolved WT and ΔIS *E. coli*. ..... 61
Supplementary Figure 4 Ancestral dose-response curves for NaCl and n-butanol ..... 61
Supplementary Figure 5. Endpoint OD at the estimated ancestral MIC after direct or gradual exposure ..... 62

## List of Tables

Table 1. Composition of the five-antibiotic mixture (MIX) used in the evolution experiments 7
Table 2. Acquired mutations, locus diversity, and IS-driven mutations in MIX- and media-adapted isolates ..... 10
Table 3. Acquired mutations, locus diversity, and IS-driven mutations in single-antibiotic- and MIX-adapted WT isolates ..... 14
Table 4. Pairwise PERMANOVA comparisons of mutation spectra among MIX-adapted strains ..... 18
Table 5. Bacterial strains used in this study. ..... 25
Table 6. Summary of turbidostat runs used to establish ethanol-selection conditions ..... 34
Table 7. Variants called in two WT-yfp populations from turbidostat run 15 ..... 36
Table 8. *B. subtilis* strains used or generated in this study. ..... 50
Table 9. Plasmids used or generated in this study. ..... 51
Table 10. Primers used in this study. LFH-PCR KO, long-flanking homology PCR knock-out .. 51

## List of Abbreviations

**BFP** Blue fluorescent protein
**BH** Benjamini-Hochberg procedure for multiple comparisons
**Bsu, *B. subtilis*** *Bacillus subtilis*
**BuOH** Butanol
**CDS** Coding sequence
**CIP** Ciprofloxacin
**DNA** Deoxyribonucleic acid
**Eco, *E. coli*** *Escherichia coli*
**EtOH** Ethanol
**FP** Fluorescent protein
**GFP** Green fluorescent protein
**IS** Insertion sequence
**KO** Gene knockout
**LB** Lysogeny broth
**LFH-PCR** Long-flanking homology polymerase chain reaction
**M9** M9 minimal medium
**MEC** Mecillinam
**MHB** Mueller-Hinton broth
**MIC** Minimum inhibitory concentration
**MIX** Five-antibiotic mixture
**MNP** Multinucleotide polymorphism
**NEB** New England Biolabs
**NIT** Nitrofurantoin
**$OD_{600}$** Optical density measured at 600 nm
**ONT** Oxford Nanopore Technologies
**PBS** Phosphate-buffered saline
**PCR** Polymerase chain reaction
**PERMANOVA** Permutational multivariate analysis of variance

**RFP** Red fluorescent protein
**RNA** Ribonucleic acid
**rRNA** Ribosomal ribonucleic acid
**SD** Standard deviation
**SNP** Single-nucleotide polymorphism
**SYFP2** Super yellow fluorescent protein 2
**TET** Tetracycline
**TMP** Trimethoprim
**WT** Wild type
**YFP** Yellow fluorescent protein
**ΔIS** IS-free *Escherichia coli* strain

# 1 Introduction

Bacteria encounter environmental changes such as shifts in nutrient availability, temperature, salinity, or chemical exposure. Although individual cells can respond physiologically, populations may adapt over generations by heritable changes [1], [2]. Evolutionary adaptation increases fitness - the relative reproductive success of a genotype under specific conditions [3]. Because fitness depends on the environment and competing genotypes, a change that is beneficial in one context may not be beneficial in another.

Adaptation depends on genetic variation arising from mutations and from the movement or recombination of genetic material within and between genomes [4]. Natural selection can increase the frequency of beneficial variants, although their emergence and persistence are also influenced by chance and population dynamics.

## *1.1 Mechanisms influencing bacterial evolutionary potential*

The potential for adaptation is influenced by genetic background. The effect of a mutation may depend on variants already present in the genome, while particular genetic variants and genetic modules can change which mutations arise and how frequently they occur [5], [6], [7]. Also, the background genetic variants can change the effects of the arising mutations on fitness. Therefore, closely related bacterial strains may follow different evolutionary trajectories under the same selective conditions.

Several genetic mechanisms illustrate this principle. Defects in the DNA repair machinery can produce hypermutator lineages with elevated mutation rates [7]. These lineages may generate beneficial mutations more rapidly, but they also accumulate more deleterious mutations [8]. Hypermutators have been observed in commensal and clinical populations, as well as in experimental evolution studies, demonstrating how genetic background can alter the supply of mutations [7], [8], [9].

Insertion sequences are highly abundant mobile genetic elements that can move within bacterial genomes [10]. Their movement may disrupt genes, modify gene expression, or cause genomic rearrangements [6], [11]. Although insertion sequences are often considered detrimental selfish genetic elements, they have been shown to occasionally generate beneficial mutations [12], [13], [14]. Whether the abundance of insertion sequences is related to their contribution in bacterial adaptation remains under debate [15].

Bacteria can also generate new genetic combinations through recombination and horizontal gene transfer [16]. Unlike mutation, which changes a DNA sequence within a lineage, horizontal transfer allows genetic material to move between cells. Transferred DNA may introduce new genes or replace related regions of the recipient chromosome through homologous recombination [17]. Several mechanisms enable such transfer, including conjugation, transduction, natural competence, and gene transfer agents [16].

Gene transfer agents are genome-encoded bacteriophage-like particles produced by certain bacteria and archaea that package fragments of chromosomal DNA and transfer them

between cells [18]. The production of these particles is typically associated with the lysis of a fraction of the producing population. Gene transfer agents are restricted to particular groups of microorganisms [19], but they provide an interesting example of a specialized genetic module that can redistribute genetic variation within a population.

Natural competence is a more broadly distributed mechanism of DNA uptake in bacteria [20]. Competent bacteria can take up extracellular DNA from their surroundings. The acquired DNA may be degraded, used as a nutrient, or incorporated into the chromosome through homologous recombination [21]. Competence can therefore introduce new variants, replace damaged or deleterious alleles, and create new combinations of existing variants. However, DNA uptake and recombination may also be costly or introduce detrimental genetic material [22]. Similarly to insertion sequences, whether the broad distribution of natural competence is due to its contribution to bacterial adaptation, remains an open question [21], [22].

## *1.2 The lack of direct comparison across similar genetic backgrounds*

Much of the evidence linking these mechanisms to bacterial adaptation is retrospective. Clinical isolates, natural populations, and experimentally evolved lineages are typically examined after adaptation occurred [12], [23], [24], [25]. Mutations associated with successful lineages may then be identified and reconstructed to determine their fitness effects. Such studies demonstrate that mobile elements, elevated mutation rates, or other genetic mechanisms can generate mutations that contribute to adaptation.

However, these observations usually lack a direct comparison with an otherwise similar genetic background in which the mechanism of interest is absent. The discovery of a beneficial mutation produced by a particular mechanism therefore shows that the mechanism contributed to one evolutionary outcome, but not that it generally increases adaptive capacity. Comparisons among naturally occurring strains provide limited evidence because the strains commonly differ at many loci in addition to the mechanism being studied.

This limitation can be addressed by comparing closely related strains that differ primarily in the gene or genetic module of interest. Replicate populations can be evolved under the same controlled conditions, allowing their changes in fitness to be compared directly. Differences between the resulting populations can then be attributed more confidently to the studied genetic feature, while minimizing the influence of unrelated genomic variation.

## *1.3 Experimental evolution*

Experimental evolution offers a prospective approach to this problem. It involves maintaining populations under defined conditions for many generations and observing the resulting genetic and phenotypic changes [26]. Bacteria are particularly suitable for this approach. They reproduce rapidly, reach large population sizes, and can often be grown under relatively simple and reproducible laboratory conditions [27].

Bacterial populations can also be frozen and revived, allowing evolved populations to be compared directly with their ancestors. Their relatively small genomes facilitate genome sequencing, while established genetic tools allow candidate mutations to be reconstructed and tested. Most importantly for this thesis, genetic engineering enables the construction of closely related backgrounds that differ in a selected gene or genetic module.

## *1.4 Scope and aim of the thesis*

This thesis uses experimental evolution and engineered bacterial strains to investigate how specific genetic mechanisms influence bacterial adaptive capacity. The projects share a common approach: closely related bacterial backgrounds that differ in a defined genetic feature are compared under controlled conditions. This approach aims to determine whether the presence of a particular mechanism changes the extent or dynamics of adaptation and whether its effect depends on the selective environment.

The first part of the thesis focuses on insertion sequences in *Escherichia coli*. Initial experiments described in Chapter 3 evaluated continuous culture for comparing insertion-sequence-containing and insertion-sequence-deficient backgrounds. Subsequent experiments used serial transfer, with butanol or sodium chloride applied as selective treatments. These studies revealed technical challenges associated with continuous culture, including contamination, as well as difficulties in establishing stress conditions that produced clear and interpretable adaptive responses during serial transfer.

Chapter 2 describes subsequent experiments employing a more robust serial-transfer design and a simpler antibiotic selection regime. Under these conditions, adaptation could be detected and compared across the tested genetic backgrounds. The results indicated that the contribution of insertion sequences to adaptation was context-dependent rather than uniformly beneficial or detrimental.

Chapter 4 focuses on natural competence in *Bacillus subtilis* as another mechanism that may influence adaptive capacity. It describes the construction of bacterial strains designed to enable controlled comparisons between competence-proficient and competence-deficient backgrounds. This work establishes the experimental system required to test how DNA uptake and homologous recombination affect adaptation in future evolution experiments.

Together, these projects examine how mechanisms that generate or redistribute genetic variation shape bacterial evolution. Their central premise is that such mechanisms do not have universally positive or negative effects. Instead, their evolutionary consequences emerge from interactions among the genetic background, the selective environment, and the design of the experiment. By directly comparing closely related bacterial backgrounds, this thesis contributes to a more prospective and experimentally controlled understanding of how genetic architecture influences adaptation.

# *2* Context-dependent contributions of insertion sequences to antibiotic adaptation in *Escherichia coli*

## *2.1 Introduction*

Insertion sequence (IS) elements are small prokaryotic mobile genetic elements that primarily encode only genes necessary for their own transposition [10]. They are found in most prokaryotic genomes, with a median abundance of approximately 12 sequences per genome, although some genomes encode hundreds or even more than a thousand IS elements [28]. It remains unclear why IS elements are so widespread despite their potential to disrupt host genes and reduce fitness.

Two main hypotheses have been proposed to explain the great abundance of IS elements throughout prokaryotic genomes. The selfish DNA hypothesis suggests that IS elements persist due to their ability to reproduce within genomes and be transferred across genomes via plasmids and other means of horizontal gene transfer [29], despite the primarily deleterious effects attributed to IS-driven mutations [30]. The alternative hypothesis suggests that IS elements are maintained because they contribute to genome plasticity and adaptation [31]. According to this hypothesis, when beneficial IS-driven mutations go to fixation, the IS copies linked within the same genetic background may persist through genetic hitchhiking [32]. The relative importance of selfish replication and benefits conferred to the host may differ among IS families because they vary in transposition activity, insertion preferences, and capacity to generate beneficial genetic changes [33]. Overall, the factors responsible for the widespread abundance of IS elements remain under debate [15].

The adaptive potential that IS elements confer to their hosts arises from the distinctive mutations they generate. In addition to new IS insertions, IS activity together with other cellular mechanisms can produce gene deletions, duplications and amplifications, inversions, and larger genomic rearrangements [6], [11]. These mutations can cause simple gene inactivation, but they can also produce functional changes that may be difficult to access through point mutations alone. For example, IS-driven mutations can activate gene expression through outward-facing or hybrid promoters, alter transcription through readthrough or derepression, create new operon structures, and remove large non-essential genomic regions [6], [11]. Gene amplifications can additionally provide a rapid response to selection for increased gene expression and facilitate the subsequent evolution of new function or regulation [34], [35], [36]. IS elements may therefore expand both the supply and diversity of mutations available to an adapting population.

IS-driven mutations can occur at considerable rates. In mutation-accumulation experiments with *E. coli*, where selection was minimized through repeated single-cell bottlenecks, IS insertions accounted for approximately 25% of detected mutations [37]. IS-driven deletions occurred less frequently, whereas amplifications and other rearrangements were not detected under these conditions. Nevertheless, such rare mutations may make a substantial contribution under selection because even rare variants can spread when they confer an adaptive advantage [38], [39]. Consistent with this possibility, various types of beneficial IS-

driven mutations have been observed in experimental evolution under multiple conditions [12], including antibiotic selection [13] and adaptation to laboratory media [14].

However, the contribution of IS elements to adaptation appears to be strongly context dependent. It may vary with the genomic positions of selection targets and their proximity to IS elements or preferred insertion sites [34], [35], the dynamics of the selection regime [36], [40], stochasticity and historical contingency of adaptation [14], and the particular selection environment and selection pressure [13]. The contribution of IS elements to adaptation may therefore depend strongly on the genetic background and selective environment. Although extensive evidence shows that IS-driven mutations can be beneficial, such observations do not reveal whether a genome containing IS elements has greater adaptive capacity than it would have in their absence, because the corresponding IS-free comparison is usually missing.

Therefore, direct comparisons between closely related IS-containing and IS-free backgrounds are needed to determine whether IS elements confer an overall adaptive advantage. Such comparisons remain limited, particularly across different selective environments. The most relevant previous comparison was performed by Steinrueck and Guet [35], who studied adaptation to increasing tetracycline concentrations using a resistance reporter inserted at several chromosomal loci in IS-containing and IS-free *E. coli* backgrounds. They showed that IS elements could facilitate adaptation by promoting amplification of the selected locus and by inserting upstream of the resistance gene and increasing its expression. However, their study focused on the activation of a single engineered resistance gene under one selective condition. Moreover, the IS-free strain was derived from the reduced-genome strain MDS42, which lacks approximately 15% of the MG1655 genome in addition to all IS elements. Thus, the general effect of genomic IS elements on adaptation across native genetic targets and different selective environments remains unclear.

Here, we addressed this gap by comparing the adaptation of wild-type (WT) MG1655 and an IS-free derivative (ΔIS) of *E. coli* under a complex antibiotic treatment and its individual components. We hypothesized that the additional mutation types supplied by IS elements could allow WT populations to adapt more rapidly, reach a higher adaptive limit, or access a different set of adaptive targets. However, construction of the ΔIS strain also restored several loci disrupted by IS elements in WT MG1655, including *wbbL*, which is required for the biosynthesis of the O-antigen, a component of outer-membrane lipopolysaccharide [41]. Restoration of O-antigen production could affect antibiotic susceptibility and adaptation independently of IS content [42]. We therefore examined additional *wbbL* backgrounds to distinguish effects associated with IS content from those associated with *wbbL* functionality.

## *2.2 Results*

### 2.2.1 IS removal did not reduce adaptation to a five-antibiotic mixture

To determine whether genomic IS elements increase the adaptive capacity under complex stress, we conducted an evolution experiment in which wild-type (WT) MG1655 and IS-free (ΔIS) *E. coli* populations adapted to increasing concentrations of a five-antibiotic mixture

(MIX). We compared the highest selection concentration reached, the rate of increase in selection concentration, and the endpoint minimum inhibitory concentration (MIC) of evolved isolates.

The ΔIS strain was derived from WT MG1655 by deleting all 45 chromosomal IS elements. Because these deletions also restored several IS-disrupted open reading frames, including *wbbL,* the rhamnosyltransferase gene involved in O-antigen synthesis, the two strains differ both in IS content and in the functionality of these loci (Figure 1).

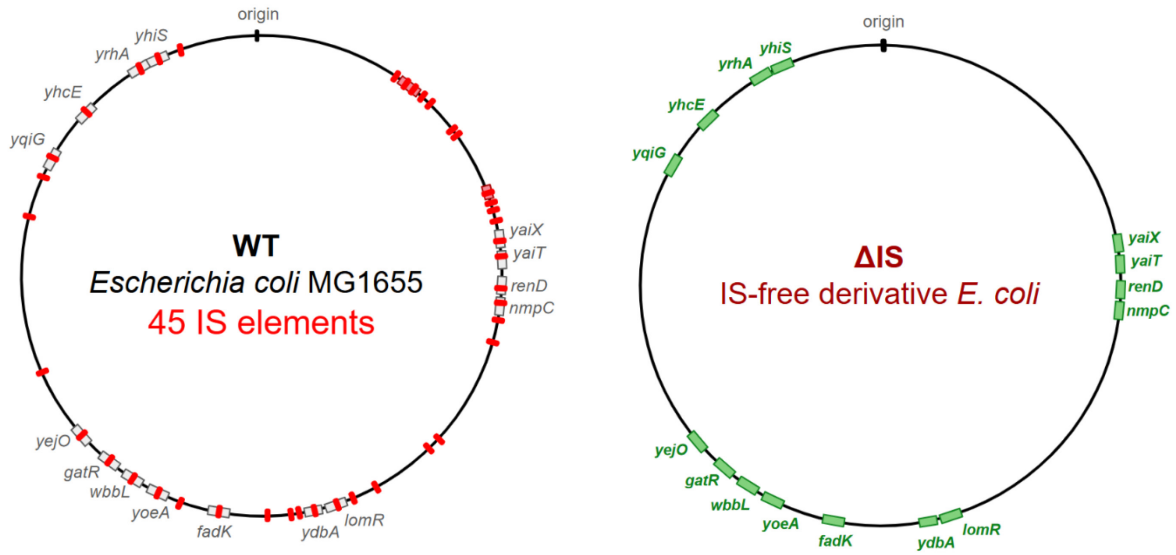



***Figure 1. Schematic representation of the genomes of the WT and ΔIS strains used in the evolution experiments.*** *The WT strain (Escherichia coli MG1655) contains 45 insertion sequence (IS) elements, indicated by red markers. The ΔIS strain was derived from WT by seamless deletion of all 45 IS elements. These deletions also restored 15 IS-disrupted protein-coding sequences (shown as gray boxes in WT and green boxes in ΔIS). Two IS elements contained insertions of one or two additional IS elements, respectively (indicated by red boxes). These nested IS elements were also removed during strain construction. The positions of genetic elements reflect their approximate genomic locations but were adjusted where necessary for visual clarity.*

To impose selection on multiple cellular processes simultaneously, we used a five-antibiotic mixture (MIX) comprising ciprofloxacin (CIP), mecillinam (MEC), nitrofurantoin (NIT), tetracycline (TET), and trimethoprim (TMP; Table 1). The antibiotics were combined in fixed relative proportions based on their individual IC90 estimates in the ancestral WT and ΔIS strains (Supplementary Figure 1A-E; Materials and Methods). Because MIX components were present at different concentrations, MIX concentration is expressed in arbitrary units (U), as defined in Table 1.

Six replicate populations of each strain (WT and ΔIS) were serially transferred every 24 h for 19 days under increasing concentrations of MIX. Selection pressure was adjusted according to culture growth: whenever a population reached a high optical density ($OD_{600} \geq 1$), the MIX concentration was multiplied by $\sqrt{2}$ (Figure 2A). This selection regime was designed to increase selection pressure as the populations adapted, minimize population loss, and promote the accumulation of multiple mutations. The initial MIX concentrations for WT and ΔIS were chosen to produce comparable effects on cell viability on day 1. The initial MIX

concentrations were 0.35 U for WT and 0.18 U for ΔIS, selected on the basis of preliminary CFU dose-response assays.

| Antibiotic | Targeted process (molecular target) | Bacteriostatic/ bactericidal | Concentration, µg/mL (in 1U MIX) |
|---|---|---|---|
| **Ciprofloxacin (CIP)** | Replication (gyrase and topoisomerase IV) | Bactericidal | 0.03 |
| **Mecillinam (MEC)** | Peptidoglycan synthesis (penicillin binding proteins) | Bactericidal | 0.30 |
| **Nitrofurantoin (NIT)** | Broad DNA and other biomolecule damage | Bactericidal | 4.00 |
| **Tetracycline (TET)** | Translation (30S ribosomal subunit) | Bacteriostatic | 4.00 |
| **Trimethoprim (TMP)** | C1 metabolism (dihydrofolate reductase) | Bacteriostatic | 0.20 |

***Table 1. Composition of the five-antibiotic mixture (MIX) used in the evolution experiments.*** *One unit of MIX is defined by the fixed component concentrations listed in the table.*

All MIX-treated populations increased the tolerated MIX concentration during the 19-day experiment and reached apparent plateaus between days 12 and 16 (Figure 2B). The highest selection concentration reached by individual populations ranged from 2.8 to 8.0 U. The endpoint selection concentrations did not differ detectably between WT and ΔIS populations (Figure 2C; two-sided Wilcoxon rank-sum test, n = 6 per strain, p = 0.672).

Relative to their respective starting concentrations, WT populations achieved a median 11.3-fold increase in MIX concentration (ranged from 11.3 to 16-fold), whereas ΔIS populations achieved a median 32-fold increase (ranged from 16 to 45.3-fold). ΔIS populations also showed a higher rate of concentration increase, expressed as concentration doublings per day (Figure 2D; two-sided Wilcoxon rank-sum test, p = 0.0202). However, the different starting concentrations complicate direct comparisons of adaptation rates between the strains. These results provide no evidence of a WT advantage in the maximum MIX concentration reached or the measured rate of concentration increase under this selection regime.

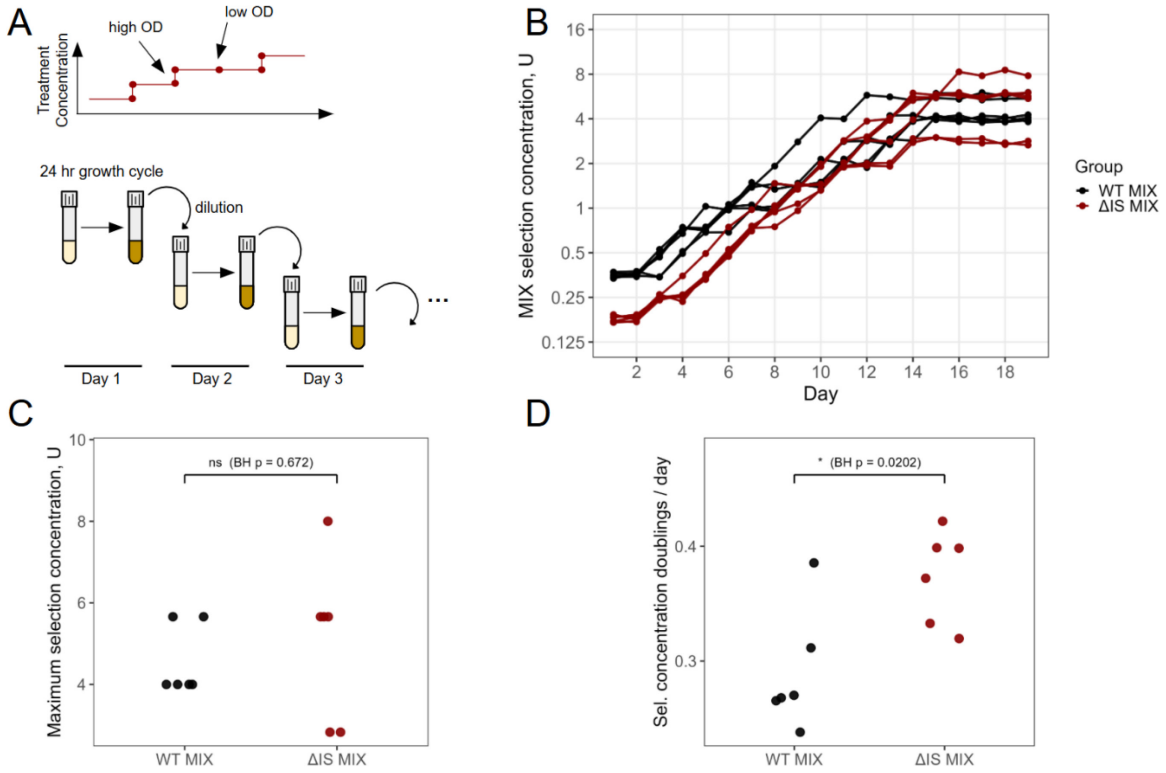



***Figure 2. Adaptation of WT and ΔIS E. coli populations to increasing MIX concentrations.*** *(A) Growth-dependent serial-transfer design. Cultures were transferred every 24 h, MIX concentration was increased $\sqrt{2}$-fold when $OD_{600}$ reached ≥1 and otherwise maintained. (B) Selection-concentration trajectories over 19 days. (C) Maximum selection concentration reached. (D) Adaptation rate, expressed as concentration doublings per day. Six independently evolving populations were analyzed per strain. Comparisons used two-sided Wilcoxon rank-sum tests; BH-adjusted p values are shown.*

To determine whether the increased selection concentrations reflected a heritable increase in resistance, we measured the minimum inhibitory concentration (MIC) of MIX for isolates from the evolved populations. All six biological replicates of each ancestral strain showed identical MIC values, reflecting the limited resolution of the twofold dilution assay and the OD-based threshold used to define MIC (see Materials and Methods). Relative to their respective ancestral strains, MICs increased significantly in both genetic backgrounds, WT and ΔIS (Figure 3A; two-sided Wilcoxon rank-sum tests; n = 6 per strain; WT, p = 0.0022; ΔIS, p = 0.0025). However, endpoint MIC did not differ detectably between MIX-adapted WT and ΔIS isolates (Figure 3B; two-sided Wilcoxon rank-sum test, p = 0.2468). These results are consistent with a heritable increase in MIX resistance and show that the two strains reached comparable endpoint resistance.

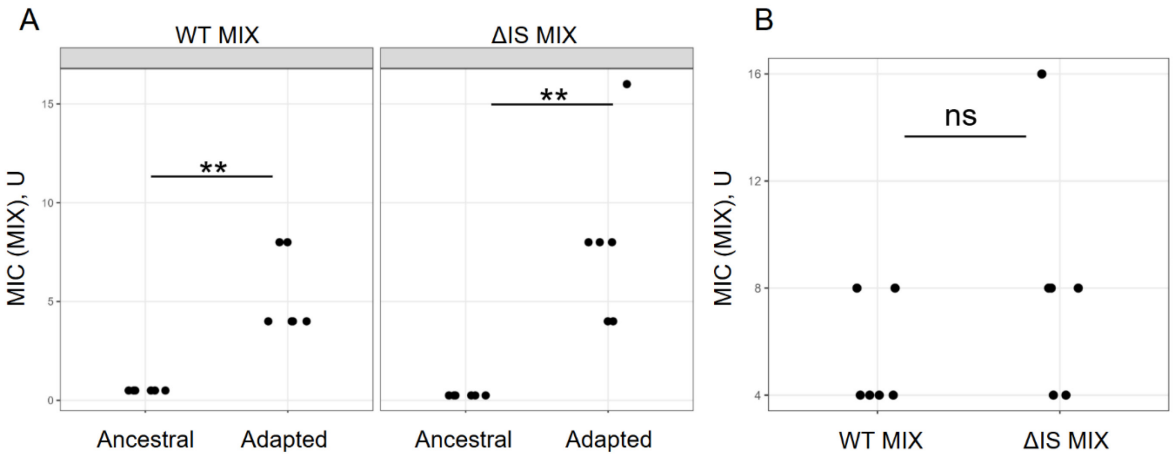



***Figure 3. Minimum inhibitory concentration of MIX in ancestral and MIX-adapted WT and ΔIS isolates.*** *(A) MICs of the ancestral strains and MIX-adapted isolates. (B) Comparison of endpoint MICs between MIX-adapted WT and ΔIS isolates. Ancestral values represent six biological replicates per strain; adapted values represent one isolate from each of six independently evolved populations. Statistics performed by two-sided Wilcoxon rank-sum tests (ns, p ≥ 0.05; **, p < 0.01).*

In summary, these results provide no evidence that genomic IS elements improved adaptation to MIX under the experimental selection regime: ΔIS populations increased resistance more rapidly and reached endpoint resistance comparable to that of WT populations. We therefore asked whether the two strains reached similar phenotypes through different mutational pathways.

### 2.2.2 WT and ΔIS evolved distinct mutation spectra under MIX selection despite minimal involvement of IS elements

To assess whether the WT and ΔIS adapted to MIX through different mutational pathways, we performed high-coverage Oxford Nanopore Technologies (ONT) whole-genome sequencing of isolates from the evolved populations, together with isolates from the corresponding media-adapted controls. This approach enabled detection of both small mutations and structural variants, including gene amplifications [43].

Across the 24 sequenced isolates, we identified 101 mutations affecting 68 distinct loci. MIX-adapted WT and ΔIS isolates acquired similar numbers of mutations, with total numbers of 43 and 42 (7.17 and 7.00 per genome) correspondingly (Table 2). Counts of mutations per isolate ranged from 6 to 10 in WT and from 6 to 9 in ΔIS, and did not differ detectably between the strains (two-sided Wilcoxon rank-sum test, n = 6 per group, p = 0.93). In contrast, media-adapted WT and ΔIS isolates accumulated only 1.17 and 1.50 mutations per isolate, respectively, significantly fewer than their corresponding MIX-adapted groups (two-sided Wilcoxon rank-sum test, n = 6 per group, p = 0.0047 in both respective comparisons). Thus, deletion of IS elements did not affect the overall number of mutations acquired during adaptation to MIX.

| Group | Mutations, n | Mutations per isolate, mean ± SD | Distinct loci, n | Group-specific loci, n | IS-driven mutations, n/N (%) | Isolates with IS-driven mutations, n/N |
|---|---|---|---|---|---|---|
| **WT MIX** | 43 | 7.17 ± 1.47 | 33 | 26 | 3/43 (7.0%) | 2/6 |
| **ΔIS MIX** | 42 | 7.00 ± 1.41 | 28 | 22 | — | — |
| **WT media** | 7 | 1.17 ± 0.75 | 7 | 7 | 1/7 (14.3%) | 1/6 |
| **ΔIS media** | 9 | 1.50 ± 0.55 | 5 | 3 | — | — |

***Table 2. Acquired mutations, locus diversity, and IS-driven mutations in MIX- and media-adapted isolates.*** *One isolate was sequenced from each of six independently evolved populations per group.*

Despite the similar numbers of mutations acquired by WT MIX and ΔIS MIX isolates, they showed significantly different mutation spectra (pairwise PERMANOVA, BH-adjusted p = 0.0029). Significant differences were also detected among the other experimental groups, including between the WT and ΔIS media controls. The ΔIS MIX and ΔIS media groups shared no mutated loci, arguing against the ΔIS MIX spectrum being produced by compensatory adaptation to the effects of ΔIS strain construction (Figure 4).

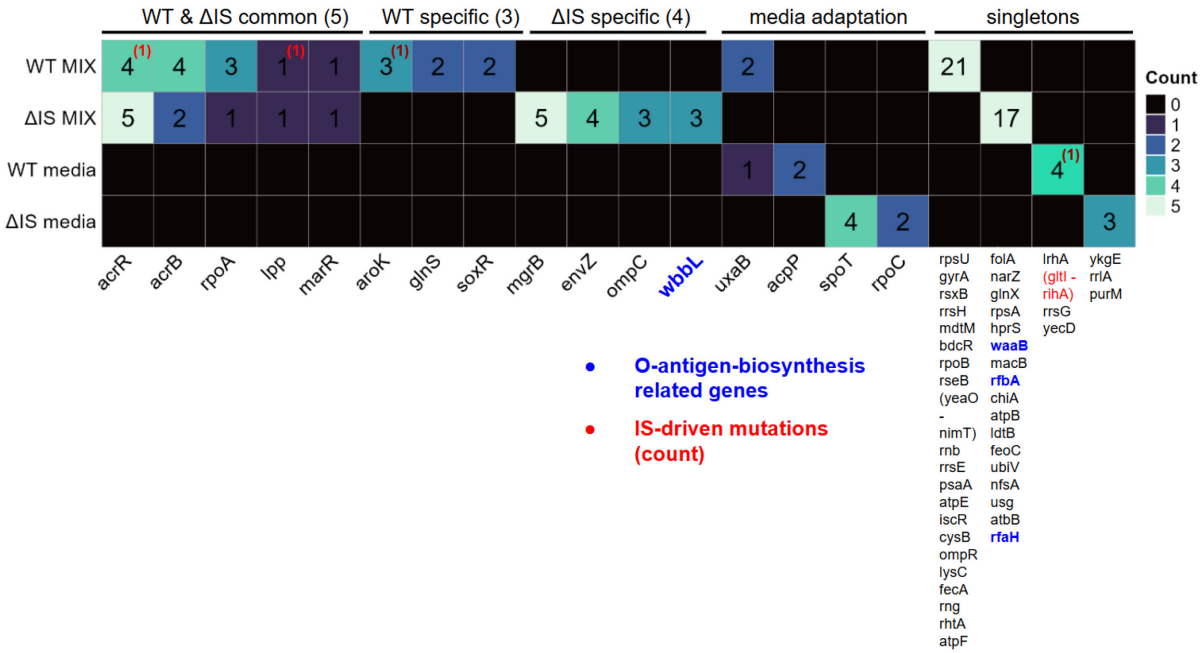



***Figure 4. Distribution of mutated loci among WT MIX, ΔIS MIX, WT media, and ΔIS media isolates.*** *Heatmap values indicate the number of independently evolved isolates carrying a mutation at each locus (n = 6 per group). Loci are grouped by their distribution among the experimental groups. Singletons are mutations found only in a single isolate across all groups. Red superscripts and labels indicate IS-driven mutations. Blue labels indicate genes involved in O-antigen biosynthesis.*

Five loci, *acrR*, *acrB*, *rpoA*, *lpp* and *marR*, were mutated in both MIX-adapted strains. Among them, *acrR* and *acrB*, which encode the transcriptional repressor and a component of the

AcrAB-TolC multidrug efflux system, were the most common (8 and 6 occurrences, respectively, among the MIX-adapted strains; Figure 4). Mutations affecting this system are consistent with selection for reduced susceptibility to CIP, TET, and TMP [44]. Overall, many mutations known to confer resistance to the individual antibiotics comprising MIX were detected in MIX-adapted isolates. However, mutations in the direct targets of the individual antibiotics comprising MIX were rare. Each strain also acquired recurrent mutations in targets that were not mutated in the other strain.

In WT MIX isolates, recurrent mutations occurred in the shared loci *acrR, acrB,* and *rpoA*. Among WT-associated targets, *aroK* was mutated in three isolates, while *soxR* and *glnS* were each mutated in two independently evolved isolates (Figure 4). These loci were not mutated in the ΔIS MIX group.

In ΔIS MIX isolates, *acrR* was mutated in 5 populations, *mgrB* was altered in 5, and *envZ* in 4. Recurrent alterations were also observed in *ompC* in 3 isolates. Two independently evolved populations carried a large deletion spanning the region from *yobD* to *mgrB*. These results identify cell envelope-related loci as prominent targets in the ΔIS background.

Notably, all six ΔIS MIX isolates carried a mutation in *wbbL* or another component of the O-antigen biosynthesis or regulation (*waaB*, *rfbA*, and *rfaH*), while no such mutations occurred in the media-adapted ΔIS isolates (Figure 4). Because functional *wbbL* was restored in ΔIS upon IS deletion, this pattern suggests that restoration of O-antigen biosynthesis was specifically disadvantageous under MIX selection rather than under serial transfer alone.

Three of the 43 mutations detected in WT MIX isolates (7.0%) were classified as IS-driven: IS5 insertions in *acrR* and *aroK*, and an IS1-associated deletion of an approximately 30-kb region containing 29 genes. These events occurred in two of the six WT isolates. IS-mediated mutations were therefore uncommon in the WT MIX mutation spectrum.

WT and ΔIS populations therefore acquired similar numbers of mutations under MIX selection but evolved significantly different mutation spectra. IS-driven mutations accounted only for 3 of 43 total mutations in WT MIX isolates and therefore made only a minor contribution to adaptation. Instead, the two backgrounds differed in the adaptive targets they used, most notably in the strong association between O-antigen biosynthesis mutations and the ΔIS background. These differences were therefore not driven by a higher overall mutation supply in WT or by recurrent IS-mediated mutagenesis.

### 2.2.3 WT populations generally reached higher relative resistance under single-antibiotic selection than under MIX selection

To better understand how treatment complexity affects the dynamics and mutation paths of adaptation, we conducted a complementary evolution experiment, in which six replicate WT populations adapted to each of the individual components of MIX - CIP, MEC, NIT, TET, or TMP, under the same 19-day, growth dependent concentration-increase selection regime as in the MIX experiment. Starting concentrations were chosen to correspond to individual starting concentrations in the MIX experiment (Materials and Methods).

Adaptation trajectories differed among antibiotics (Figure 5A). Most TET populations reached an apparent plateau within 19 days, whereas populations selected with CIP, MEC, NIT, or TMP had not plateaued by the end of the experiment. MEC- and TMP-treated populations increased in selection concentration at the maximum rate permitted by the selection regime, whereas CIP-treated populations increased more slowly. NIT-treated populations maintained high growth through most of the experiment but failed to meet the growth threshold at the highest concentrations during the final days (Figure 5A). Except for one TET-treated population that plateaued earlier, all cultures achieved larger maximum selection concentration increases than the MIX-treated populations. However, at the treatment level, the maximum increase under TET did not differ detectably from MIX (BH-adjusted p = 0.0562; Figure 5B). Rates of concentration increase were also higher under CIP, MEC, NIT, and TMP than under MIX, whereas the rate of concentration increase under TET treatment did not differ detectably from MIX treatment (BH-adjusted p=0.809; Figure 5C).

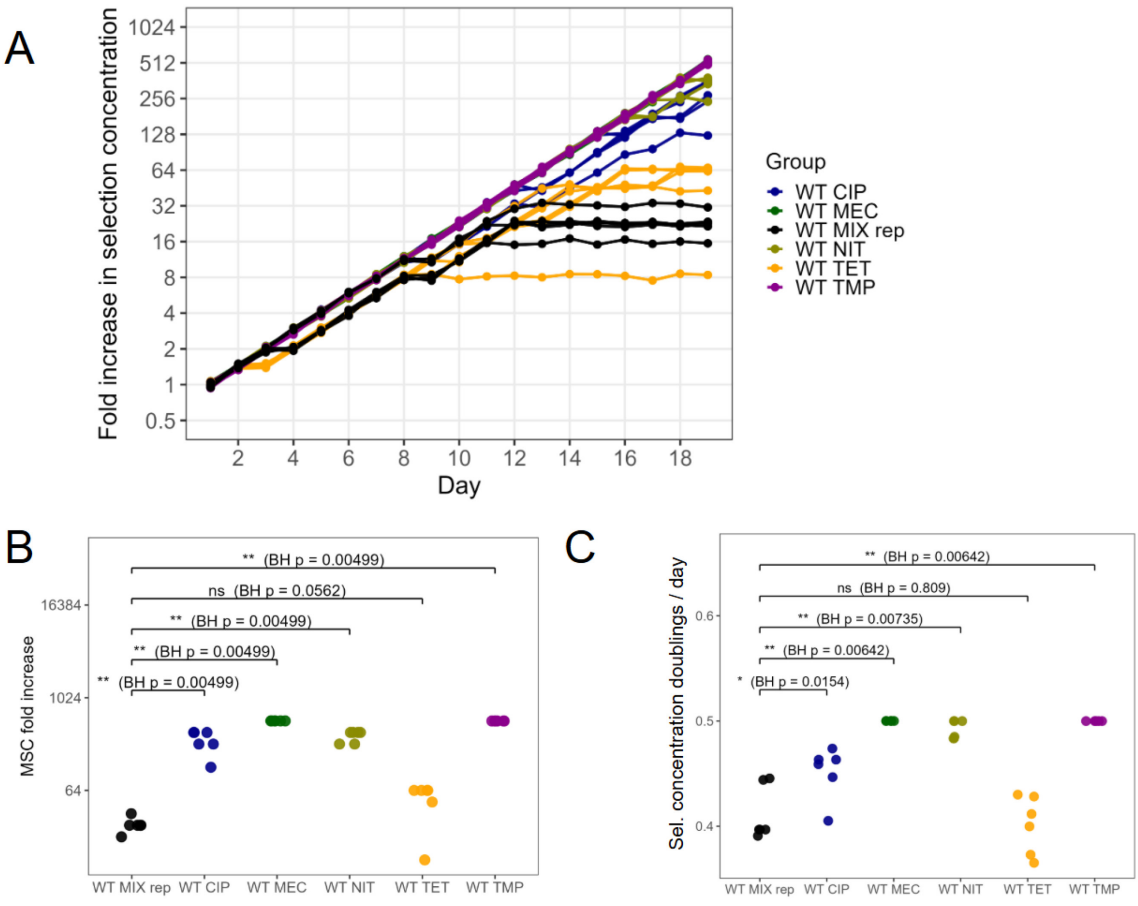



***Figure 5. Adaptation of WT E. coli populations under single-antibiotic and MIX selection.*** *(A) Fold increase in selection concentration relative to the treatment-specific starting concentration over 19 days. (B) Maximum fold increase in selection concentration. (C) Adaptation rate, expressed as concentration doublings per day. Six independently evolving populations were analyzed per treatment. Each single-antibiotic treatment was compared to MIX using two-sided Wilcoxon rank-sum tests, BH-corrected p-values are shown.*

Because the highest selection concentration is constrained by the stepwise selection regime and does not necessarily correspond directly to resistance, we measured the MIC of the selecting antibiotics against isolates of the respective evolved populations. All five single-

antibiotic treatments produced significant increases in MIC relative to the corresponding ancestral values (Figure 6). Mean MIC fold increases were larger than the 10.7-fold increase in MIX-adapted isolates as the result of CIP, MEC, NIT, and TMP selection, whereas TET-adapted isolates showed the same mean 10.7-fold increase as MIX-adapted isolates (Figure 6). MICs exceeded the tested range for one of six NIT-adapted isolates and five of six TMP-adapted isolates. Thus, the corresponding mean fold increases of >26.7-fold and >2,150.4-fold are lower-bound estimates.

Together, the selection trajectories and MIC measurements show that single-antibiotic selection generally generated larger antibiotic-specific phenotypic gains than MIX selection over the same duration of the experiment. TET was the exception: its selection-concentration trajectory did not differ detectably from MIX, and TET- and MIX-adapted isolates showed identical mean MIC fold increases. We next asked whether this difference was associated with greater involvement of IS-driven mutations.

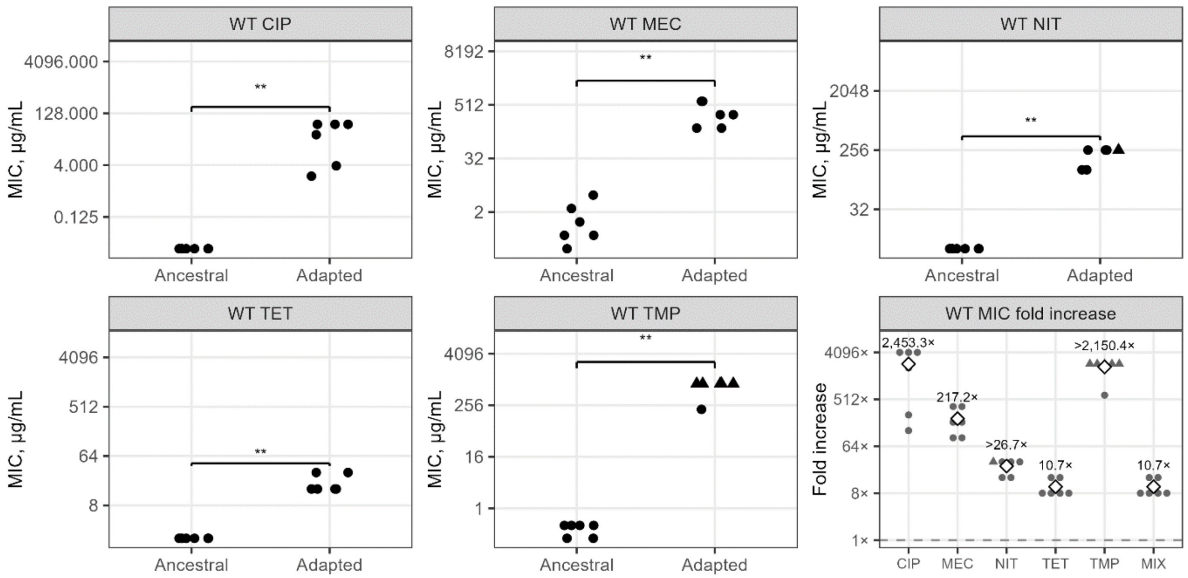



***Figure 6. Treatment-specific minimum inhibitory concentrations and fold increases of ancestral and antibiotic-adapted WT E. coli.*** *The first five panels show absolute MIC of the indicated antibiotic in the ancestral strain and in endpoint isolates evolved under that antibiotic. Adapted values represent one isolate from each of six independently evolved populations, ancestral values represent six biological replicates. The bottom-right panel shows MIC fold increases for WT isolates adapted to single antibiotics or MIX, calculated as each isolate's MIC divided by the mean ancestral MIC in the corresponding assay. Small markers denote individual isolates; diamonds and numerical labels show mean MIC fold increases. Triangles indicate MICs above the tested range; ">" mean labels denote lower bounds. Statistics performed by two-sided Wilcoxon rank-sum tests with Benjamini-Hochberg correction across the five ancestral-versus-adapted comparisons (adjusted p = 0.00375 for CIP, NIT, TET and TMP; adjusted p = 0.00477 for MEC; **, adjusted p < 0.01).*

### 2.2.4 The contribution of IS-driven mutations varied among antibiotics

To determine whether the prevalence of IS-driven mutations depended on the treatment, we whole-genome sequenced isolates from each of the populations adapted to individual antibiotics. The fraction of detected IS-driven mutations differed markedly among antibiotic treatments: 1/36 (2.8%) under CIP, 4/22 (18.2%) under MEC, 4/30 (13.3%) under NIT, 13/39

(33.3%) under TET, and 0/23 (0%) under TMP, compared with 3/43 (7.0%) under MIX selection. Total mutation counts also varied among treatments, ranging from 22 in MEC-evolved isolates to 43 in MIX-evolved isolates (Table 3).

We compared the per-isolate fractions of IS-driven mutations between WT MIX and each single-antibiotic treatment. Only the TET group differed significantly from the MIX group after correction (two-sided Wilcoxon rank-sum test, n = 6 per group, BH-adjusted p = 0.0435). None of the other comparisons was statistically significant. Thus, although the fractions varied widely among treatments, the available sample size provided statistical support specifically for a higher fraction of IS-driven mutations under TET than under MIX selection.

| Group | Mutations, n | Mutations per isolate, mean ± SD | Distinct loci, n | Group-specific loci, n | IS-driven mutations, n/N (%) | Isolates with IS-driven mutations, n/N |
|---|---|---|---|---|---|---|
| **WT CIP** | 36 | 6.00 ± 1.55 | 17 | 10 | 1/36 (2.8%) | 1/6 |
| **WT MEC** | 22 | 3.67 ± 0.82 | 15 | 12 | 4/22 (18.2%) | 4/6 |
| **WT NIT** | 30 | 5.00 ± 1.26 | 14 | 8 | 4/30 (13.3%) | 3/6 |
| **WT TET** | 39 | 6.50 ± 0.84 | 22 | 15 | 13/39 (33.3%) | 6/6 |
| **WT TMP** | 23 | 3.83 ± 0.75 | 9 | 7 | 0/23 (0.0%) | 0/6 |
| **WT MIX** | 43 | 7.17 ± 1.47 | 33 | 26 | 3/43 (7.0%) | 2/6 |

***Table 3. Acquired mutations, locus diversity, and IS-driven mutations in single-antibiotic- and MIX-adapted WT isolates****. One isolate was sequenced from each of six independently evolved populations per treatment.*

### 2.2.5 Single-antibiotic selection produced more parallel and treatment-specific genetic adaptation

Across all five single-antibiotic treatments, mutations were more recurrent across replicate populations than under MIX selection (Figure 7, Figure 8). Each single-antibiotic treatment resulted in at least one locus mutated in five or six of the six isolates, whereas no locus was mutated in more than four MIX-adapted isolates (Figure 7). In contrast, MIX adaptation produced 23 singleton loci and 33 distinct mutated loci overall, compared with 7-14 singleton loci and 9-22 distinct loci in the single-antibiotic groups (Table 3). Thus, MIX selection produced a broader but less repeatable locus spectrum.

Single-antibiotic selection repeatedly targeted loci previously associated with resistance to the corresponding antibiotics (Figure 8), whereas MIX selection produced a broader and less repeatable mutation spectrum. CIP-adapted populations recurrently acquired mutations in *gyrA* and *parC*, while *envZ* was mutated in five of the six MEC-adapted isolates. All six NIT-adapted isolates carried mutations in *emrR*, *nfsA*, and *nfsB*. Likewise, all TMP-adapted populations acquired mutations associated with the *folA* locus, including both promoter and

coding-sequence mutations, and all TET-adapted populations carried mutations in *lon*. These recurrent mutations associated with single drugs were absent or rare in MIX-adapted populations, including mutations affecting the CIP targets *gyrA* and *parC*, the TMP-associated locus *folA*, and the NIT-associated loci *emrR*, *nfsA*, and *nfsB.*

Taken together, single-antibiotic and MIX selection produced largely non-overlapping mutation spectra. MIX-adapted populations showed a broader mutation spectrum lacking direct drug targets and more recurrent mutations in loci associated with efflux and gene regulation (Figure 8). This pattern is compatible with selection for mutations that affect responses to multiple components of MIX.

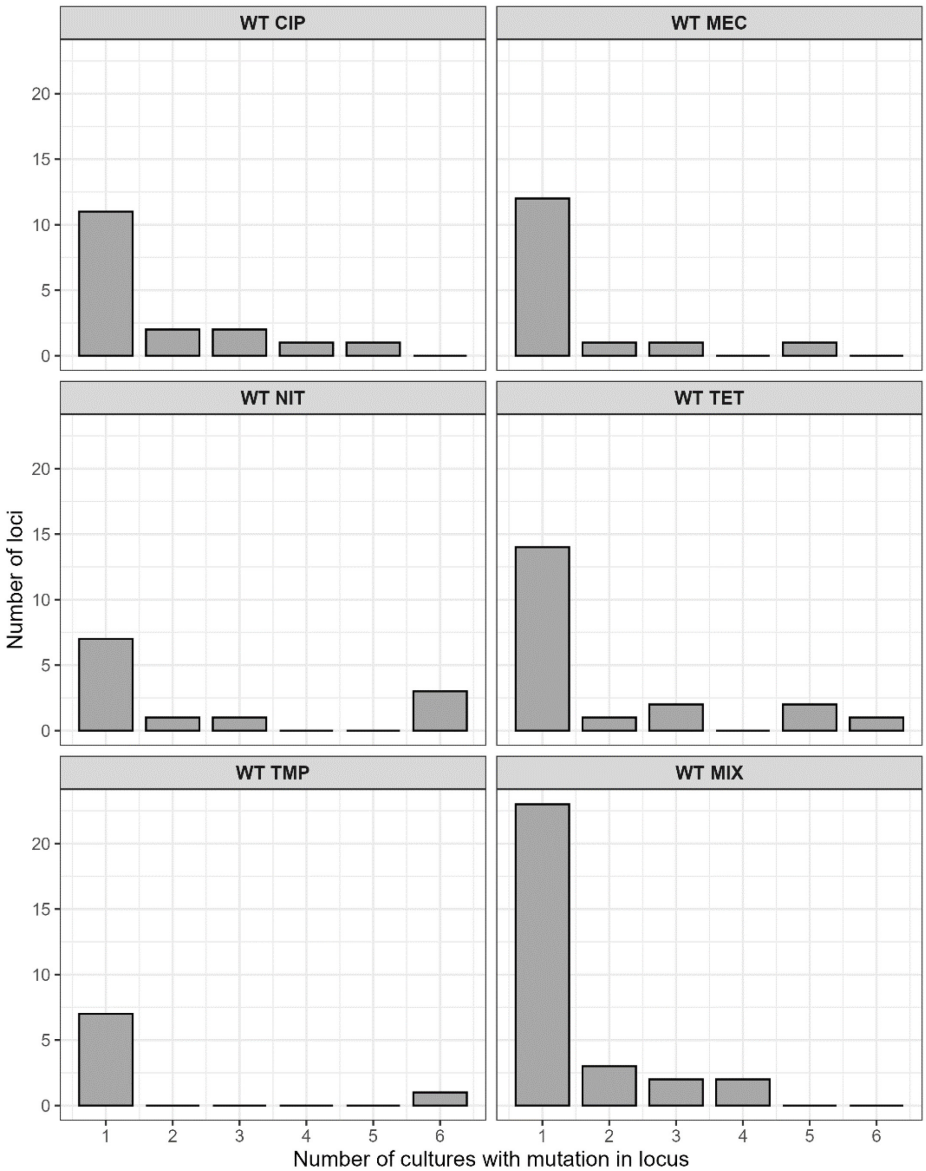



***Figure 7. Recurrence of mutated loci across replicate WT isolates adapted to MIX and individual antibiotics.*** *Bars indicate the number of distinct loci mutated in one to six replicate populations after adaptation to CIP, MEC, NIT, TET, TMP, or MIX. A higher value on the horizontal axis therefore indicates greater parallelism among replicate populations. Mutations were more strongly concentrated in recurrent loci under single-antibiotic selection, whereas MIX adaptation produced more loci found in only one population and no locus mutated in more than four populations.*

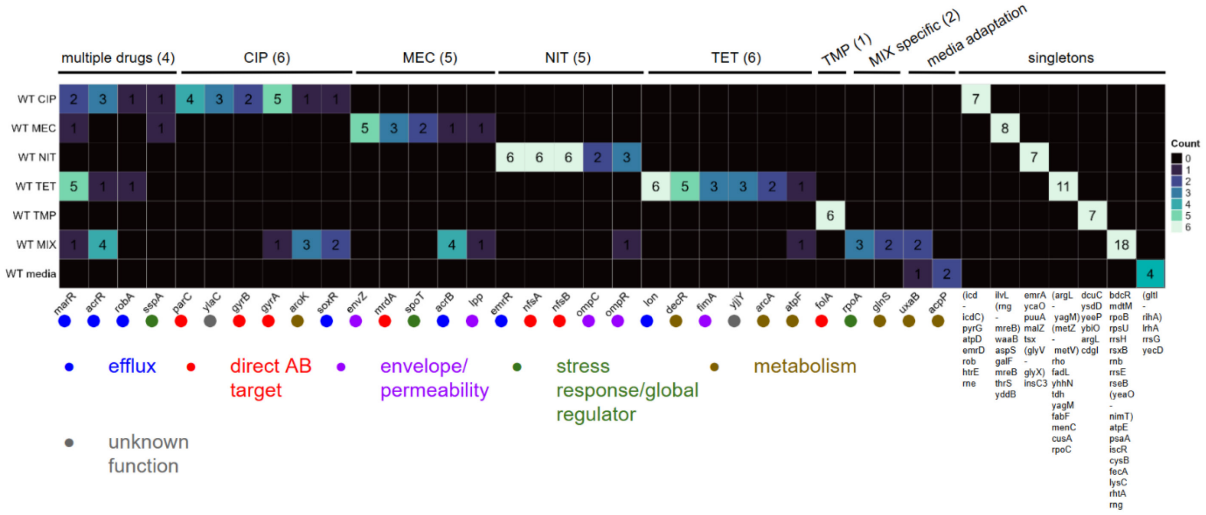



***Figure 8. Mutation spectra of WT isolates adapted to MIX and individual antibiotics.*** *Heatmap values indicate the number of independently evolved isolates carrying a mutation at each locus (n = 6 per treatment). Loci are grouped by treatment association. Singletons are mutations found only in a single isolate across all groups. Colored markers denote functional categories.*

### 2.2.6 Inactivation of *wbbL* shifts the ΔIS mutation spectrum toward that of WT

The WT and ΔIS strains differ not only in IS content but also in the functionality of *wbbL*. In WT, *wbbL* is disrupted by an IS insertion, whereas removal of this insertion during ΔIS construction precisely restored the functional gene. To determine whether this difference in *wbbL* status contributed to the divergent mutation spectra of MIX-adapted WT and ΔIS populations, we performed a complementary evolution experiment using two additional strains, *wbbL*+ and ΔIS *wbbL**. The *wbbL*+ strain is a WT derivative in which only the IS insertion disrupting *wbbL* was removed, thereby restoring gene function while retaining the other IS elements. In contrast, ΔIS *wbbL** is a ΔIS derivative in which *wbbL* was inactivated by introducing two consecutive stop codons followed by a frameshift. Together, these strains allowed us to examine the possible contribution of *wbbL* functionality from those of genome-wide IS removal.

The complementary experiment included six replicate populations each of WT, *wbbL*+ and ΔIS *wbbL**. ΔIS was not evolved again, and its data were taken from the original MIX experiment. The trajectory analysis uses the repeated WT populations, which began selection at the same MIX concentration of 0.18 U as the other strains. In contrast, the mutation-spectrum analysis uses the original WT and ΔIS isolates together with the newly evolved *wbbL*+ and ΔIS *wbbL** isolates. Sequencing data from the repeated WT populations were not included in this analysis.

Repeated WT populations reached maximum selection concentrations that did not differ detectably from those of the original WT or ΔIS populations (both BH-adjusted p = 0.440; Supplementary Figure 2A, B). Their adaptation rate was higher than that of the original WT populations (BH-adjusted p = 0.0143). However, the WT-ΔIS rate difference was no longer detected when WT began selection at the same MIX concentration as ΔIS (0.18 U; BH-adjusted

p = 0.375; Supplementary Figure 2C). Thus, WT again showed no detectable advantage over ΔIS in maximum selection concentration or adaptation rate.

All replicate populations in the four strain groups reached an apparent plateau in MIX selection concentration (Figure 9A). Pairwise comparisons with WT detected no significant differences in maximum selection concentration for ΔIS, ΔIS *wbbL**, or *wbbL*+ populations (two-sided Wilcoxon rank-sum test, n = 6 per strain, BH-adjusted p = 0.326, 0.718, and 0.272, respectively; Figure 9B). These results provide no evidence that *wbbL* status affected the maximum MIX concentration reached under this selection regime.

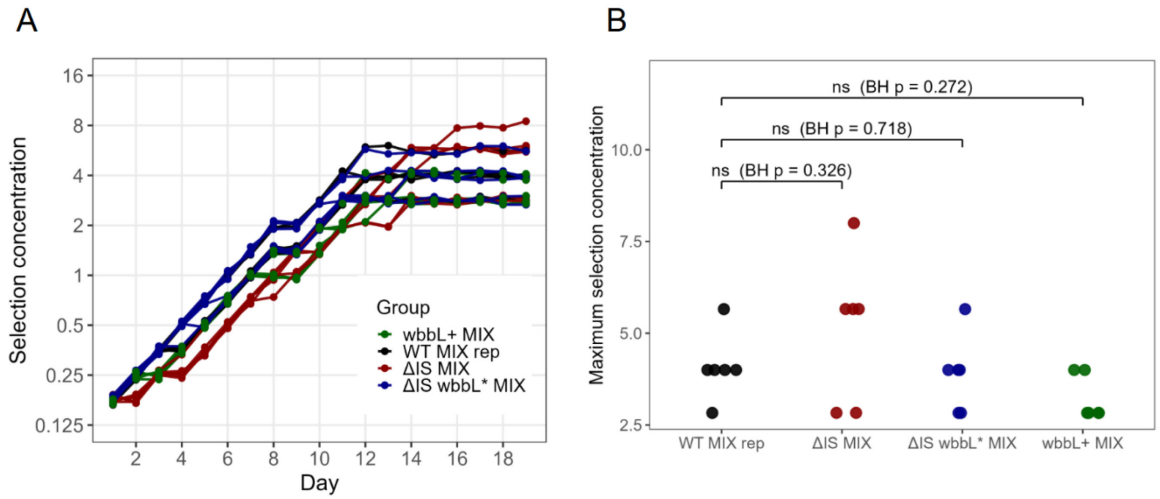



***Figure 9. Adaptation of WT, ΔIS, ΔIS wbbL*, and wbbL+ E. coli populations under MIX selection.*** *(A) Selection concentration trajectories over 19 days. (B) Maximum MIX selection concentration reached by each population. Six independently evolving populations were analyzed per strain. Each modified strain was compared with WT using a two-sided Wilcoxon rank-sum test, BH-corrected p-values are shown.*

We then performed whole-genome sequencing of isolates from the adapted populations (Figure 10). The mutation spectra of all four MIX-adapted groups differed significantly from one another in pairwise PERMANOVA comparisons after Benjamini-Hochberg correction (adjusted p = 0.0039-0.0221; Table 4). Among comparisons with WT, ΔIS *wbbL** resulted in the smallest effect size estimate ($R^2$ = 0.15, F = 1.71), compared with ΔIS ($R^2$ = 0.18, F = 2.18) and *wbbL*+ ($R^2$ = 0.21, F = 2.61). This pattern is consistent with a partial shift of the ΔIS mutation spectrum toward that of WT upon *wbbL* inactivation, although the WT and ΔIS *wbbL** spectra remained significantly different.

ΔIS *wbbL** shared several recurrent mutated loci with WT, including *acrB*, *soxR*, and *aroK*. In contrast, loci that mutated recurrently in ΔIS, including *mgrB*, *envZ*, *ompC*, and *wbbL*, were unaltered in ΔIS *wbbL** isolates (Figure 10). The reciprocal change of *wbbL* status did not produce an analogous ΔIS-like pattern in the *wbbL*+ strain. These results suggest that the effect of *wbbL* status depends on genomic background and does not fully account for the difference between WT and ΔIS.

| group1 | group2 | $R^2$ | F | p | BH-adjusted p |
|---|---|---|---|---|---|
| WT MIX | ΔIS MIX | 0.18 | 2.18 | 0.0024 | 0.0039 |
| WT MIX | ΔIS *wbbL** MIX | 0.15 | 1.71 | 0.0221 | 0.0221 |
| WT MIX | *wbbL*+ MIX | 0.21 | 2.61 | 0.0044 | 0.0053 |
| ΔIS MIX | ΔIS *wbbL** MIX | 0.28 | 3.82 | 0.0026 | 0.0039 |
| ΔIS MIX | *wbbL*+ MIX | 0.27 | 3.75 | 0.0023 | 0.0039 |
| ΔIS *wbbL** MIX | *wbbL*+ MIX | 0.32 | 4.70 | 0.0016 | 0.0039 |

***Table 4. Pairwise PERMANOVA comparisons of mutation spectra among MIX-adapted strains.*** *$R^2$ indicates the proportion of variation explained by strain, and F is the pseudo-F statistic - the ratio of between-group to within-group variation. p-values were adjusted using the Benjamini-Hochberg correction.*

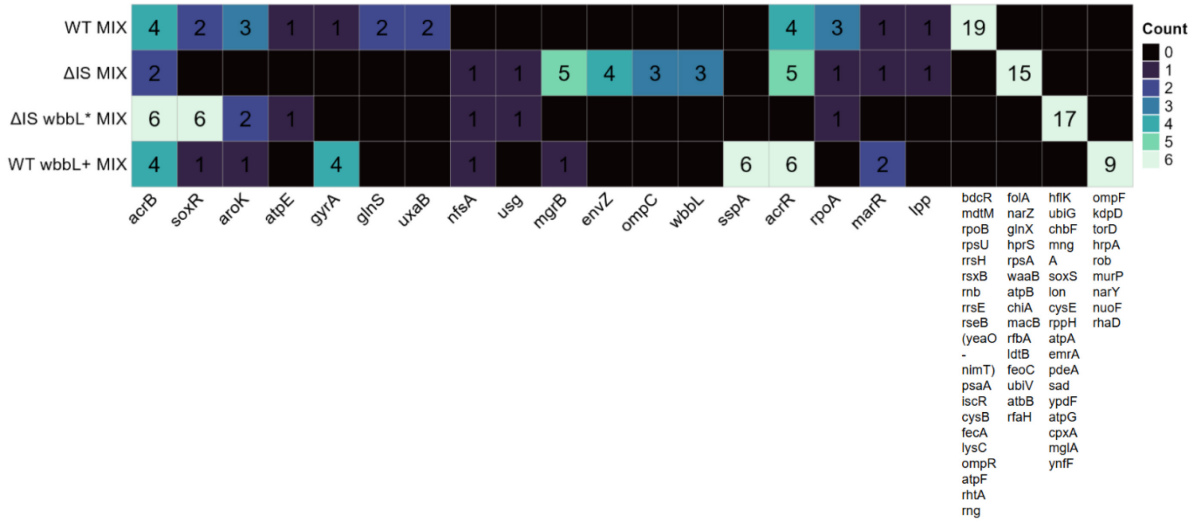



***Figure 10. Mutation spectra of MIX-adapted WT, wbbL+, ΔIS, and ΔIS wbbL* isolates under MIX selection.*** *Heatmap values indicate the number of independently evolved isolates carrying a mutation at each locus (n = 6 per strain). Singletons are mutations found only in a single isolate across all groups.*

### 2.2.7 IS background and *wbbL* status both affected adaptive capacity under TET selection

To determine whether genomic IS elements increase the adaptive capacity and mutational pathways to individual antibiotics, we conducted a complementary evolution experiment where replicate populations of ΔIS and ΔIS *wbbL** *E. coli* strains were adapted to individual antibiotics MEC, NIT, and TET under the same selection regime. These antibiotics were selected because they produced the highest numbers of IS-driven mutations in the corresponding WT experiments (Table 3). The inclusion of ΔIS *wbbL** allowed us to partially distinguish the effect of *wbbL* status from differences associated with the IS-removal background.

The effect of *wbbL* inactivation on adaptation depended on the antibiotic (Figure 11). Under MEC treatment, neither ΔIS nor ΔIS *wbbL** populations reached an apparent plateau during the experiment. ΔIS *wbbL** populations adapted at the maximum rate permitted by the selection regime producing selection concentration trajectories identical to those of WT,

whereas ΔIS populations demonstrated similar trajectories but one to two concentration increases behind as they failed to meet the growth threshold within the first one or two days in the beginning of the experiment (Figure 11A). Under NIT, the two strains followed similar trajectories and reached comparable final selection concentrations (Figure 11B).

The most striking difference among the strains was observed under TET selection. ΔIS and ΔIS *wbbL** populations reached an apparent selection concentration plateau. ΔIS populations attained significantly lower selection concentrations than WT and ΔIS *wbbL** populations, whereas ΔIS *wbbL** reached values intermediate between WT and ΔIS (Figure 11D). The maximum selection concentration of ΔIS *wbbL** was significantly different from ΔIS (two-sided Wilcoxon rank-sum test, n=6 per strain, BH-adjusted p = 0.00683) and showed no detectable difference with WT (two-sided Wilcoxon rank-sum test, n=6 per strain, BH-adjusted p = 0.0767). Adaptation rates differed significantly among the three strains: WT populations adapted faster than ΔIS *wbbL** populations, which adapted faster than ΔIS populations (Figure 11E; two-sided Wilcoxon rank-sum test, n=6 per strain, BH-adjusted p = 0.00683 for both comparisons). These results indicate that restoration of functional *wbbL* in the ΔIS background accounts for a substantial part of its reduced adaptation to TET, particularly its lower maximum attained selection concentration.

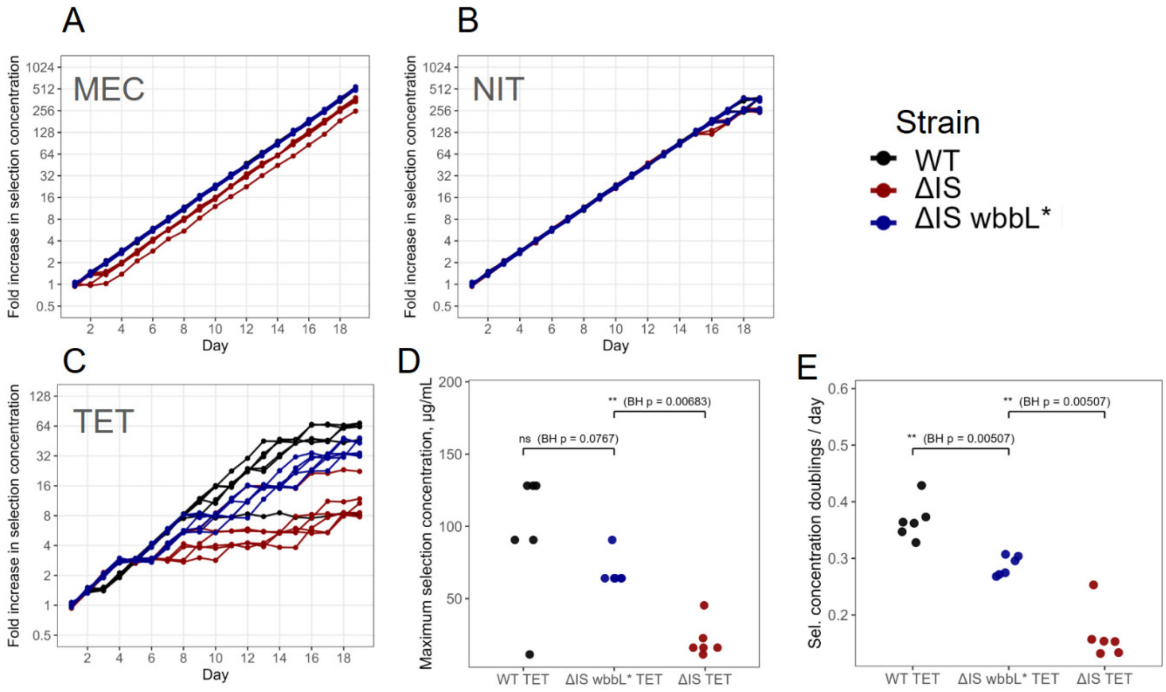



***Figure 11. Adaptation of WT, ΔIS, and ΔIS wbbL* populations under MEC, NIT, and TET selection.*** *(A-C) Fold increase in selection concentration over 19 days under MEC, NIT, and TET, respectively. (D) Maximum TET selection concentration reached. (E) Adaptation rate under TET, expressed as concentration doublings per day. Six independently evolving populations were analyzed per strain. Statistics performed by two-sided Wilcoxon rank-sum test, BH-corrected p-values are shown.*

To assess whether different strains adapted to antibiotics through different genetic mechanisms, we whole-genome sequenced isolates of the adapted populations. After sequencing-quality filtering, genomes were available for 1/6 ΔIS and 4/6 ΔIS *wbbL** MEC populations, 5/6 ΔIS and 6/6 ΔIS *wbbL** NIT populations, and 6/6 ΔIS and 5/6 ΔIS *wbbL** TET

populations. Because only one ΔIS MEC genome was available, the MEC mutation spectra were not used for between-strain comparisons. Analyses of NIT- and TET-adapted isolates should be interpreted with the remaining imbalance in sample sizes taken into account. The low number of successfully sequenced ΔIS MEC isolates may reflect technical difficulties during sample processing or sequencing, as a deterioration in sequencing quality was observed during this stage of the study. However, the underlying cause could not be determined, and it remains unclear whether the particularly low recovery in this group was coincidental or associated with strain- or treatment-specific factors.

The NIT-adapted WT, ΔIS, and ΔIS *wbbL** isolates showed broadly overlapping mutation spectra (Figure 12B), consistent with their similar adaptation trajectories (Figure 11B). In contrast, the TET-adapted isolates differed in several recurrently mutated loci (Figure 12A).

The *lon* locus was mutated in all 6/6 WT isolates but in only 1/6 ΔIS and 1/5 ΔIS *wbbL** isolates. In WT, all *lon* mutations were IS421 insertions in its promoter region, whereas the *lon* mutations detected in the IS-free strains were point mutations. Mutations in *fimA* and *yjjY* were also detected in half of the WT isolates but not in the ΔIS or ΔIS *wbbL** isolates. The WT *yjjY* mutations were IS421 promoter insertions. These observations indicate that TET adaptation in WT repeatedly involved mutational routes unavailable to the IS-free strains.

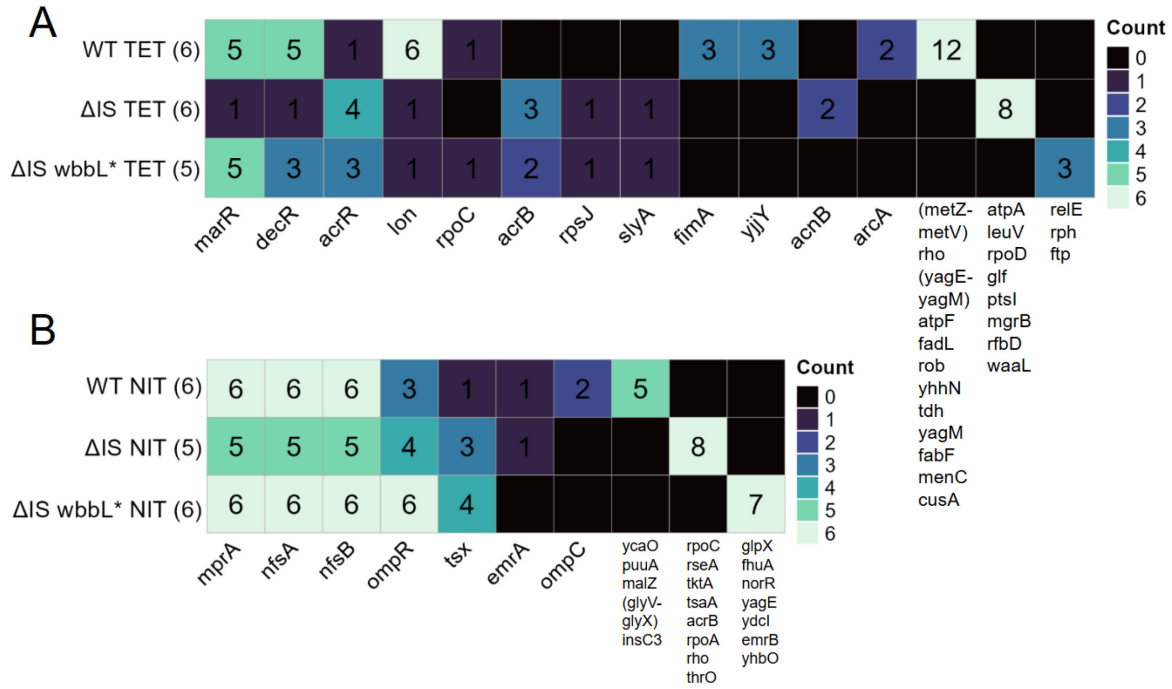



***Figure 12. Mutation spectra of WT, ΔIS, and ΔIS wbbL* isolates under TET and NIT selection.*** *Heatmaps show the number of isolates carrying a mutation at each locus after adaptation to TET (A) or NIT (B). The number of sequenced isolates in each experimental group is given in parentheses in the row labels, as some genomes were excluded after sequencing-quality filtering. Singletons are mutations found only in a single isolate across all groups.*

## *2.3 Discussion*

### 2.3.1 IS removal did not reduce adaptation under MIX selection

We hypothesized that genomic IS elements may increase adaptive capacity of bacteria by providing additional mutation types with potentially different fitness effects. However, under MIX selection, WT populations did not achieve higher endpoint MIX resistance or adapt faster than ΔIS populations under the tested selection regime, although the two strains followed different mutational pathways. The subsequent experiments showed that the effects related to IS content depended on both the selection environment and *wbbL* status. In particular, IS-driven mutations were uncommon and provided no detectable phenotypic advantage under MIX selection, whereas TET selection resulted in both recurrent IS-driven mutations and a WT adaptive advantage that was only partly explained by *wbbL*. Collectively, these results suggest that IS elements expand the available repertoire of mutations, but the expanded repertoire leads to an adaptive advantage only when IS-driven mutations provide particularly beneficial adaptive routes in the relevant environment.

During adaptation to increasing MIX concentrations, WT and ΔIS reached comparable maximum MIX selection concentrations (Figure 2). Both strains acquired heritable increases in MIX resistance, with no detectable difference in endpoint MIC (Figure 3). Although ΔIS showed a higher adaptation rate than WT in the original experiment, this difference was no longer detected when WT was repeated from the same starting MIX concentration as ΔIS (Supplementary Figure 2C). This suggests that the different starting concentrations contributed to the original rate difference. However, WT was also repeated in a separate experiment, so variation between experiments could also have contributed. Overall, WT showed no detectable advantage over ΔIS in adaptation to MIX under the tested conditions.

Whole-genome sequencing of adapted isolates showed that WT and ΔIS acquired similar numbers of mutations, but the two strains acquired significantly different mutation spectra. In both strains, mutations affected multidrug efflux, particularly the AcrAB-TolC system, whereas other recurrently mutated loci differed between strains. WT-associated mutations included *aroK*, *glnS*, and *soxR*, while ΔIS-associated mutations included envelope-associated loci and O-antigen biosynthesis or regulation. The occurrence of O-antigen-associated mutations in all MIX-adapted ΔIS isolates, but not in the corresponding media controls, is consistent with selection against the ancestral ΔIS O-antigen recovered state specifically under MIX, but not under media selection. Thus, similar phenotypic outcomes were reached through partly distinct and background-dependent mutational pathways.

Only 3 of the 43 mutations detected in MIX-adapted WT isolates were classified as IS-driven. Therefore, IS-driven mutations constituted only a small fraction of the mutations detected in MIX-adapted WT isolates and cannot explain the difference in mutation spectra between WT and ΔIS. The observed fraction of IS-driven mutations was also lower than fractions reported in several previous studies, including no-selection mutation-accumulation experiments (25%) [37], Lenski long-term evolution experiment (35%) [14], and adaptation to some individual antibiotics (NIT - 35-54%; TET - 54%) [13]. These comparisons should be interpreted cautiously because the studies differ in selection regime, duration, strains, and mutation detection

methodology. Nevertheless, the observed low fraction of IS-driven mutations suggests that beneficial IS-mediated adaptation routes were relatively inaccessible or weakly favored under MIX selection.

### 2.3.2 The contribution of IS elements in adaptation depended on the selection environment

WT populations adapted to the individual antibiotics generally achieved larger antibiotic-specific gains in resistance than populations adapted to MIX. TET was the exception to this general adaptation trajectory pattern: neither its maximum selection concentration increase nor its rate of concentration increase differed detectably from MIX. The mean MIC fold increase relative to the corresponding ancestral MIC was also identical for TET- and MIX-adapted WT isolates (10.7-fold in both groups; Figure 6). Together, these phenotypic similarities raise the possibility that TET constrained adaptation to MIX.

Single-antibiotic selection also produced more parallel mutation spectra and repeatedly targeted known drug-specific resistance loci, whereas MIX adaptation produced a broader and less repeatable mutation spectrum with mutations mainly affecting efflux, envelope, and regulatory pathways. This pattern is consistent with the possibility that MIX favored mutations with simultaneous effects on its components, while individual antibiotics favored narrower sets of highly beneficial resistance mutations.

However, the experiment compared one particular mixture with its five constituents, such that treatment complexity is not a systematically tested variable. Because the concentrations of all five MIX components were increased together in constant proportions, the experiment cannot determine whether TET, another component, or interactions among components constrained further MIX adaptation. Moreover, the largely distinct mutation spectra show that similar phenotypic outcomes do not imply equivalent evolutionary responses under TET and MIX. Differences in selection strength and in whether populations reached an apparent plateau may also have contributed to the observed contrast in achieved resistance.

Previous studies in *E. coli* demonstrated antagonism between CIP and TET [45] and between MEC and NIT, as well as strain-dependent synergy between TMP and MEC or NIT [46]. However, these pairwise results do not show whether the five antibiotics together inhibit growth more or less strongly than expected from their individual effects under the conditions used here. Drug interactions were not formally quantified in this study, and their contributions to MIX inhibition and adaptation remain unresolved.

The fraction of IS-driven mutations varied substantially in WT isolates among antibiotic treatments, but only TET differed significantly from MIX after correction for multiple comparisons. Therefore, these data provide statistical support for increased IS contribution in adaptation under TET selection, while there is insufficient evidence for the apparent differences for CIP, MEC, NIT, and TMP selection. These results suggest that the contribution of IS elements is not fixed or equal across different antibiotic environments. However, additional replication and more tested conditions are required to estimate the extent of this

variation and determine which properties of a treatment make IS-mediated adaptive routes advantageous.

### 2.3.3 *wbbL* status partly explained mutation spectrum differences between WT and ΔIS under MIX selection

Deletion of the genomic IS elements restored 15 previously interrupted open reading frames, including *wbbL*. Therefore, interpretation of the WT-ΔIS mutation spectra comparison is complicated. All MIX-adapted ΔIS isolates acquired mutations in *wbbL* or related O-antigen pathways, suggesting that functional O-antigen biosynthesis was disadvantageous under MIX selection. Inactivation of *wbbL* in ΔIS shifted its mutation spectrum partially toward that of WT and removed several recurrent ΔIS-associated loci from the spectrum, including *mgrB*, *envZ*, and *ompC*. However, the ΔIS *wbbL** spectrum remained significantly different from the WT spectrum, and restoring *wbbL* in WT did not produce the reciprocal ΔIS-like spectrum. These asymmetric effects are consistent with background-dependent interactions (epistasis) among *wbbL*, IS content, and other restored loci. Therefore, ΔIS *wbbL** strain helps substantially to distinguish the effect of *wbbL* restoration from other consequences of IS removal. However, other genes restored during ΔIS construction remain potential sources of differences from WT.

### 2.3.4 TET selection demonstrated an adaptive advantage of WT over ΔIS not fully explained by *wbbL* status

Under TET selection, WT populations achieved higher selection concentrations and adapted faster than ΔIS populations. Inactivation of *wbbL* in ΔIS substantially increased the achieved maximum concentration, which indicates that functional *wbbL* contributed to the adaptive disadvantage of ΔIS. However, WT populations still adapted faster than ΔIS *wbbL** populations, showing that *wbbL* status alone did not explain the adaptive advantage of WT.

The sequencing results suggest that access to IS-driven mutations may account for part of the remaining difference. All WT isolates acquired IS421 promoter insertions affecting *lon*, whereas *lon* mutations were rare in both the IS-free strains and occurred by point mutations. WT isolates also recurrently acquired IS-driven mutations affecting *yjjY*. These results are consistent with WT having access to potentially beneficial mutational pathways that are accessible exclusively through IS-driven mutations, although the causal effects of these mutations remain to be experimentally confirmed. In contrast, the WT and both the IS-free strains showed similar adaptation trajectories and broadly overlapping mutation spectra under NIT selection. Thus, the advantage associated with the WT repertoire of potentially beneficial IS-driven mutations was specific to a particular antibiotic environment.

### 2.3.5 Limitations and implications

The findings of this study should be interpreted considering several limitations. Six replicate populations provided limited power for comparing the fractions of IS-driven mutations,

particularly after correction for multiple comparisons. Sequencing a single isolate per adapted population could not capture within-population polymorphism, competing lineages, earlier events, or the order in which mutations arose. The concentration-increase selection regime imposed an upper bound on the measurable adaptation rate, and some populations had not reached an apparent selection concentration plateau by the end of the experiment. Differences in starting MIX concentration complicate direct interpretation of the measured rates. Unequal sequencing sample sizes limited comparisons among TET- and NIT-adapted strains, while the low number of successfully sequenced MEC-adapted ΔIS isolates prevented a meaningful comparison of MEC mutation spectra. Finally, the phenotypic effects of the identified mutations were not experimentally studied, and the restoration of multiple open reading frames during ΔIS construction prevents the interpretation of all WT-ΔIS differences as being related only to the activity of IS elements.

Overall, the results do not show that genomic IS elements confer a universal advantage in adaptation. Instead, they support that IS elements increase the diversity of accessible mutations, while the fitness benefits of that diversity depend on the environment and genetic background. Under MIX and NIT selection, IS-positive and IS-free populations achieved comparable phenotypic results, whereas TET selection provided evidence consistent with an advantage from mutational pathways enabled by IS-driven mutations. A broader understanding of the role of IS elements in adaptation will therefore require systematic investigation of the environments in which IS-driven mutations provide advantageous pathways, the environments in which they do not, and the factors underlying these differences.

## *2.4 Materials and methods*

### 2.4.1 Bacterial strains and genotypes

All *E. coli* strains used in this study were obtained from the laboratory collection and were derived from K-12 MG1655 (Table 5). The ΔIS, ΔIS *wbbL**, and *wbbL*+ strains were constructed previously in our laboratory by Roderich Roemhild (manuscript in preparation). The ΔIS strain was generated by seamless deletion of all 45 annotated IS elements from the WT genome. Removal of IS elements interrupting coding sequences restored 15 open reading frames, including *wbbL*, which encodes a rhamnosyltransferase involved in O-antigen biosynthesis. ΔIS *wbbL** carries an inactivating insertion in *wbbL* in the ΔIS background. *wbbL*+ was derived from WT by deleting the IS5I copy interrupting *wbbL*.

### 2.4.2 Media, antibiotics, and growth conditions

If not stated otherwise, experiments were conducted in Mueller-Hinton broth (MHB; 2.0 g/L beef infusion solids, 17.5 g/L casein hydrolysate, 1.5 g/L starch, pH was adjusted to 7.4 at 25°C), and solid medium used was MHB agar (MHB supplemented with 15 g/L Bacto agar). All antibiotics were obtained from Sigma-Aldrich. Liquid cultures were grown at 37 °C with shaking at 180 rpm.

| Strain | Genotype |
|---|---|
| *E. coli* MG1655 (WT) | *E. coli* K-12 F– λ– *ilvG*– *rfb*-50 *rph*-1 |
| ΔIS | *E. coli* MG1655 ΔIS3ABCDE ΔIS2ADEFHIK ΔIS150 ΔIS911AB ΔIS600 ΔISX ΔIS30ABCD ΔIS609 ΔISZ ΔIS4 ΔIS186ABC ΔIS5ABDIFYKLoRTH ΔIS1ABCDEFH |
| ΔIS *wbbL** | *E. coli* ΔIS *wbbL*-mut* |
| *wbbL+* | *E. coli* MG1655 ΔIS5I |

***Table 5. Bacterial strains used in this study.*** *. Bacterial strains used in this study. mut* indicates the replacement of the deleted IS sequence with 5'-TAATAGG-3' introducing a double stop codon followed by a frameshift.*

### 2.4.3 Composition and calibration of MIX

The five-antibiotic mixture MIX contained ciprofloxacin (CIP), mecillinam (MEC), nitrofurantoin (NIT), tetracycline (TET), and trimethoprim (TMP). The relative concentrations of the components were selected using preliminary single-antibiotic dose-response assays in the ancestral WT and ΔIS strains (Supplementary Figure 1A-E), with two independent biological replicates per strain-antibiotic combination.

Assays were performed in MHB media using a Bioscreen C MBR automated growth curve analyzer (Oy Growth Curves Ab Ltd., Finland). Overnight cultures were normalized to the optical density of the culture with the lowest OD and diluted 1:500 in fresh medium. Wells containing 150 µL of twofold serial antibiotic dilutions were inoculated with 150 µL of diluted culture, giving a final inoculum dilution of 1:1000 relative to the OD-normalized overnight cultures. Cultures were incubated for 24 h at 37 °C with agitation.

Baseline-corrected endpoint OD at 24 h was normalized to the corresponding antibiotic-free controls. Four-parameter log-logistic models were fitted to the mean relative OD for each strain-antibiotic combination using the R package *drc* (LL.4 model; Nelder-Mead optimization; [47]). IC90 was estimated as the concentration corresponding to 10% of the untreated-control endpoint OD. The IC90 estimates were similar between the two strains. MIX concentration is reported in arbitrary units (U), with one unit containing approximately one single-antibiotic IC90 of each component at the concentrations listed in Table 1. Other MIX concentrations were prepared by proportionally scaling all components. The overall MIX dose response was subsequently measured under the same Bioscreen conditions, with six independent biological replicates per ancestral strain (Supplementary Figure 1F). No IC90 or MIC was calculated from these preliminary MIX curves, and drug interactions were not formally quantified.

### 2.4.4 Experimental evolution

For each strain-treatment combination, six independent colonies of the corresponding ancestral strain were grown separately for 16 h in treatment-free MHB. Each culture was then diluted 1:100 into the first treatment concentration to begin one independently evolving population. Populations were propagated in 2 mL MHB in 15-mL round-bottom culture tubes. Every 24 h, cultures were diluted 1:100 into fresh medium containing the appropriate treatment. Selection concentration was adjusted separately for each population according to its growth during the preceding cycle. If a culture reached $OD_{600} \geq 1$, it was transferred to a $\sqrt{2}$-fold higher treatment concentration (two consecutive steps produced a twofold increase). Otherwise, it was maintained at the same concentration. This growth-dependent regime increased selection pressure along with culture adaptation while reducing the risk of population loss. At selected time points, culture samples were mixed with glycerol to a final concentration of 15% and frozen at -70°C.

### 2.4.5 Experimental design and treatment groups

Four evolution experiments were conducted, with six independently evolving populations per strain-treatment combination. In the first experiment, WT and ΔIS populations were propagated for 19 days under MIX selection together with antibiotic-free media controls. MIX selection began at 0.35 U for WT and 0.18 U for ΔIS, based on preliminary CFU dose-response assays performed at a 1:1000 inoculum dilution. Subsequent assays at the 1:100 dilution used in the evolution experiment did not show a difference in MIX susceptibility between WT and ΔIS. For subsequent isolate analyses, frozen populations that reached a selection concentration plateau were used: five WT populations were frozen on day 16 and one on day 14, while three ΔIS populations were frozen on day 15 and three on day 16.

In the second experiment, WT populations were propagated for 19 days under each individual component of MIX. Starting concentrations were 0.01062 µg/mL CIP, 0.1062 µg/mL MEC, 1.415 µg/mL NIT, 1.415 µg/mL TET, and 0.0708 µg/mL TMP.

In the third experiment, ΔIS *wbbL** and *wbbL*+ populations were propagated for 19 days under MIX selection beginning at 0.18 U. WT was evolved again to provide a reference starting at the same MIX concentration as ΔIS and the two *wbbL*-modified strains. ΔIS was not evolved again.

For the complementary MIX trajectory comparisons, WT, ΔIS *wbbL**, and *wbbL*+ data came from the third experiment, whereas ΔIS data were reused from the first experiment. For the corresponding mutation-spectrum comparisons, WT and ΔIS isolates came from the first experiment, while ΔIS *wbbL** and *wbbL*+ isolates came from the third experiment. Although the repeated WT populations were also sequenced, those sequencing data were not included in the analyses presented here. The WT trajectory and mutation-spectrum data in these complementary comparisons therefore represent different sets of independently evolved populations.

In the fourth experiment, ΔIS and ΔIS *wbbL** populations were propagated for 19 days under MEC, NIT, or TET selection, beginning at 0.1062, 1.415, and 1.415 µg/mL, respectively.

### 2.4.6 Analysis of adaptation trajectories

The maximum selection concentration was defined as the highest concentration observed during the experiment, regardless of whether a population reached an apparent selection concentration plateau by the end of experiment. For each population, the adaptation rate was estimated as the slope of a linear regression of $\log_2$(concentration/starting concentration) against day, from the first through the last concentration increase. The concentration change rates are expressed as concentration doublings per day.

### 2.4.7 MIC measurements and dose-response assays

Cultures were streaked on MHB agar and grown for 16 h in antibiotic-free MHB. Twofold serial dilutions of MIX or the relevant antibiotic were prepared in 100 µL MHB per well in 96-well plates. An equal volume of diluted culture was added to a final volume of 200 µL and $OD_{600}$ of 0.003. Plates were incubated for 24 h at 37°C with shaking at 750 rpm on a Titramax plate shaker (Heidolph). Endpoint $OD_{600}$ was measured using an H1 plate reader (BioTek). MIC was defined as the lowest concentration yielding $OD_{600} < 0.05$. One isolate from each evolved population (n = 6 per group) and six biological replicates of each ancestral strain were measured.

For WT ancestral and corresponding single-antibiotic-adapted isolates, respectively, the tested concentration ranges (µg/mL) were 0.002-1.92 and 0.12-122.88 for CIP; 0.038-38.4 and 0.6-614.4 for MEC; 0.031-32 and 0.25-256 for NIT; 0.031-32 and 2-512 for TET; and 0.006-6.4 and 0.8-819.2 for TMP. MIX was tested at 0.008-8 U in ancestral strains and 0.016-16 U in MIX-adapted isolates. Antibiotic-free controls were included.

MICs exceeded the tested range for one of six NIT-adapted WT isolates (>256 µg/mL) and five of six TMP-adapted WT isolates (>819.2 µg/mL), and were reported as greater than the highest tested concentration. MIC fold increases were calculated relative to the corresponding ancestral mean and summarized using arithmetic means. For above-range MICs, the highest tested concentrations were used in these calculations, and the resulting mean fold increases were reported as lower bounds. The dose-response curves used for MIC determination are shown in Supplementary Figure 3.

### 2.4.8 DNA extraction and whole-genome sequencing

For each experimental group, one isolate was obtained from each independently evolved population by streaking the frozen population on MHB agar supplemented with the respective treatment at 1x MIC. A single colony was grown for 24 h in 25 mL MHB containing the same treatment at 1x MIC. For the samples from the first and second evolution experiments, genomic DNA was extracted using the Blood & Cell Culture DNA Midi Kit

(Qiagen) according to the manufacturer's instructions. For the samples from the third and fourth evolution experiments, genomic DNA extraction was performed by Microsynth. Overnight cultures were harvested at a total biomass equivalent to six $OD_{600}$ units. Cell pellets were washed twice with PBS buffer, resuspended in 1 mL of NAP buffer, and submitted to Microsynth for DNA extraction. Oxford Nanopore Technologies long-read sequencing, de novo genome assembly, and genome annotation were performed using the BacterialSeq service from Microsynth (Balgach, Switzerland). Unless stated otherwise, six genomes were analyzed per experimental group. After sequencing-quality filtering, the numbers of available ΔIS and ΔIS *wbbL** genomes were 1 and 4 under MEC, 5 and 6 under NIT, and 6 and 5 under TET treatment, respectively (out of six populations per group).

### 2.4.9 Mutation identification and annotation

The de novo genome assemblies provided by Microsynth were aligned against the corresponding ancestral reference genome using progressiveMauve [48] implemented in Mauve v2.4.0 [49], and the alignments were inspected in Geneious Prime v2026.1 [50]. Candidate single-nucleotide variants, small insertions and deletions, IS insertions, inversions, amplifications, and large deletions were identified by manual comparison of the assembled genomes. Gene and IS annotations supplied by Microsynth were used to annotate the detected mutations. A mutation was classified as IS-driven when comparison of the assembled genomes supported insertion of an annotated IS element or a deletion or rearrangement associated with an IS element. Mutation identification was therefore based on high-coverage long-read assemblies rather than independent read-level variant calling.

Mutations within coding regions were assigned to the corresponding annotated coding-sequence feature. Mutations in non-coding regions were assigned to the nearest coding sequence and annotated as upstream or downstream. The recurrent ycfK-tfaP-tfaE-stfE inversion, a common phase-variable inversion observed in approximately half of the sequenced genomes, was excluded from the analysis. For locus-level mutation-spectrum comparisons, overlapping large deletions affecting multiple genes were represented by the narrowest shared affected locus.

### 2.4.10 Mutation-spectrum comparisons

One isolate was sequenced from each of six independently evolved populations per experimental group. Mutation spectra were represented as an isolate-by-locus binary matrix indicating the presence (1) or absence (0) of at least one acquired mutation at each locus. Multiple mutations affecting the same locus within an isolate were counted once, while independent occurrences across isolates were retained. Differences in mutation spectra among experimental groups were assessed using permutational multivariate analysis of variance (PERMANOVA) [51] based on Jaccard distances, which quantify the proportion of mutated loci not shared between two isolates. The analysis partitions variation in mutation spectra into between-group and within-group components, with statistical significance assessed using 9,999 permutations of group labels.

For descriptive purposes, loci were classified based on their occurrence across all populations included in a given comparison. Singleton loci were mutated in only one population, whereas recurrent loci were mutated independently in two or more populations, irrespective of experimental group.

# 3 Adaptation of *Escherichia coli* to complex stress environments

## *3.1 Introduction*

Laboratory evolution can reveal how bacteria respond to environmental stress and whether particular genetic mechanisms contribute to this response. This chapter describes an initial attempt to investigate the contribution of IS elements to adaptation under complex stress conditions. Ethanol was used in continuous-culture experiments because it affects several cellular processes and because adaptation of *E. coli* to ethanol has been described previously [52], [53]. Additional experiments examined adaptation to increasing concentrations of NaCl and n-butanol using daily transfers in 96-well plates.

Continuous culture allows microbial populations to be maintained over extended periods while controlling nutrient supply or population density, making it useful for studying adaptation under defined conditions. However, wall-associated growth can complicate the interpretation of these experiments. Early studies in *Escherichia coli* demonstrated selective advantages associated with attachment to culture-vessel walls [54]. Subsequently, Chao and Ramsdell showed that wall populations could maintain strains that were less competitive in the liquid phase by releasing cells into suspension [55]. Consequently, changes in population composition can reflect differences in attachment and retention as well as differences in planktonic growth. Aggregation also repeatedly arises during chemostat evolution in yeast, illustrating the broader importance of this problem in continuous-culture experiments [56].

These observations also show that the physical organization of a culture can influence its evolutionary dynamics. In static *Pseudomonas fluorescens* microcosms, spatial heterogeneity favors diversification, including the emergence of biofilm-forming variants that colonize the air-liquid interface [57]. Although this system differs from a stirred continuous culture, it demonstrates how spatial niches can introduce selective pressures beyond those intended by the experimental design. In an OD-controlled turbidostat, wall-associated growth and aggregation are therefore potential complications both for population comparisons and for the measurement used to control dilution.

The first aim was to compare wild-type (WT) and IS-free (ΔIS) strains during prolonged ethanol exposure in a small-scale turbidostat. Several experimental configurations were tested, including constant ethanol concentrations and growth-dependent increases in ethanol concentration. These experiments showed that the device could maintain and dilute cultures, but they also revealed recurrent cross-contamination between vials and the formation of soft cell aggregates on the vial walls. These technical problems prevented a reliable long-term comparison of independent populations.

A second set of experiments therefore used daily pin replication in 96-well plates. Independent cultures of WT and ΔIS strains carrying fluorescent markers were exposed to gradually increasing NaCl or n-butanol concentrations. Frozen populations from selected time points were later tested after one day of growth without stress. In the well-plate experiments, growth was observed at high NaCl and n-butanol concentrations during selection, but this

growth advantage was not clearly retained after the populations were recovered without stress.

## *3.2 Results and discussion*

### 3.2.1 Continuous ethanol exposure in the turbidostat was limited by recurrent cross-contamination

The Replifactory turbidostat contains seven culture vials with automated stirring, optical-density measurements, medium addition and waste removal (Figure 13; [58]). This configuration was selected to maintain several independently evolving populations under similar conditions. Two ethanol-selection strategies were tested. In the first, a constant ethanol concentration was supplied from one medium reservoir. In the second, ethanol-free LB and LB containing 10% (v/v) ethanol were mixed in proportions determined by the measured growth response. The conditions and outcomes of the individual runs are summarized in Table 6.

The OD profiles were interpreted by distinguishing gradual increases caused by culture growth from abrupt decreases caused by dilution. When the OD reached the dilution threshold, fresh medium was added and an equivalent volume of culture was removed, approximately halving the OD. Continued growth therefore produced a repeating sawtooth pattern: OD increased between dilution events and dropped sharply after each dilution (Figure 14A). At a fixed dilution threshold and dilution volume, longer intervals between successive dilution events indicated slower culture growth.

Increasing the ethanol concentration often slowed growth, visible as smaller increases in OD and longer intervals between dilution events. In the example shown in Figure 14B, growth slowed after the increase to approximately 4.9% ethanol and subsequently recovered, as indicated by the return of more frequent growth-dilution cycles. This illustrates temporary inhibition followed by recovery during continued ethanol exposure; it does not by itself establish heritable adaptation. Small concentration increases, for example a multiplication factor of 1.04, were generally more stable than large increases. A concentration multiplication factor of 1.33 combined with a rescue concentration decrease produced repeated oscillations between inhibition and recovery rather than a steady increase in tolerance (Table 6).

The main limitation was cross-contamination between culture vials. The first sign was a change in the size of the OD decrease following dilution. Whereas dilution with cell-free medium normally approximately halved the OD, affected cultures often showed alternating normal and smaller decreases, with the smaller decreases approximately half the expected magnitude (Figure 14C). Incoming medium containing cells could produce a smaller decrease because it would introduce cells while diluting the culture. However, this OD pattern alone could not establish contamination, because aggregation also affected OD measurements. Growth in an uninoculated control vial provided additional evidence of contamination (Figure 14D), and subsequent fluorescence-based checks confirmed transfer between cultures. The

medium reservoirs remained visibly clear, suggesting contamination within the vial and supply-line system.

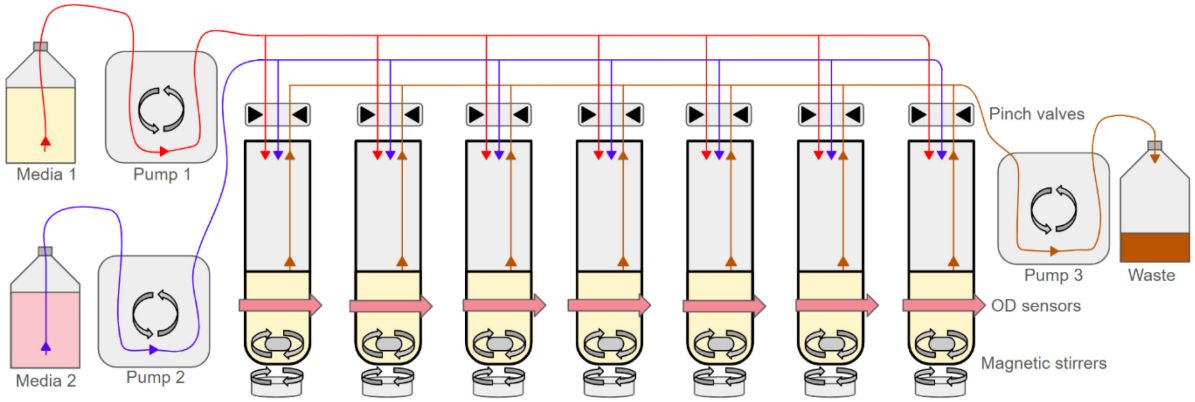



***Figure 13. Diagram of the Replifactory turbidostat system.*** *The system consists of seven independently maintained culture vials equipped with magnetic stirrers and optical density sensors. Two medium reservoirs supply fresh medium through separate peristaltic pumps, allowing the composition of the supplied medium to be adjusted by varying the mixing ratio. Pinch valves control medium delivery to individual vials, while a third pump removes excess culture into a waste container.*

A second recurring observation was the formation of soft, opaque material on the inner vial wall. This material readily detached and resuspended when stirring was stopped and vials were shaken. We therefore describe it as loosely attached aggregates, in contrast to the firmly attached biofilms observed in a later run, described below. The composition of the aggregates was not characterized. Cell aggregation made OD measurements unreliable. Because OD measurements controlled dilution, aggregation could also have affected dilution timing. Preferential retention of wall-associated cells could additionally have altered their residence time relative to suspended cells. In *E. coli* chemostats, wall populations have been shown to continually release cells into the medium, allowing strains that were less competitive in the liquid phase to persist [55]. Such a process could confound population comparisons because persistence would reflect wall-associated growth and retention as well as growth in suspension. Affected runs therefore could not provide a reliable comparison of adaptation between WT and ΔIS populations (Table 6).

In run 15, fluorescently labelled WT and ΔIS populations were grown at a constant ethanol concentration of 4.3% (v/v). Most vials developed visible biofilm formation that appeared much different from previously observed cell aggregation, as the material on the vial walls was firm and did not resuspend when vials were shaken. Two WT-yfp cultures did not show signs of cross-contamination and cell aggregate or biofilm formation. They were selected for population sequencing. One DNA sample was prepared from each population. Both populations contained the same set of seven called variants (Table 7). The occurrence of the same seven variants in two independent populations was unlikely to represent parallel mutation, which supports that cells were transferred between cultures.

| Run # | Duration, (days) | Strains | Starting EtOH | Selection setup | Culture dilution OD threshold | Purpose | Main outcome | Termination reason |
|---|---|---|---|---|---|---|---|---|
| 2 | 4 | WT | 4% | Increasing (x1.33 concentration increase) | 0.2 | Establish culture maintenance and concentration increase protocol | Culture maintenance and growth-dependent concentration increase works | Cross-contamination |
| 4 | 4 | WT | 4%, 4.25%, 4.5% | Constant | 0.3, 0.25, 0.2, 0.15 | Identify OD thresholds for EtOH concentrations allowing continuous culture maintenance | Identified working OD thresholds for concentrations. EtOH concentration (OD threshold): 4.0% (0.2); 4.25% (0.2); 4.5% (0.15) | Cross-contamination and aggregate formation |
| 5 | 3 | WT | LB; LB + 0.1% Tween 20 | Constant | 0.2 | Assess effect of Tween 20 addition on aggregate formation | Tween 20 is not useful against cell aggregate formation | - |
| 7 | 3 | WT | 3.80% | Increasing (x1.33 concentration increase; x1.67 rescue conc. decrease) | 0.2 | Establish adaptation to increasing concentrations | The setup with high concentration increase, and rescue concentration decrease values led to concentration fluctuations back and forth | - |
| 8 | < 1 | WT | 4% | Constant | 0.2 | Establish adaptation under constant stress | Did not maintain constant stress due to a bug in the code | Concentration was not maintained correctly due to bug in the updated software |
| 9 | 4 | WT | 3.80% | Increasing (x1.04 concentration increase) | 0.2 | Determine maximum selection concentration | Concentration increased up to 5.5% | Cross-contamination |
| 10 | 3 | FP-labeled WT ΔIS | 4.25% | Constant | 0.2 | Establish adaptation under constant stress | *E. coli* doubling time in 4.25% EtOH decreased from 40 to 18 min | Cross-contamination |
| 12 | 3 | FP-labeled WT ΔIS | 4.50% | Constant | 0.15 | Compare WT and ΔIS growth rate increase | Premature termination | Incorrect dilution frequency due to bug in the updated software |
| 13 | 3 | FP-labeled WT ΔIS | 3.80% | Increasing (x1.04 concentration increase) | 0.3 | Compare WT and ΔIS maximum selection concentration | Premature termination | Unstoppable recurrent dilutions due to bug in the updated software |
| 14 | 2 | FP-labeled WT ΔIS | 4.30% | Constant | 0.2 | Assess the effect of the stirrer RPM rate on cell aggregate formation | Aggregation does not occur at 3500 rpm/vortex reaching middle tube. Higher and lower RPMs lead to aggregation | - |
| 15 | 2 | FP-labeled WT ΔIS | 4.30% | Constant | 0.2 | Compare WT and ΔIS growth rate increase | Biofilm formation except 2 WT cultures. Detected mutations suggested cross-contamination | Cell aggregate formation |

| Run # | Duration, (days) | Strains | Starting EtOH | Selection setup | Culture dilution OD threshold | Purpose | Main outcome | Termination reason |
|---|---|---|---|---|---|---|---|---|
| 17 | 6 | FP-labeled WT ΔIS | 4.30% | Constant | 0.3 | Assess the dynamics of cross-contamination by plating fluorescent cells | Cross-contamination occurred after ~140h | Cross-contamination |
| 18 | 6 | FP-labeled WT ΔIS | 4.30% | Constant | 0.3 | Assess the effect of the media-feeding needle contact on cross-contamination | Cross-contamination occurred after ~140h. Tube shaking did not affect the dynamics | Cross-contamination |

***Table 6. Summary of turbidostat runs used to establish ethanol-selection conditions.*** *The table lists the strains, selection regime, OD threshold, duration and main observations for each run. FP labeled WT ΔIS - WT-yfp, WT-bfp, ΔIS-yfp, ΔIS-bfp. EtOH, ethanol.*

Ethanol exposure may itself have contributed to aggregate or biofilm formation. Lim et al. demonstrated that ethanol stimulated the production of curli, extracellular amyloid protein fibers that promote cell-cell and cell-surface adhesion and form part of the biofilm matrix in *E. coli* [59]. Under their tested conditions, increased curli production was accompanied by aggregation and enhanced biofilm formation. However, the mechanism responsible for the material observed here was not determined. The experiments also did not distinguish an environmentally induced response from heritable adaptation or establish whether aggregation increased ethanol tolerance.

Cross-contamination was examined more directly in two further runs by alternating YFP- and BFP-labelled strains between neighboring vials. Samples were streaked on agar plates and colonies were examined for fluorescence. Fluorescence inconsistent with the inoculated strain was detected at 140 h, whereas at 100 h it was still consistent with the inoculated strain (Figure 15A). To assess whether the contact of the culture with the media-feeding needle affects cross-contamination, in a subsequent run, we thoroughly shook vials at indicated time points (Figure 15B). Vigorous shaking of the vials did not change the timing of contamination.

Together, these trials showed that the turbidostat could maintain cultures and apply constant or dynamically changing ethanol concentrations over periods of a few days. However, independent multi-day evolution experiments were not reliable under the tested configurations because cross-contamination became detectable after approximately six days. The experiments were therefore not continued as a comparison of adaptation between WT and ΔIS populations.

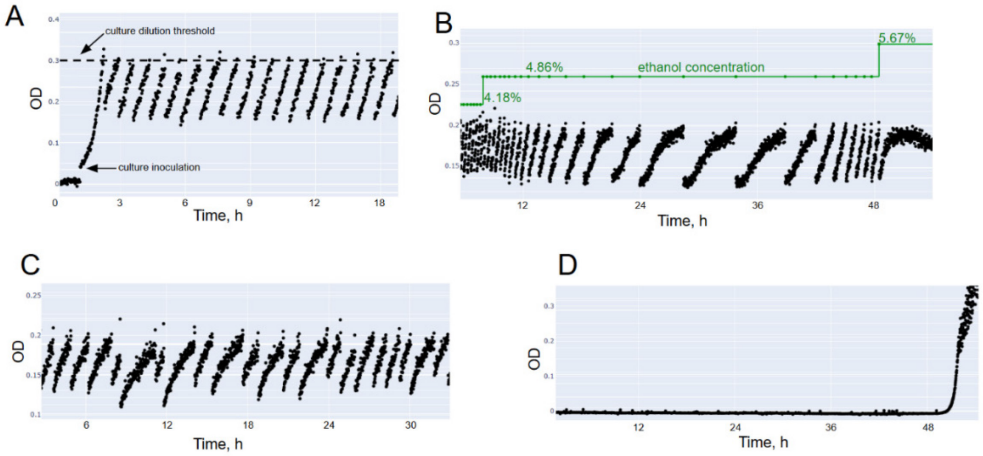



***Figure 14. Representative OD profiles illustrating culture maintenance, responses to ethanol exposure, and signs of contamination during turbidostat experiments.*** *Black points show OD measurements. (A) Normal growth-dilution cycles. OD rises as the culture grows. Reaching the dilution threshold (dashed line) triggers medium addition and culture removal, approximately halving the OD. (B) Response to increasing ethanol concentration, indicated by the green stepped line and percentage labels. Longer intervals between dilution events indicate slower growth; the subsequent return of more frequent cycles indicates recovery. (C) Irregular dilution responses. Some dilution events produce smaller OD decreases than expected for dilution with cell-free medium, suggesting possible introduction of cells through the medium supply. (D) OD remains near baseline before increasing sharply in an uninoculated control vial, indicating contamination. Panels show representative runs summarized in Table 6.*

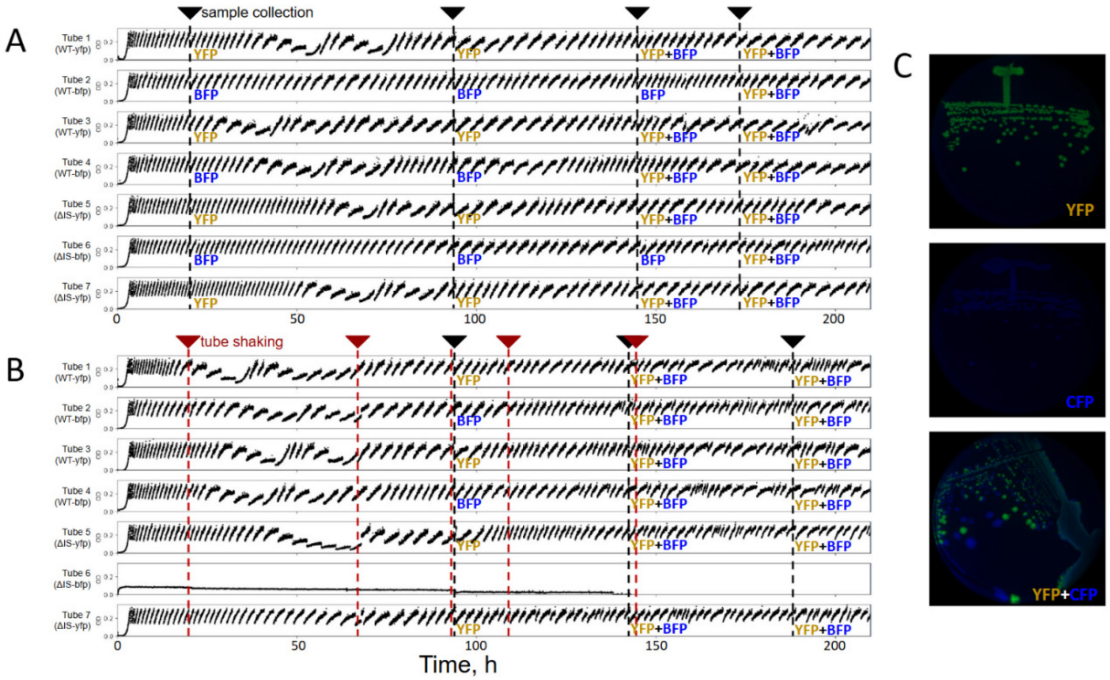



***Figure 15. Cross-contamination repeatedly appeared in turbidostat runs after approximately 6 days and was not affected by tube shaking.*** *YFP- and BFP-labelled WT and ΔIS strains were inoculated in alternating vials. OD profiles per vial are shown. Cultures were maintained in LB+4.3% (v/v) ethanol. Samples were collected and examined for fluorescence at time-points indicated by black arrows. Detected fluorescence of the colonies is indicated. In both runs, cross-contamination was detected at approximately 140 h. (A) First trial with no additional tube shaking. (B) Second run, where tubes were manually vigorously shaken at time-points indicated by red arrows to examine the effect of the contact of the culture with the media-feeding needle. Early shaking did not alter the time of cross-contamination occurrence. Vial 6 showed no growth as its stirrer had failed. (C) Representative plates demonstrating detected YFP-only, BFP-only, and YFP and BFP fluorescent cell containing cultures.*

| Replicate # | Mutation # | Type | Feature type | Gene | Effect | Product | Support (reads mutant / reads ancestral) |
|---|---|---|---|---|---|---|---|
| **1** | 1 | SNP | CDS | ampE | Val68= | protein AmpE | 469 / 5 |
| | 2 | SNP | non-coding DNA | | nt position: 121792 | | 500 / 0 |
| | 3 | SNP | CDS | intF | Glu203= | putative phage integrase | 161 / 0 |
| | 4 | Deletion | multiple CDS | | nt position: 696753. deletion 109 bp | | 109 / 0 |
| | 5 | SNP | CDS | cdgI | Gly49= | putative c-di-GMP binding protein CdgI | 513 / 0 |
| | 6 | SNP | CDS | yohK | Leu34= | putative 3-hydroxypropanoate export protein YohK | 453 / 0 |
| | 7 | MNP | rRNA | rrlD | Non-coding transcript variant | 23S ribosomal RNA | 434 / 0 |
| **2** | 1 | SNP | CDS | ampE | Val68= | protein AmpE | 286 / 2 |
| | 2 | SNP | non-coding DNA | | nt position: 121792 | | 294 / 0 |
| | 3 | SNP | CDS | intF | Glu203= | putative phage integrase | 92 / 0 |
| | 4 | Deletion | multiple CDS | | nt position: 696753. deletion 109 bp | | 45 / 0 |
| | 5 | SNP | CDS | cdgI | Gly49= | putative c-di-GMP binding protein CdgI | 315 / 0 |
| | 6 | SNP | CDS | yohK | Leu34= | putative 3-hydroxypropanoate export protein YohK | 279 / 2 |
| | 7 | MNP | rRNA | rrlD | Non-coding transcript_variant | 23S ribosomal RNA | 277 / 0 |

***Table 7. Variants called in two WT-yfp populations from turbidostat run 15.*** *One population DNA sample was analyzed per culture. The same seven variants were detected in both samples, supporting cross-contamination between the populations.*

### 3.2.2 No detectable adaptation to butanol and NaCl

To avoid the cross-contamination observed in the turbidostat, adaptation was next tested by daily pin replication in 96-well plates, where populations were maintained in separate wells. Four fluorescently labelled strains were used: WT-yfp, WT-bfp, ΔIS-yfp and ΔIS-bfp. For each strain, 15 independent cultures were started from separate colonies, giving 60 inoculated wells per plate. The outer wells contained medium only and served as contamination controls. Three plates were serially transferred in parallel: a stress-free control plate, a plate with increasing NaCl and a plate with increasing n-butanol (Figure 16A).

The experiment lasted 12 days. Day 0 cultures were grown from colonies without stress. On days 1-11, cultures were exposed to the stress and transferred every 24 h with a pin replicator. Approximately 0.2 µL was transferred into 200 µL of fresh medium, corresponding to a nominal 1:1000 dilution. A copy of each plate was frozen daily. The cultures were grown in M9 medium containing 0.4% glucose at 37°C, and optical density was measured before each transfer.

NaCl exposure started at 300 mM and increased by 50 mM per day. The measured minimum inhibitory concentration (MIC) of the ancestral strains was 500 mM. If applied directly from inoculation, this concentration was expected to yield endpoint OD below 0.05 (rather than necessarily zero, according to the threshold-based MIC determination procedure), as observed in all replicates of the four labelled ancestral strains in preliminary dose-response assays (Supplementary Figures 4, 5). Mean optical density decreased as the concentration increased, but growth remained detectable for approximately two transfers beyond the initial MIC (Figure 16C). The ΔIS cultures showed an earlier decline in growth than the WT cultures.

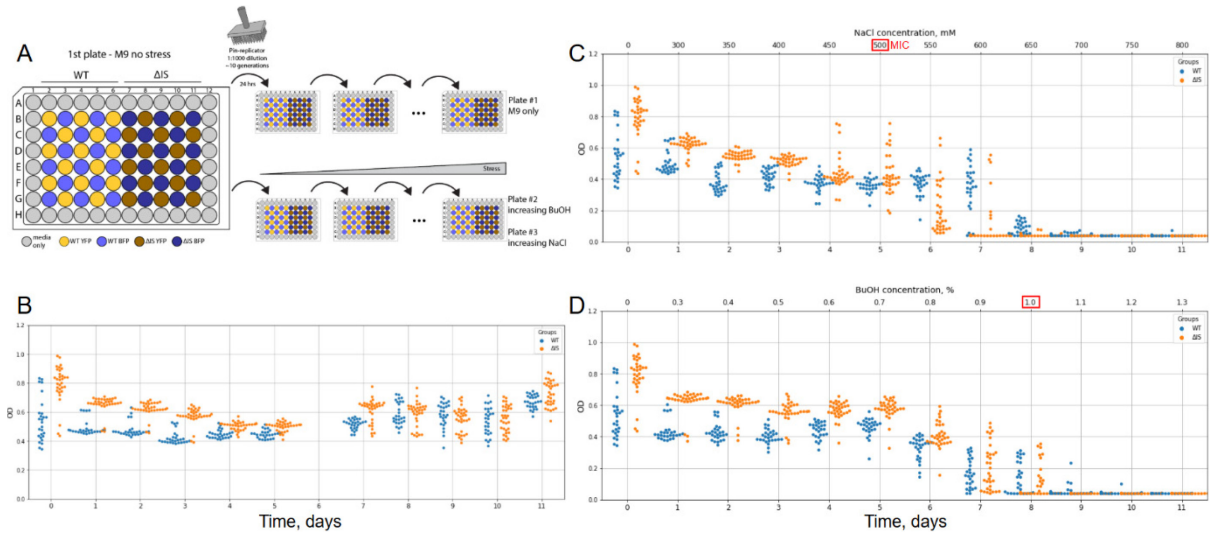


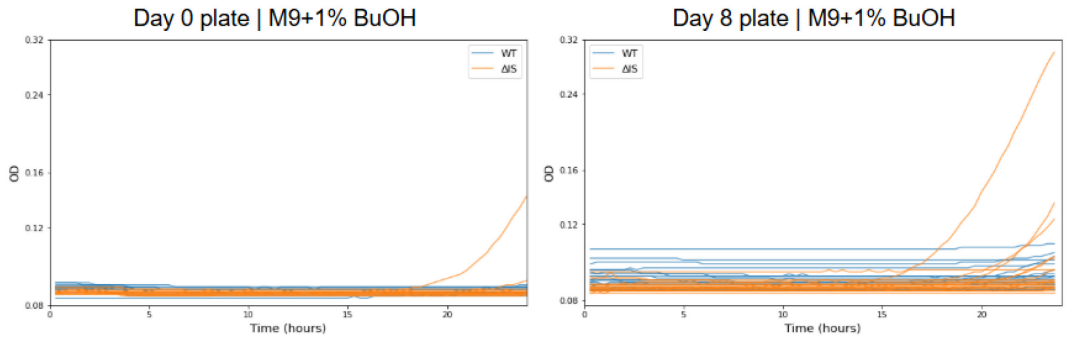

***Figure 16. Pin-replication experiments with increasing NaCl and butanol concentrations.*** *(A) Experimental design and 96-well plate layout. Fifteen independent cultures of each of four strains were arranged in a checkerboard pattern. Outer wells contained medium only. Cultures were daily transferred. (B) Optical density of cultures propagated without stress. (C-D) Ancestral MICs are indicated in red: 500 mM NaCl and 1.0% butanol. Points represent individual wells, colors represent WT (blue) and ΔIS (orange) backgrounds. (C) Optical density during exposure to NaCl, starting at 300 mM and increasing by 50 mM per day. (D) Optical density during exposure to butanol, starting at 0.3% (v/v) and increasing by 0.1% (v/v) per day.*

Butanol exposure started at 0.3% (v/v) and increased by 0.1% (v/v) per day. The ancestral MIC was 1.0% (v/v). Direct exposure from inoculation at this concentration likewise yielded OD below 0.05 in all replicates of the four labelled ancestral strains (Supplementary Figures 4, 5). Cultures retained measurable growth as the concentration approached the MIC, but little growth was detected above it (Figure 16D). The stress-free control plate maintained growth throughout the experiment (Figure 16B), showing that the daily transfer itself supported continued propagation.

To test whether growth at high stress was retained after removal of the stress, frozen populations were revived from the selected plates. NaCl populations from day 7, which had been exposed to 600 mM NaCl, and butanol populations from day 8, which had been exposed to 1.0% n-butanol, were compared with their corresponding day 0 populations. Frozen cultures were first pin-replicated into stress-free M9 medium and incubated for 24 h at 37°C. This stress-free growth step was included to distinguish stable adaptation from a temporary physiological response.

After recovery, the butanol populations were transferred to M9 medium containing 1.0% butanol and OD growth curves were recorded for 24 h. Day 8 populations did not show a substantial general improvement relative to day 0 populations, and most populations showed little or no growth (Figure 17A). A few wells showed apparent rescue. However, endpoint optical density on the original day 8 plate depended strongly on well position (Figure 17B). This pattern was consistent with a plate effect, potentially involving evaporation or aeration, and made the butanol assay unsuitable for a robust comparison of adaptation.

A




B

| | 1 | 2 | 3 | 4 | 5 | 6 | 7 | 8 | 9 | 10 | 11 | 12 |
|---|---|---|---|---|---|---|---|---|---|---|---|---|
| A | 0.038 | 0.039 | 0.038 | 0.04 | 0.038 | 0.038 | 0.038 | 0.038 | 0.038 | 0.038 | 0.038 | 0.041 |
| B | 0.039 | 0.274 | 0.159 | 0.038 | 0.038 | 0.038 | 0.037 | 0.038 | 0.039 | 0.04 | 0.116 | 0.039 |
| C | 0.038 | 0.235 | 0.045 | 0.04 | 0.038 | 0.04 | 0.038 | 0.038 | 0.038 | 0.039 | 0.054 | 0.038 |
| D | 0.039 | 0.143 | 0.076 | 0.039 | 0.05 | 0.065 | 0.039 | 0.039 | 0.039 | 0.038 | 0.047 | 0.038 |
| E | 0.039 | 0.24 | 0.17 | 0.039 | 0.038 | 0.084 | 0.039 | 0.041 | 0.039 | 0.039 | 0.086 | 0.039 |
| F | 0.039 | 0.265 | 0.289 | 0.182 | 0.104 | 0.091 | 0.152 | 0.101 | 0.137 | 0.122 | 0.192 | 0.039 |
| G | 0.048 | 0.297 | 0.142 | 0.291 | 0.311 | 0.289 | 0.354 | 0.34 | 0.331 | 0.283 | 0.265 | 0.039 |
| H | 0.039 | 0.04 | 0.039 | 0.039 | 0.039 | 0.04 | 0.039 | 0.039 | 0.039 | 0.041 | 0.039 | 0.039 |

C

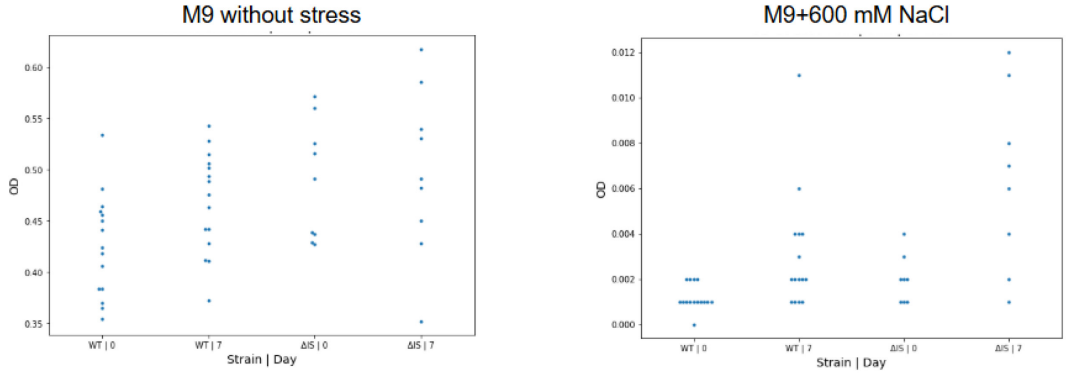



***Figure 17. Validation of growth after selection in butanol and NaCl.*** *Frozen populations were first recovered for 24 h in stress-free M9. (A) Growth during 24 h in M9+1.0% (v/v) butanol for day 0 and day 8 butanol-exposed WT and ΔIS populations. (B) Endpoint optical density by well position from the original day 8 butanol selection plate, showing a strong positional effect. (C) Endpoint optical density of day 0 and day 7 NaCl-exposed WT and ΔIS populations in stress-free M9 or M9 supplemented with 600 mM NaCl. NaCl-treated cultures remained close to the lower limit of reliable optical-density measurement.*

For the NaCl validation, recovered cultures were grown either without stress or with 600 mM NaCl. At 600 mM NaCl, both day 0 and day 7 populations reached only very low endpoint optical densities, close to the measurement limit and at most approximately 1% of the WT carrying capacity in stress-free M9 medium (Figure 17C). Therefore, the small difference

between time points was not considered as biologically meaningful evidence of stable adaptation. Thus, the earlier observed growth decline of ΔIS populations during serial transfer may be related to higher NaCl tolerance of the ancestral WT strain and does not by itself demonstrate more efficient adaptation of WT populations.

### 3.2.3 Concluding remarks

The experiments described in this chapter did not provide a reliable test of whether IS elements improve adaptation to complex stress environments. The turbidostat maintained cultures and applied ethanol selection, but cross-contamination between vials became detectable after approximately six days. The pin-replication experiments avoided contamination problems related to an interconnected liquid system, but apparent growth at high NaCl or butanol concentrations was not retained after recovery of the populations for one day without stress.

Unsuccessful or inconclusive experimental evolution studies are rarely reported. A comprehensive review citing 697 experimental evolution studies did not identify studies reporting an absence of adaptation [27]. Although these results do not show that adaptation to these stresses is impossible, they demonstrate the importance of distinguishing stable adaptation from temporary physiological responses and technical effects. The limitations faced in these experiments motivated the switch to daily serial transfer in physically separate culture tubes under antibiotic selection, as described in the previous chapter.

## *3.3 Materials and methods*

### 3.3.1 Bacterial strains

All *E. coli* strains used in this study were obtained from the laboratory collection. The WT-yfp, WT-bfp, ΔIS-yfp, and ΔIS-bfp strains were constructed previously in our laboratory by Roderich Roemhild (manuscript in preparation). The turbidostat experiments used the WT MG1655, WT-yfp, WT-bfp, ΔIS-yfp and ΔIS-bfp *E. coli* strains. The pin-replication experiments used WT-yfp, WT-bfp, ΔIS-yfp and ΔIS-bfp *E. coli* strains.

| Strain | Genotype |
|---|---|
| WT (MG1655) | *E. coli* K-12 F– λ– *ilvG*– *rfb*-50 *rph*-1 |
| WT-yfp | *E. coli* MG1655 ΔglnW ptsS/glmS::cat-J23101-SYFP2 |
| WT-bfp | *E. coli* MG1655 ΔglnW ptsS/glmS::cat-J23101-mtagBFP2 |
| ΔIS-yfp | *E. coli* MG1655 arsB-mut* mdtH-mut* creC-mut* ΔIS3ABCDE ΔIS2ADEFHIK ΔIS150 ΔIS911AB ΔIS600 ΔISX ΔIS30ABCD ΔIS609 ΔISZ ΔIS4 ΔIS186ABC ΔIS5ABDIFYKLoRTH ΔIS1ABCDEFH ptsS/glmS::cat-J23101-SYFP2 |
| ΔIS-bfp | *E. coli* MG1655 arsB-mut* mdtH-mut* creC-mut* ΔIS3ABCDE ΔIS2ADEFHIK ΔIS150 ΔIS911AB ΔIS600 ΔISX ΔIS30ABCD ΔIS609 ΔISZ ΔIS4 ΔIS186ABC ΔIS5ABDIFYKLoRTH ΔIS1ABCDEFH ptsS/glmS::cat-J23101-mtagBFP2 |

### 3.3.2 Media and growth conditions

Turbidostat cultures were grown in lysogeny broth (LB) supplemented with the indicated concentration of ethanol. Pin-replication cultures were grown in M9 minimal medium supplemented with 0.4% glucose. Unless stated otherwise, cultures were incubated at 37°C.

### 3.3.3 Turbidostat device and evolution experiments

Continuous culture experiments were performed using a custom-built Replifactory turbidostat (model ISTA1; Figure 13) developed and provided by Catalin Rusnac [58]. A turbidostat maintains cultures below a defined cell density by adding fresh medium and removing an equal volume of culture when a specified optical density threshold is reached. The device contained seven culture vials and separate pumps and silicone tubing for medium supply, dilution and waste removal. Tubing sections were joined using Luer connectors.

Two input reservoirs contained ethanol-free LB and LB supplemented with 10% (v/v) ethanol. This configuration allowed the supplied ethanol concentration to be adjusted by changing the mixing ratio of the two media. Depending on the experiment, the ethanol concentration was either kept constant or increased when the culture doubling time fell below 2 h (and kept constant for at least 5 culture doublings). Diluted culture was transferred to a waste container.

Culture vials were closed with rubber inserts fitted with stainless-steel needles for medium supply, waste removal and sampling. Samples were collected using sterile syringes, and the sampling ports were disinfected with 70% ethanol before and after sampling. The tubing and culture vial assemblies were autoclaved before each experiment.

Pump volumes and optical-density measurements were calibrated before use. Each vial contained 12 mL LB with the indicated ethanol concentration. Stirring was adjusted to produce a vortex extending approximately halfway down the liquid column. When the optical-density threshold was reached, the culture was diluted approximately 1:2 with fresh medium. The conditions used in individual experiments are summarized in Table 6.

### 3.3.4 Population DNA extraction, sequencing and variant calling

Population DNA was extracted from the two selected WT-yfp cultures from turbidostat run 15. DNA extraction and sequencing were performed as described in Chapter 2. Variants were called with Snippy v4.6.0 using the raw sequence reads and the corresponding reference genome with default settings for each strain.

### 3.3.5 Pin-replication evolution experiments

Ancestral MICs were estimated using a blank-corrected endpoint OD threshold of 0.05 (Supplementary Figure 4, Materials and Methods). The concentrations indicated in Figure 16 represent conservative common MIC estimates across the four fluorescently labelled ancestral strains.

Four strains were distributed across 96-well plates in a checkerboard arrangement. Each plate contained 15 independent cultures of WT-yfp, WT-bfp, ΔIS-yfp and ΔIS-bfp (60 total). The outer wells contained medium only. Three plates were propagated in parallel: one without stress, one with increasing NaCl and one with increasing n-butanol.

Cultures were transferred every 24 h with a calibrated pin replicator. The pins transferred approximately 0.2 µL into 200 µL of fresh medium, corresponding to ~1:1000 dilution and 10 generations. The experiment lasted 12 days. Day 0 was inoculated from independent colonies and grown without stress. Then, 11 daily transfers were performed under increasing stress concentrations. The NaCl concentration was 300 mM on day 1 and increased by 50 mM per day. The n-butanol concentration was 0.3% (v/v) on day 1 and increased by 0.1% (v/v) per day. OD was measured daily before transfer, and a copy of each plate was frozen at each time point.

For validation, frozen day 0 populations were compared with populations collected on day 7 after exposure to 600 mM NaCl or on day 8 after exposure to 1.0% n-butanol. All populations were first recovered for 24 h at 37°C in stress-free M9 medium. The butanol-treated populations and their day 0 controls were then tested in 1.0% n-butanol. The NaCl-treated populations and their day 0 controls were normalised to OD600 = 0.003 and tested in M9 with or without 600 mM NaCl.

# 4 Construction of strains to study the role of natural competence in adaptation

## *4.1 Introduction*

Unlike eukaryotes, bacteria reproduce asexually, but their evolution is not strictly clonal. DNA can move between cells by horizontal gene transfer mechanisms, including conjugation, transduction, and natural transformation. Horizontal gene transfer moves DNA not only between distant species, but can lead to homologous recombination within populations. When transferred DNA recombines with the chromosome, an allele can move from one genetic background to another. This is supported by population-genomic studies, which detect less linkage between loci than expected under strictly clonal evolution, and in many bacterial species recombination has been shown to introduce more sequence variation than mutation [60], [61], [62]. Thus, homologous recombination is common in bacteria, but it remains unclear whether recombination improves adaptation.

Natural transformation provides a suitable system for investigating the contribution of homologous recombination to bacterial adaptation. It involves the active uptake of extracellular DNA from the environment with subsequent integration into the genome [63]. The physiological state in which bacteria can be transformed is called natural competence.

The molecular mechanism of natural transformation is broadly conserved across Gram-positive and Gram-negative bacteria (Figure 18) [63]. In most characterized systems, extracellular double-stranded DNA is initially captured by type IV pili. The DNA is then brought into a compartment between the cell wall and cytoplasmic membrane in Gram-positive bacteria, or into the periplasm in Gram-negative bacteria, where it interacts with the DNA-binding protein ComEA. Subsequently, DNA is transported across the cytoplasmic membrane through the conserved membrane channel ComEC. During this process, one DNA strand is degraded, while the other enters the cytoplasm as single-stranded DNA. The incoming strand is protected by DprA, which also facilitates RecA loading and subsequent homologous recombination with the bacterial chromosome. An exception to the typical pilus-dependent uptake mechanism is found in *Helicobacter pylori*, which uses a type IV secretion system for DNA uptake [64].

The main differences in natural transformation between Gram-positive and Gram-negative bacteria arise from differences in their cell envelope architecture. In both groups, extracellular DNA is captured by type IV pilus-related structures [63]. In Gram-positive bacteria, such as *Bacillus subtilis*, retractile competence pili facilitate DNA transport across the thick peptidoglycan cell wall [65], bringing it into contact with membrane-anchored ComEA. In Gram-negative bacteria, such as *Haemophilus influenzae*, DNA must additionally cross the outer membrane through the secretin channel PilQ associated with the pilus machinery. Once in the periplasm, DNA interacts with ComEA. Unlike the membrane-anchored ComEA of Gram-positive bacteria, ComEA in characterized Gram-negative systems is a soluble periplasmic protein. Despite these differences, the core machinery involved in DNA transport across the cytoplasmic membrane and homologous recombination is broadly conserved. However, other aspects of natural transformation, including accessory

components of the DNA-uptake machinery, regulation of competence [20], and DNA-uptake specificity [66], vary among bacterial species.

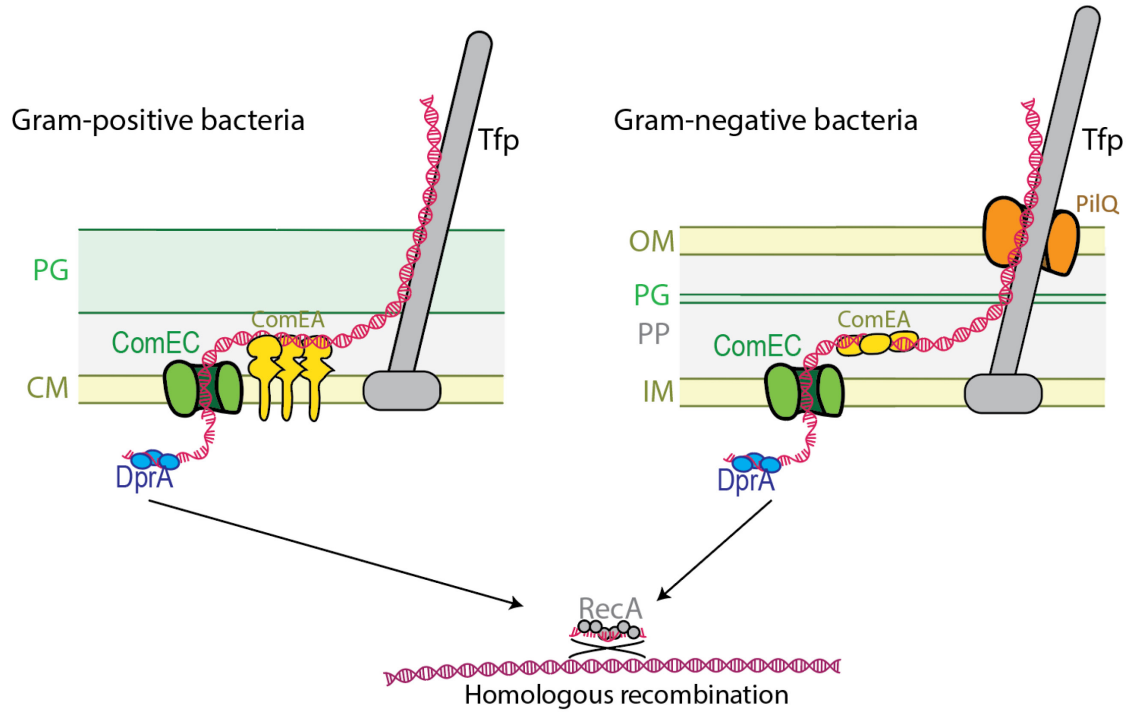



***Figure 18. Schematic representation of natural transformation in Gram-positive and Gram-negative bacteria.*** *Extracellular DNA is captured by transformation pili and transported across the cell envelope, where it interacts with ComEA. In Gram-positive bacteria, ComEA is membrane-anchored, whereas in Gram-negative bacteria it is located in the periplasm, and DNA uptake across the outer membrane occurs through the secretin PilQ. DNA is subsequently transported across the cytoplasmic membrane through ComEC, with one strand degraded during uptake. The incoming single-stranded DNA interacts with DprA, which facilitates RecA loading and subsequent homologous recombination with the bacterial chromosome. CM, cytoplasmic membrane; PG, peptidoglycan; OM, outer membrane; IM, inner membrane; PP, periplasm; Tfp, transformation pilus.*

Natural transformation has been demonstrated in more than 80 bacterial species across diverse bacterial taxa [20]. However, its real prevalence may be higher because competence is often induced only under specific conditions and varies between isolates. One genomic study identified a ComEC homologue in 96% of analyzed bacterial genomes [67], and another comparative analysis showed that homologs of the core competence proteins ComEC and DprA are conserved and mainly inherited vertically among diverse bacteria [20]. Therefore, natural transformation appears to be an ancient and widespread chromosomally encoded mechanism of horizontal gene transfer, making it a suitable model for studying the role of homologous recombination in bacterial adaptation.

### 4.1.1 Potential effect of natural transformation on adaptation

Homologous recombination caused by natural transformation may lead to the breakdown of linkage between alleles [68]. In a strictly clonal population, a beneficial mutation remains linked to every other allele in the genome in which it arose. If different beneficial mutations arise in different lineages, those lineages compete, and one useful mutation may be lost when

the other lineage fixes. Transformation can place both beneficial alleles into the same genome and may therefore increase the rate or extent of adaptation [69], [70], [71]. This benefit should be strongest when several beneficial mutations are present at the same time, for example in large populations, at high mutation supply, or during adaptation to a new or stressful environment [72].

Transformation may also separate a beneficial allele from linked deleterious mutations. Without recombination, selection for the beneficial allele can carry harmful passenger mutations to high frequency. Recombination can move the beneficial allele into a fitter background and reduce this genetic load [73]. At the population level, both processes are expected to reduce correlations among allele-frequency trajectories and to allow adaptive alleles to spread without a complete genome-wide selective sweep. Narrow, gene-specific sweeps have been inferred in environmental populations of *Vibrio cyclitrophicus* and *Sulfolobus* [74], [75] consistent with fixation of beneficial alleles without linkage constraints.

Competence is not expected to be beneficial in every environment. Producing the uptake machinery has a physiological cost, and imported DNA can disrupt favorable combinations of alleles or introduce deleterious variants [20], [22], [76]. Natural transformation may also be maintained for reasons other than evolutionary beneficial recombination, including the use of extracellular DNA as a nutrient or as a template for DNA repair [21], [77], [78]. Therefore, the total effect of competence on adaptation should depend on the availability and relatedness of donor DNA, the frequency and duration of the competent state, the supply of beneficial mutations, population size, and the strength of selection.

### 4.1.2 Experimental evidence and open questions

A few previous evolution experiments address the effect of genetic recombination on the adaptive capacity of bacteria. These studies compare the adaptation efficiency of recombination proficient and deficient genetic backgrounds.

One study compared recombination-proficient and recombination-deficient *Escherichia coli* populations adapting to standard laboratory conditions [79]. Recombination was enabled by chromosomal integration of the F plasmid. At the normal mutation rate, recombination-proficient populations did not adapt better than recombination-deficient populations. An advantage of recombination was detected only in *mutS* mutants, which had an artificially increased mutation rate. Under these conditions, many mutations arose simultaneously, increasing competition among beneficial mutations in different lineages. This result supports the idea that recombination becomes useful when the supply of beneficial mutations is high. However, the dependence on an artificial mutator background limits its relevance to populations with normal mutation rates. In addition, the recombination system was artificially introduced and did not represent a naturally competent bacterium. The study followed the frequency of one adaptive allele, but this provided only limited information about genome-wide allele dynamics.

Experiments with naturally competent bacteria produced variable results. In *Streptococcus pneumoniae*, transformation-proficient populations adapted better than transformation-

deficient populations under stressful conditions, whereas transformation-deficient populations performed better under benign conditions [80]. Naturally competent *Helicobacter pylori* also evolved higher fitness than a competence-deficient strain in one experimental system [81]. However, this work compared different isolates rather than otherwise similar backgrounds, which limits the conclusions of this study. Studies with *Acinetobacter baylyi* produced mixed results. In one study, competence increased fitness during exponential growth but reduced it during stationary phase, resulting in no overall fitness benefit [77]. Another study showed no benefit of transformation and found that transformability decreased during evolution [82].

Together, these studies show that the effect of recombination depends on mutation rate, environmental stress, and the physiological state of the population. However, each study examined only a limited set of conditions, and the results are difficult to compare across different organisms and experimental systems. Most studies measured adaptation rate or endpoint fitness but did not directly test whether transformation combined beneficial alleles from different lineages. Comparisons between competence-proficient and competence-deficient strains can also be affected by physiological differences between the backgrounds. Finally, genome-wide allele-frequency dynamics were generally not followed to determine how recombination changed associations among adaptive mutations.

Therefore, the first aim of the proposed project was a direct mechanistic proof-of-concept test. Two distinguishable *B. subtilis* lineages would each carry a different beneficial allele, represented by an antibiotic resistance cassette. The experiment would test whether natural transformation combines these two cassettes in the same genome and whether this allows competent populations to acquire double resistance earlier than competence-deficient populations. This design would provide direct proof that transformation can bring together beneficial mutations that originated in separate lineages.

The second aim was to compare changes in fitness over time between naturally competent and competence-deficient populations evolving under constant conditions. Measurements at several time points would determine whether competence changes the rate or final extent of adaptation. As a secondary and more ambitious objective, selected intermediate populations would be sequenced to follow mutation frequencies. Following an approach used to study meiotic sex in evolving yeast populations [83], associations among allele-frequency trajectories could indicate whether adaptive alleles remained linked to their original backgrounds or spread more independently in competent populations.

The evolution experiments were not initiated during this thesis. The completed work consisted of constructing and initially characterizing the strains required for these comparisons.

## *4.2 Experimental framework*

The proposed experiments required matched Com+ and Com- strains carrying distinguishable fluorescent markers and antibiotic-resistance cassettes at different chromosomal loci. The

same strain collection would support both the direct detection of recombination and the measurement of fitness during experimental evolution.

### 4.2.1 Model system and strain design

*Bacillus subtilis* was selected because natural competence is efficient and well characterized in this organism [20], [63], [84]. The central comparison would be between the naturally competent parental strain W168 (Com+) and an otherwise matched strain lacking competence membrane channel *comEC* (Com-). Deleting *comEC* blocks DNA uptake, leaving the upstream regulation of competence intact.

Two labelled strains would be required for the direct recombination experiment. The first strain would carry one fluorescent marker linked to a chloramphenicol-resistance cassette at the *amyE* locus. This construct could be integrated using pBS1C, which targets *amyE* and confers chloramphenicol resistance.

The second strain would carry a distinct fluorescent marker linked to a spectinomycin-resistance cassette at the *thrC* locus, which is located distantly from *amyE*. This construct could be generated using pBS4S, which targets *thrC* and confers spectinomycin resistance [85]. Both labelled strains would be produced in Com+ and Com- versions. Integration at separate loci would allow both marker-resistance cassettes to be combined in the same genome by transformation.

### 4.2.2 Direct detection of recombination

The two labelled strains would be introduced at low frequencies into a larger, otherwise unlabelled ancestral population with the same competence background. Com+ labelled strains would be introduced into W168 populations, while Com- labelled strains would be introduced into Δ*comEC* populations. Both groups would be propagated under constant sublethal concentrations of chloramphenicol and spectinomycin.

Samples would be collected and plated at several time points on medium containing high concentrations of both antibiotics to select for cells carrying both resistance cassettes. A colony displaying both fluorescent markers would be expected to contain both chromosomal integrations and would therefore represent a candidate recombinant. The linked fluorescent markers would help distinguish recombination from double resistance arising through spontaneous mutations. A cell that acquired resistance to both antibiotics through mutation would not acquire both fluorescent markers. The primary readouts would be the time at which double-fluorescent, double-resistant colonies first appeared and their frequency in Com+ and Com- populations. This would allow us to test whether natural competence speeds up adaptation by recombination of beneficial alleles under these conditions.

### 4.2.3 Fitness trajectories during adaptation

The second experiment would compare replicate Com+ and Com- populations evolving under constant conditions. At regular time points, fitness would be measured by competition against an otherwise isogenic ancestral reference strain carrying an alternative fluorescent marker. The primary readouts would be the rate of fitness increase and the final fitness reached by the Com+ and Com- populations.

As a secondary objective, populations at selected time points would be sequenced to identify occurred mutations. Associations among these trajectories would be compared between Com+ and Com- populations. Strongly correlated trajectories would suggest that mutations remained linked within the same propagating lineage. More independent trajectories in competent populations could be consistent with transformation moving alleles between genetic backgrounds.

## *4.3 Results and discussion*

### 4.3.1 Construction of the Δ*comEC* strain

One of the required strains for the proposed experimental system was a competence-deficient strain. The *comEC* gene of wild-type *B. subtilis* W168 was replaced with a kanamycin-resistance cassette using long-flanking homology PCR. The assembled replacement fragment was transformed into W168 to replace *comEC*. The Δ*comEC*::*kanR* genotype was verified by colony PCR.

This construction produced the Com- background required for comparison with naturally competent W168. Transformation efficiency of the Δ*comEC* strain was not measured, and the loss of competence needs to be quantitatively confirmed before using the strain in the subsequent experiments. The fluorescent and resistance-marker integrations would also need to be introduced into this background to produce the final Com- strains.

### 4.3.2 Construction and testing of fluorescent strains

A panel of integrative plasmids was assembled using pBS1C as the backbone (Table 9). This vector integrates at the *amyE* locus and carries a chloramphenicol-resistance cassette. It was combined with genes coding for different fluorescent proteins under the control of *PliaI*, *PxylA*, or *PliaG*. The resulting plasmids were transformed into the wild-type *B. subtilis* strain W168 to integrate the combinations of promoters and fluorescent markers into the chromosome.

The bacitracin-inducible promoter P*liaI* was initially tested because inducible expression was expected to reduce the fitness cost of fluorescent markers during growth in liquid culture. Strains carrying BFP, GFP, YFP, or RFP under the control of P*liaI* produced clear fluorescence after bacitracin induction in liquid LB medium (Figure 19A). For each fluorophore,

fluorescence was more than one order of magnitude above the signal measured for W168 at the corresponding excitation and emission wavelengths.

However, the same strains did not produce clear fluorescence on bacitracin-containing agar (Figure 19B). Only the P*liaI*-YFP strain showed a weak visible signal. Testing additional bacitracin concentrations and batches did not improve colony fluorescence (data not shown). P*liaI* was therefore unsuitable for the proposed competition fitness assays and detection of recombinants.

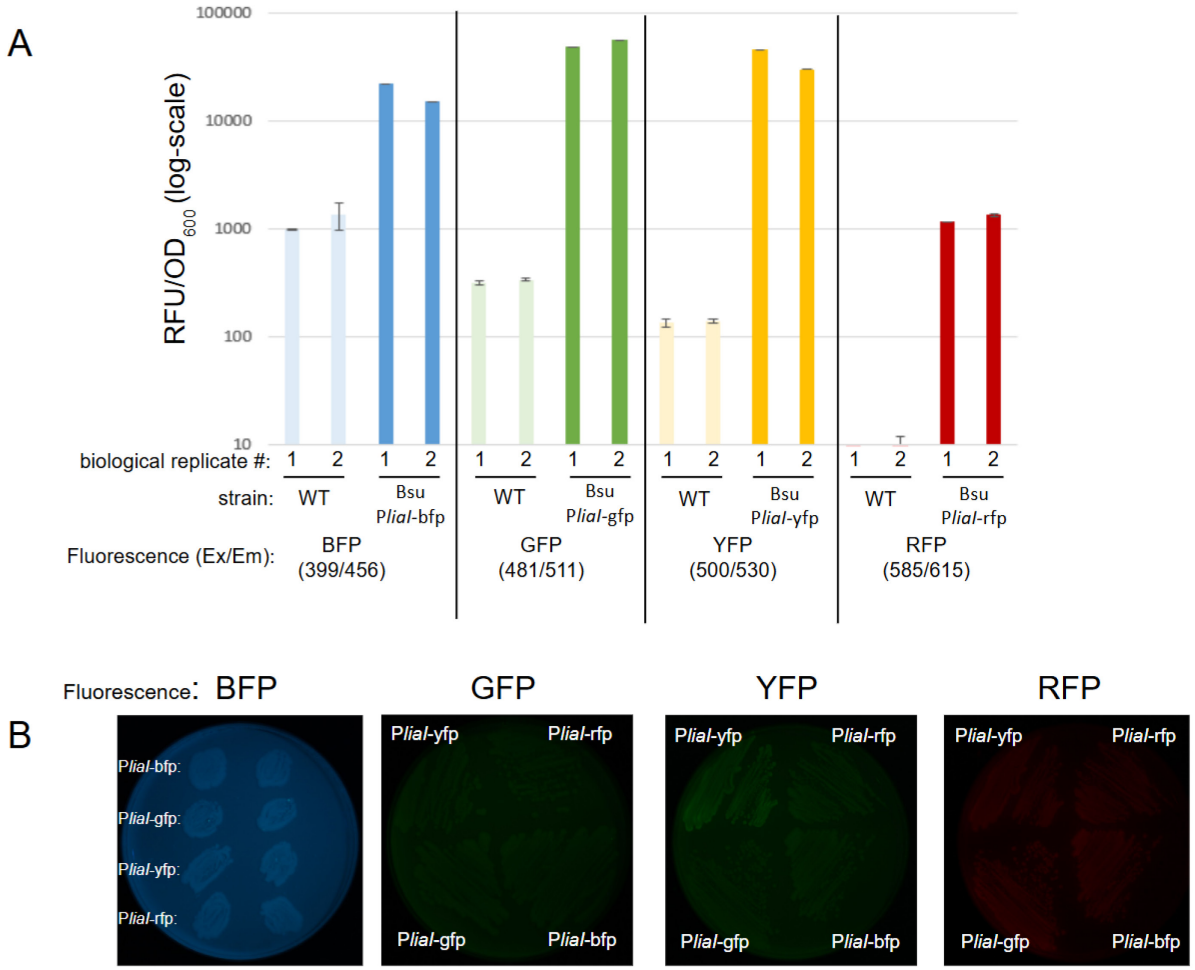



***Figure 19. Bacitracin-inducible fluorescent markers produced strong signals in liquid medium but weak signals on solid medium.*** *(A) Endpoint fluorescence of B. subtilis W168 and strains carrying BFP, GFP, YFP, or RFP under PliaI control after induction in liquid LB. Normalized to OD600, measured at the indicated excitation/emission settings. Two biological replicates per strain, three technical replicates per biological replicate. Mean ± SD per strain. (B) The four PliaI marker strains were streaked on LB agar containing 30 µg/mL bacitracin and imaged in the indicated channels. Only the PliaI-YFP strain showed a weak visible signal.*

Because P*liaI* did not enable colony identification, fluorescent proteins were also cloned under the xylose-inducible promoter P*xylA* and the constitutive promoter P*liaG*. Both promoters showed visible fluorescence on agar plates (Figure 20). P*xylA*-YFP showed some background fluorescence without added xylose, but its signal strongly increased after induction with 0.5% xylose (Figure 20A,B). P*liaG*-YFP showed constitutive fluorescence. P*xylA*-GFP and P*xylA*-RFP colonies could be distinguished when the strains were grown together on

xylose plates and the green and red fluorescence channels were merged (Figure 20C), showing that differently labelled colonies can be distinguished on the same plate.

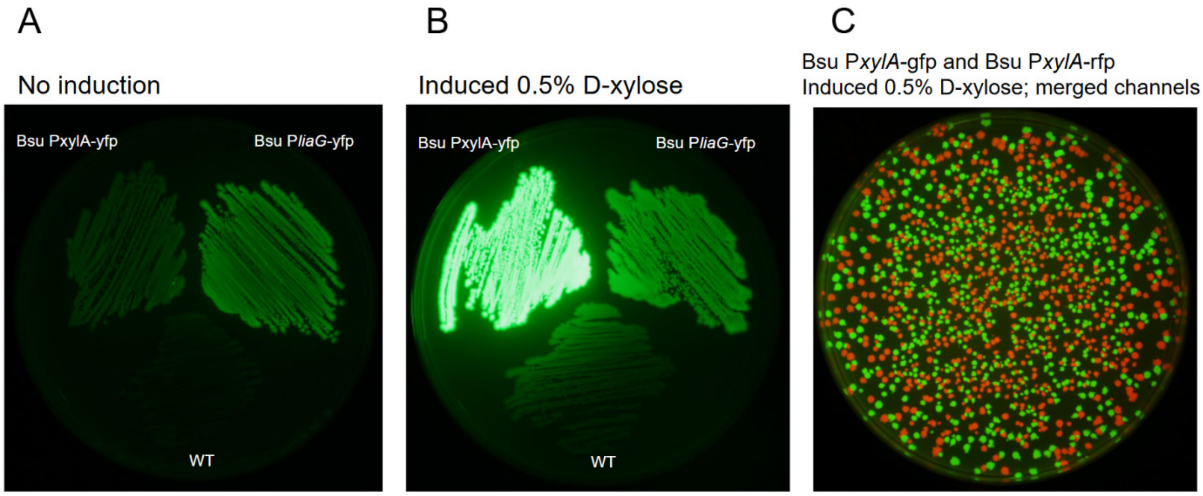



***Figure 20. Fluorescent marker expression on agar plates.*** *(A) W168, Bsu PxylA-YFP, and Bsu PliaG-YFP without xylose induction. (B) The same strains on a plate with 0.5% D-xylose induction. (C) Merged green and red fluorescence channels from a trial plate competition fitness assay containing a mixture of Bsu PxylA-GFP and Bsu PxylA-RFP colonies grown with 0.5% D-xylose.*

### 4.3.3 Progress toward the proposed experimental system

The completed work established two components of the proposed system: a genotypically verified Δ*comEC* background and fluorescent, chloramphenicol resistant strains carrying the markers at *amyE*. In addition, the promoter tests identified P*xylA* as the most suitable tested promoter for distinguishing *B. subtilis* colonies on agar plates.

The second strain required for the direct recombination detection experiment was not constructed. This strain would carry a distinct fluorescent marker linked to spectinomycin resistance at *thrC* and could be generated using pBS4S using similar methodology. The *comEC* gene would then need to be deleted from the *amyE* and *thrC* integrant strains. The resulting strains would require tests of transformation efficiency, marker stability, resistance, and relative fitness.

The linked resistance and fluorescence markers would provide a useful readout of recombination. Double-antibiotic selection would identify cells with double resistance, while fluorescence in both channels would distinguish candidate recombinants from cells that acquired resistance through mutation.

No direct recombination or experimental-evolution experiment was initiated. Consequently, recombinant frequencies, fitness trajectories, and allele-frequency dynamics were not measured. The completed strains provided a starting point for the proposed experiments but did not test whether natural competence affects adaptation.

## *4.4 Materials and methods*

### 4.4.1 Bacterial strains, plasmids, and primers

The bacterial strains (Table 8) and plasmids (Table 9) used and constructed in this study are listed below. All the constructed strains were derived from *B. subtilis* W168. The primers used in this study are listed in Table 10. The commercial *E. coli* NEB 5-alpha strain was used for plasmid propagation. The source plasmids used for cloning were obtained from the Bacillus Genetic Stock Center (Columbus, Ohio, USA) or from the laboratory collection.

| Name | Genotype | Description | Source |
|---|---|---|---|
| W168 | *B. subtilis* trpC2 | Wild-type *B. subtilis* strain | Lab collection |
| Bsu PliaI-bfp | *B. subtilis* W168 amyE::PliaI-mTagBFP_Bsu cam | Bsu with optimized BFP under bacitracin promoter in amyE | This study |
| Bsu PliaI-gfp | *B. subtilis* W168 amyE::PliaI-GFPmut1 cam | Bsu with GFP under bacitracin promoter in amyE | This study |
| Bsu PliaI-yfp | *B. subtilis* W168 amyE::PliaI-SYFP2 cam | Bsu with SYFP under bacitracin promoter in amyE | This study |
| Bsu PliaI-rfp | *B. subtilis* W168 amyE::PliaI-mCherry_Bsu cam | Bsu with optimized mCherry under bacitracin promoter in amyE | This study |
| Bsu PliaG-yfp | *B. subtilis* W168 amyE::PliaG-SYFP2 cam | Bsu with SYFP under a constitutive promoter in amyE | This study |
| Bsu xylA-yfp | *B. subtilis* W168 amyE::PxylA-SYFP2 cam | Bsu with SYFP under xylose promoter in amyE | This study |
| Bsu xylA-bfp | *B. subtilis* W168 amyE::PxylA-mTagBFP_Bsu cam | Bsu with optimized BFP under xylose promoter in amyE | This study |
| Bsu xylA-gfp | *B. subtilis* W168 amyE::PxylA-GFPmut1 cam | Bsu with GFP under xylose promoter in amyE | This study |
| Bsu xylA-rfp | *B. subtilis* W168 amyE::PxylA-mCherry_Bsu cam | Bsu with optimized mCherry under xylose promoter in amyE | This study |
| Bsu Δ*comEC* | *B. subtilis* W168 Δ*comEC*::kanR | Bsu with natural competence channel *comEC* gene deletion | This study |

***Table 8. B. subtilis strains used or generated in this study.***

| Plasmid | Description | Source |
|---|---|---|
| pBS1C | Backbone for Bsu amyE integration chloramphenicol resistance | Lab collection |
| pSB1C3-mTagBFP_Bsu | source plasmid for mTagBFP | Bacillus Genetic Stock Center |
| pSB1C3-GFPmut1 | source plasmid for GFPmut1 | Bacillus Genetic Stock Center |
| pSB1C3-SYFP2 | source plasmid for SYFP2 | Bacillus Genetic Stock Center |
| pSB1C3-mCherry_Bsu | source plasmid for mCherry_Bsu | Bacillus Genetic Stock Center |
| pSB1C3-PliaI | source plasmid for PliaI bacitracin inducible promoter | Lab collection |
| pSB1C3-PliaG | source plasmid for PliaG (constitutive promoter) | Lab collection |
| pSB1C3-PxylA | source plasmid for PxylA (xylose inducible promoter) | Lab collection |
| pDG780 | kanamycin cassette for long-flanking homology PCR in Bsu | Bacillus Genetic Stock Center |

| Plasmid | Description | Source |
|---|---|---|
| pBS1C-PliaI-mTagBFP_Bsu | Integration into amyE bacitracin inducible expression of mTagBFP_Bsu in Bsu | This study |
| pBS1C-PliaI-GFPmut1 | Integration into amyE bacitracin inducible expression of GFPmut1 in Bsu | This study |
| pBS1C-PliaI-SYFP2 | Integration into amyE bacitracin inducible expression of SYFP2 in Bsu | This study |
| pBS1C-PliaI-mCherry_Bsu | Integration into amyE bacitracin inducible expression of mCherry_Bsu in Bsu | This study |
| pBS1C-PliaG-SYFP2 | Integration into amyE, constitutive expression of SYFP in Bsu | This study |
| pBS1C-PxylA-SYFP2 | Integration into amyE, xylose-inducible expression of SYFP in Bsu | This study |
| pBS1C-PxylA-GFPmut1 | Integration into amyE, xylose-inducible expression of GFPmut1 in Bsu | This study |
| pBS1C-PxylA-mCherry_Bsu | Integration into amyE, xylose-inducible expression of mCherry_Bsu in Bsu | This study |

***Table 9. Plasmids used or generated in this study.***

| Name | Sequence | Purpose |
|---|---|---|
| amyE-seq-Fwd | AAAGGTCATTGTTGACGCGG | Sanger sequencing of amyE locus integration, and colony-PCR verification |
| amyE-seq-Rev | atcatcgctcatccatgtc | Sanger sequencing of amyE locus integration |
| mTagBFP_Bsu-check-Rev | CAGTTTATGGCCCAGTTTTG | colony-PCR verification of BFP integrated strains |
| GFPmut1-check-Rev | GTAGAGCTCATCCATGCCATG | colony-PCR verification of GFP integrated strains |
| SYFP2-check-Rev | atacagctcatccatacccagg | colony-PCR verification of YFP integrated strains |
| LFH-comEC-up-fwd | CATCCAGCGTAATTTCTTC | LFH-PCR KO of *comEC* using pDG series cassettes in Bsu |
| LFH-comEC-up-rev | cgagcgcctacgaggaatttgtatcgGGGCAGTCGCTGTTATGA | LFH-PCR KO of *comEC* using pDG series cassettes in Bsu |
| LFH-comEC-down-fwd | cctatcacctcaaatggttcgctgCGCATTCATCACACGTAG | LFH-PCR KO of *comEC* using pDG series cassettes in Bsu |
| LFH-comEC-down-rev | AGGCAATTGAGAAAGCGG | LFH-PCR KO of *comEC* using pDG series cassettes in Bsu |
| kanR-R | AAATGGAGTGTCTTCTTCCC | colony-PCR verification of *comEC* deletion |
| d_comEC-check-Fwd | TTAAACGCCTGTTCGCAAGC | colony-PCR verification of *comEC* deletion |
| d_comEC-check-Rev | GGCGGACAAGTGGTATGACA | colony-PCR verification of *comEC* deletion |

***Table 10. Primers used in this study. LFH-PCR KO, long-flanking homology PCR knock-out.***

### 4.4.2 Growth and culture conditions

*B. subtilis* strains were routinely grown in lysogeny broth (LB) at 37°C at 180 rpm shaking. LB agar was used as solid medium supplemented with appropriate selection as indicated below.

MNGE medium was used to induce competence for transformation of *B. subtilis*. A 10x MN stock contained 136 g $K_2HPO_4 \cdot 3H_2O$, 60 g $KH_2PO_4$, and 10 g sodium citrate·$2H_2O$ per 1 L. For 10 mL MNGE, 0.92 mL 10x MN stock, 7.75 mL sterile deionized water, 1 mL 20% glucose, 50 µL 40% potassium glutamate, 50 µL Fe(III) ammonium citrate (2.2 mg/mL), 100 µL tryptophan (5 mg/mL), 100 µL threonine (5 mg/mL) and 30 µL 1 M $MgSO_4$ were combined. Expression Mix contained 500 µL 5% yeast extract, 250 µL 10% casamino acids, 250 µL sterile deionized water, and 50 µL tryptophan (5 mg/mL).

### 4.4.3 Strain construction

Plasmids for integration of fluorescent marker into the *B. subtilis amyE* locus were assembled in the pBS1C integrative plasmid backbone. The backbone was digested with EcoRI and PstI. Promoter fragments were obtained from the corresponding source plasmids by digestion with EcoRI and SpeI, and fluorescent-protein-coding fragments were obtained by digestion with XbaI and PstI. The fragments were gel-purified, ligated with T4 ligase at equimolar amounts, and transformed into *E. coli* NEB 5-alpha according to the manufacturer's instructions. Transformants were selected on ampicillin plates (100 µg/mL), pure-streaked and verified by colony PCR. Confirmed clones were grown overnight, and plasmid DNA was purified using the QIAprep Spin Miniprep Kit (Qiagen).

Confirmed pBS1C derivative plasmids were linearized with ScaI and transformed into *B. subtilis* W168. Transformants were selected on chloramphenicol plates (5 µg/mL). Integration at *amyE* was screened by loss of α-amylase activity on starch agar: transformants and a W168 control were grown overnight and the plate was covered with Lugol iodine. Uninterrupted *amyE* locus produced a clear zone around the colony, while correct integration did not. Then the clones were verified by colony PCR and Sanger sequencing.

To construct the Δ*comEC* strain, *comEC* was replaced with a kanamycin-resistance cassette using the long-flanking homology PCR method. ~1 kb regions upstream and downstream of *comEC* were amplified from W168 genomic DNA. The primers used to amplify the upstream and downstream regions added short sequences homologous to opposite ends of the kanamycin-resistance cassette from pDG780, allowing the three fragments to be joined. The two flanking fragments (100 ng each) and the cassette (200 ng) were fused for nine PCR cycles. Then primers LFH-comEC-up-fwd and LFH-comEC-down-rev were added, and the full-length replacement fragment was amplified for further 30 cycles. The product was gel-purified and transformed into W168. The transformants were selected on kanamycin plates (10 µg/mL), colonies were pure-streaked, and the replacement was verified by colony PCR.

### 4.4.4 Transformation of *Bacillus subtilis*

An overnight culture was diluted 1:100 into 10 mL MNGE medium and grown to $OD_{600}$ of 1.2. For each transformation, 400 µL of culture was transferred to a glass test tube and mixed with 1 µg of the linearized plasmid. Cultures were incubated for 1 h, then 100 µL of Expression Mix was added, and the cultures were incubated for 1 h. Chloramphenicol was added to 0.125

μg/mL for pre-induction during the expression step. Next, cells were plated on the appropriate selection and incubated for 16-24 h.

### 4.4.5 Fluorescence characterization

Fresh overnight cultures of P*liaI* strains were diluted 1:100 into 10 mL LB in 100-mL flasks. Expression was induced at $OD_{600}$ = 1 with 30 μg/mL bacitracin, and the cultures were incubated for 85 min. 2 mL of culture was washed with 1 mL PBS and resuspended in 1 mL PBS. BFP, GFP, YFP, and RFP fluorescence was measured at excitation/emission wavelengths of 399/456, 481/511, 500/530, and 585/615 nm, respectively, and normalized to $OD_{600}$. Two biological replicates were tested per strain, with three technical replicates per biological replicate. For plate imaging, P*liaI* strains were streaked on LB agar supplemented with 30 μg/mL bacitracin. P*xylA* and P*liaG* strains were imaged on LB agar with or without 0.5% D-xylose using the appropriate fluorescence channel.

## References


[1] J. E. Barrick and R. E. Lenski, “Genome dynamics during experimental evolution,” *Nat Rev Genet*, vol. 14, no. 12, pp. 827–839, Dec. 2013, doi: 10.1038/nrg3564.

[2] M. J. Wiser, N. Ribeck, and R. E. Lenski, “Long-Term Dynamics of Adaptation in Asexual Populations,” *Science*, vol. 342, no. 6164, pp. 1364–1367, Dec. 2013, doi: 10.1126/science.1243357.

[3] I. Gordo, L. Perfeito, and A. Sousa, “Fitness effects of mutations in bacteria,” *Journal of Molecular Microbiology and Biotechnology*, vol. 21, no. 1–2, pp. 20–35, Jan. 2012, doi: 10.1159/000332747.

[4] R. E. Lenski, “What is adaptation by natural selection? Perspectives of an experimental microbiologist,” *PLOS Genetics*, vol. 13, no. 4, p. e1006668, Apr. 2017, doi: 10.1371/journal.pgen.1006668.

[5] M. S. Breen, C. Kemena, P. K. Vlasov, C. Notredame, and F. A. Kondrashov, “Epistasis as the primary factor in molecular evolution,” *Nature*, vol. 490, no. 7421, pp. 535–538, Oct. 2012, doi: 10.1038/nature11510.

[6] P. Siguier, E. Gourbeyre, and M. Chandler, “Bacterial insertion sequences: their genomic impact and diversity,” *FEMS Microbiology Reviews*, vol. 38, no. 5, pp. 865–891, Sep. 2014, doi: 10.1111/1574-6976.12067.

[7] P. D. Sniegowski, P. J. Gerrish, and R. E. Lenski, “Evolution of high mutation rates in experimental populations of E. coli,” *Nature*, vol. 387, no. 6634, pp. 703–705, Jun. 1997, doi: 10.1038/42701.

[8] A. Giraud *et al.*, “Costs and Benefits of High Mutation Rates: Adaptive Evolution of Bacteria in the Mouse Gut,” *Science*, vol. 291, no. 5513, pp. 2606–2608, Mar. 2001, doi: 10.1126/science.1056421.

[9] I. Matic *et al.*, “Highly Variable Mutation Rates in Commensal and Pathogenic Escherichia coli,” *Science*, vol. 277, no. 5333, pp. 1833–1834, Sep. 1997, doi: 10.1126/science.277.5333.1833.

[10] P. Siguier, E. Gourbeyre, A. Varani, B. Ton-Hoang, and M. Chandler, “Everyman’s Guide to Bacterial Insertion Sequences,” *Microbiology Spectrum*, vol. 3, no. 2, Apr. 2015, doi: 10.1128/microbiolspec.mdna3-0030-2014.

[11] E. Darmon and D. R. F. Leach, “Bacterial Genome Instability,” *Microbiology and Molecular Biology Reviews*, vol. 78, no. 1, pp. 1–39, 2014, doi: 10.1128/mmbr.00035-13.

[12] D. Schneider and R. E. Lenski, “Dynamics of insertion sequence elements during experimental evolution of bacteria,” *Research in Microbiology*, vol. 155, no. 5, pp. 319–327, Jun. 2004, doi: 10.1016/j.resmic.2003.12.008.

[13] C. Pereira, O. M. Warsi, and D. I. Andersson, “Pervasive Selection for Clinically Relevant Resistance and Media Adaptive Mutations at Very Low Antibiotic Concentrations,” *Molecular Biology and Evolution*, vol. 40, no. 1, p. msad010, Jan. 2023, doi: 10.1093/molbev/msad010.

[14] J. Consuegra *et al.*, “Insertion-sequence-mediated mutations both promote and constrain evolvability during a long-term experiment with bacteria,” *Nat Commun*, vol. 12, no. 1, p. 980, Feb. 2021, doi: 10.1038/s41467-021-21210-7.

[15] M. Touchon and E. P. C. Rocha, “Causes of Insertion Sequences Abundance in Prokaryotic Genomes,” *Molecular Biology and Evolution*, vol. 24, no. 4, pp. 969–981, Apr. 2007, doi: 10.1093/molbev/msm014.

[16] T. G. Villa, L. Feijoo-Siota, A. Sánchez-Pérez, JL. R. Rama, and C. Sieiro, “Horizontal Gene Transfer in Bacteria, an Overview of the Mechanisms Involved,” *Horizontal Gene Transfer*, pp. 3–76, 2019, doi: 10.1007/978-3-030-21862-1_1.

[17] B. J. Arnold, I.-T. Huang, and W. P. Hanage, “Horizontal gene transfer and adaptive evolution in bacteria,” *Nat Rev Microbiol*, vol. 20, no. 4, Art. no. 4, Apr. 2022, doi: 10.1038/s41579-021-00650-4.

[18] A. S. Lang, O. Zhaxybayeva, and J. T. Beatty, “Gene transfer agents: Phage-like elements of genetic exchange,” *Nature Reviews Microbiology*, vol. 10, no. 7, pp. 472–482, Jul. 2012, doi: 10.1038/nrmicro2802.

[19] A. S. Lang, A. B. Westbye, and J. T. Beatty, “The Distribution, Evolution, and Roles of Gene Transfer Agents in Prokaryotic Genetic Exchange,” *Annual Review of Virology*, vol. 4, pp. 87–104, 2017, doi: 10.1146/annurev-virology-101416-041624.

[20] C. Johnston, B. Martin, G. Fichant, P. Polard, and J. P. Claverys, “Bacterial transformation: Distribution, shared mechanisms and divergent control,” *Nature Reviews Microbiology*, vol. 12, no. 3, pp. 181–196, Mar. 2014, doi: 10.1038/nrmicro3199.

[21] M. Vos, “Why do bacteria engage in homologous recombination?,” *Trends in Microbiology*, vol. 17, no. 6, pp. 226–232, Jun. 2009, doi: 10.1016/j.tim.2009.03.001.

[22] R. J. Redfield, “Evolution of bacterial transformation: is sex with dead cells ever better than no sex at all?,” *Genetics*, vol. 119, no. 1, pp. 213–221, May 1988, doi: 10.1093/genetics/119.1.213.

[23] D. Boutoille *et al.*, “Detection of an IS21 insertion sequence in the mexR gene of Pseudomonas aeruginosa increasing β-lactam resistance,” *FEMS Microbiol Lett*, vol. 230, no. 1, pp. 143–146, Jan. 2004, doi: 10.1016/S0378-1097(03)00882-6.

[24] Z. M. Kunze, S. Wall, R. Appelberg, M. T. Silva, F. Portaels, and J. J. McFadden, “IS901, a new member of a widespread class of atypical insertion sequences, is associated with pathogenicity in Mycobacterium avium,” *Molecular Microbiology*, vol. 5, no. 9, pp. 2265–2272, 1991, doi: 10.1111/j.1365-2958.1991.tb02157.x.

[25] A. Lichter, S. Manulis, L. Valinsky, B. Karniol, and I. Barash, “IS1327, a new insertion-like element in the pathogenicity-associated plasmid of Erwinia herbicola pv. gypsophilae,” *Mol Plant Microbe Interact*, vol. 9, no. 2, pp. 98–104, Mar. 1996.

[26] T. J. Kawecki, R. E. Lenski, D. Ebert, B. Hollis, I. Olivieri, and M. C. Whitlock, “Experimental evolution,” *Trends in Ecology & Evolution*, vol. 27, no. 10, pp. 547–560, Oct. 2012, doi: 10.1016/j.tree.2012.06.001.

[27] B. Van den Bergh, T. Swings, M. Fauvart, and J. Michiels, “Experimental Design, Population Dynamics, and Diversity in Microbial Experimental Evolution,” *Microbiology and Molecular Biology Reviews*, vol. 82, no. 3, p. 10.1128/mmbr.00008-18, Jul. 2018, doi: 10.1128/mmbr.00008-18.

[28] S. Tempel, J. Bedo, and E. Talla, “From a large-scale genomic analysis of insertion sequences to insights into their regulatory roles in prokaryotes,” *BMC Genomics*, vol. 23, no. 1, p. 451, Jun. 2022, doi: 10.1186/s12864-022-08678-3.

[29] W. F. Doolittle and C. Sapienza, “Selfish genes, the phenotype paradigm and genome evolution,” *Nature*, vol. 284, no. 5757, pp. 601–603, Apr. 1980, doi: 10.1038/284601a0.

[30] S. F. Elena, L. Ekunwe, N. Hajela, S. A. Oden, and R. E. Lenski, “Distribution of fitness effects caused by random insertion mutations in Escherichia coli,” *Genetica*, vol. 102–103, no. 1–6, pp. 349–358, 1998.

[31] M. Blot, “Transposable elements and adaptation of host bacteria,” *Genetica*, vol. 93, no. 1, pp. 5–12, Feb. 1994, doi: 10.1007/BF01435235.

[32] J.-L. Martiel and M. Blot, “Transposable Elements and Fitness of Bacteria,” *Theoretical Population Biology*, vol. 61, no. 4, pp. 509–518, Jun. 2002, doi: 10.1006/tpbi.2002.1603.
[33] Y. Kanai, S. Tsuru, and C. Furusawa, “Insertion sequences: Simple mobile elements with rich ecological and evolutionary structures,” *Current Opinion in Systems Biology*, vol. 36, p. 100481, Dec. 2023, doi: 10.1016/j.coisb.2023.100481.
[34] I. Tomanek and C. C. Guet, “Adaptation dynamics between copy-number and point mutations,” *eLife*, vol. 11, p. e82240, Dec. 2022, doi: 10.7554/eLife.82240.
[35] M. Steinrueck and C. C. Guet, “Complex chromosomal neighborhood effects determine the adaptive potential of a gene under selection,” *eLife*, vol. 6, p. e25100, Jul. 2017, doi: 10.7554/eLife.25100.
[36] D. J. Van Hofwegen, C. J. Hovde, and S. A. Minnich, “Rapid Evolution of Citrate Utilization by Escherichia coli by Direct Selection Requires citT and dctA,” *Journal of Bacteriology*, vol. 198, no. 7, pp. 1022–1034, Mar. 2016, doi: 10.1128/jb.00831-15.
[37] H. Lee, E. Popodi, H. Tang, and P. L. Foster, “Rate and molecular spectrum of spontaneous mutations in the bacterium Escherichia coli as determined by whole-genome sequencing,” *Proceedings of the National Academy of Sciences*, vol. 109, no. 41, pp. E2774–E2783, Oct. 2012, doi: 10.1073/pnas.1210309109.
[38] P. J. Hastings, “Adaptive Amplification,” *Critical Reviews in Biochemistry and Molecular Biology*, vol. 42, no. 4, pp. 271–283, Jan. 2007, doi: 10.1080/10409230701507757.
[39] D. I. Andersson and D. Hughes, “Gene Amplification and Adaptive Evolution in Bacteria,” *Annual Review of Genetics*, vol. 43, pp. 167–195, 2009, doi: 10.1146/annurev-genet-102108-134805.
[40] J. C. Crow, H. Geng, T. J. Sullivan, S. M. Soucy, and D. Schultz, “Dynamics of drug delivery determines course of evolution of antibiotic responses in bacteria,” *bioRxiv*, p. 2023.11.29.569327, Sep. 2024, doi: 10.1101/2023.11.29.569327.
[41] D. F. Browning *et al.*, “Laboratory adapted Escherichia coli K-12 becomes a pathogen of Caenorhabditis elegans upon restoration of O antigen biosynthesis,” *Molecular Microbiology*, vol. 87, no. 5, pp. 939–950, 2013, doi: 10.1111/mmi.12144.
[42] K. L. May, T. Akiyama, B. G. Parker, M. Kim, and M. Grabowicz, “LPS O-antigen polysaccharide length impacts outer membrane permeability of enteric gram-negative bacteria,” *mBio*, vol. 16, no. 12, pp. e02518-25, Nov. 2025, doi: 10.1128/mbio.02518-25.
[43] A. Magi, B. Giusti, and L. Tattini, “Characterization of MinION nanopore data for resequencing analyses,” *Brief Bioinform*, vol. 18, no. 6, pp. 940–953, Nov. 2017, doi: 10.1093/bib/bbw077.
[44] S. Nasrollahian, J. P. Graham, and M. Halaji, “A review of the mechanisms that confer antibiotic resistance in pathotypes of E. coli,” *Front. Cell. Infect. Microbiol.*, vol. 14, Apr. 2024, doi: 10.3389/fcimb.2024.1387497.
[45] J. Broughton, A. Fraisse, and M. El Karoui, “Suppression of bacterial cell death underlies the antagonistic interaction between ciprofloxacin and tetracycline,” *Mol Syst Biol*, vol. 22, no. 1, p. 7, Oct. 2025, doi: 10.1038/s44320-025-00162-w.
[46] N. Fatsis-Kavalopoulos, R. Roemhild, P.-C. Tang, J. Kreuger, and D. I. Andersson, “CombiANT: Antibiotic interaction testing made easy,” *PLOS Biology*, vol. 18, no. 9, p. e3000856, Sep. 2020, doi: 10.1371/journal.pbio.3000856.
[47] C. Ritz, F. Baty, J. C. Streibig, and D. Gerhard, “Dose-Response Analysis Using R,” *PLOS ONE*, vol. 10, no. 12, p. e0146021, Dec. 2015, doi: 10.1371/journal.pone.0146021.

[48] A. E. Darling, B. Mau, and N. T. Perna, “progressiveMauve: Multiple Genome Alignment with Gene Gain, Loss and Rearrangement,” *PLOS ONE*, vol. 5, no. 6, p. e11147, Jun. 2010, doi: 10.1371/journal.pone.0011147.

[49] A. C. E. Darling, B. Mau, F. R. Blattner, and N. T. Perna, “Mauve: Multiple Alignment of Conserved Genomic Sequence With Rearrangements,” *Genome Research*, vol. 14, no. 7, pp. 1394–1403, Jul. 2004, doi: 10.1101/gr.2289704.

[50] M. Kearse *et al.*, “Geneious Basic: An integrated and extendable desktop software platform for the organization and analysis of sequence data,” *Bioinformatics*, vol. 28, no. 12, pp. 1647–1649, Jun. 2012, doi: 10.1093/bioinformatics/bts199.

[51] M. J. Anderson, “A new method for non-parametric multivariate analysis of variance,” *Austral Ecology*, vol. 26, no. 1, pp. 32–46, 2001, doi: 10.1111/j.1442-9993.2001.01070.pp.x.

[52] H. Goodarzi *et al.*, “Regulatory and metabolic rewiring during laboratory evolution of ethanol tolerance in E. coli,” *Molecular Systems Biology*, vol. 6, no. 1, p. 378, Jan. 2010, doi: 10.1038/msb.2010.33.

[53] T. Swings *et al.*, “Adaptive tuning of mutation rates allows fast response to lethal stress in Escherichia coli,” *eLife*, vol. 6, p. e22939, May 2017, doi: 10.7554/eLife.22939.

[54] R. J. Munson and B. A. Bridges, “‘Take-over’—an Unusual Selection Process in Steady-State Cultures of Escherichia coli,” *Microbiology*, vol. 37, no. 3, pp. 411–418, 1964, doi: 10.1099/00221287-37-3-411.

[55] L. CHAO and G. RAMSDELL, “The Effects of Wall Populations on Coexistence of Bacteria in the Liquid Phase of Chemostat Cultures,” *Microbiology*, vol. 131, no. 5, pp. 1229–1236, 1985, doi: 10.1099/00221287-131-5-1229.

[56] E. A. Hope, C. J. Amorosi, A. W. Miller, K. Dang, C. S. Heil, and M. J. Dunham, “Experimental Evolution Reveals Favored Adaptive Routes to Cell Aggregation in Yeast,” *Genetics*, vol. 206, no. 2, pp. 1153–1167, Jun. 2017, doi: 10.1534/genetics.116.198895.

[57] P. B. Rainey and M. Travisano, “Adaptive radiation in a heterogeneous environment,” *Nature*, vol. 394, no. 6688, pp. 69–72, Jul. 1998, doi: 10.1038/27900.

[58] C. Rusnac, “Replifactory: a multiplexed, automated, and scalable platform for continuous evolution experiments.” Accessed: Oct. 20, 2026. [Online]. Available: https://docs.replifactory.com/

[59] J. Y. Lim, J. M. May, and L. Cegelski, “Dimethyl Sulfoxide and Ethanol Elicit Increased Amyloid Biogenesis and Amyloid-Integrated Biofilm Formation in Escherichia coli,” *Applied and Environmental Microbiology*, vol. 78, no. 9, pp. 3369–3378, May 2012, doi: 10.1128/AEM.07743-11.

[60] O. X. Cordero and M. F. Polz, “Explaining microbial genomic diversity in light of evolutionary ecology,” *Nature Reviews Microbiology*, vol. 12, no. 4, pp. 263–273, Mar. 2014, doi: 10.1038/nrmicro3218.

[61] M. Vos and X. Didelot, “A comparison of homologous recombination rates in bacteria and archaea,” *ISME Journal*, vol. 3, no. 2, pp. 199–208, Oct. 2009, doi: 10.1038/ismej.2008.93.

[62] M. J. Rosen, M. Davison, D. Bhaya, and D. S. Fisher, “Fine-scale diversity and extensive recombination in a quasisexual bacterial population occupying a broad niche,” *Science*, vol. 348, no. 6238, pp. 1019–1023, May 2015, doi: 10.1126/science.aaa4456.

[63] D. Dubnau and M. Blokesch, “Mechanisms of DNA Uptake by Naturally Competent Bacteria,” *Annual Review of Genetics*, vol. 53, pp. 217–237, Dec. 2019, doi: 10.1146/annurev-genet-112618-043641.

[64] D. Hofreuter, S. Odenbreit, and R. Haas, “Natural transformation competence in Helicobacter pylori is mediated by the basic components of a type IV secretion system,” *Molecular Microbiology*, vol. 41, no. 2, pp. 379–391, 2001, doi: 10.1046/j.1365-2958.2001.02502.x.

[65] J. D. Zuke, R. Erickson, K. R. Hummels, and B. M. Burton, “Visualizing dynamic competence pili and DNA capture throughout the long axis of Bacillus subtilis,” *Journal of Bacteriology*, vol. 205, no. 9, pp. e00156-23, Sep. 2023, doi: 10.1128/jb.00156-23.

[66] J. C. Mell and R. J. Redfield, “Natural competence and the evolution of DNA uptake specificity,” *Journal of Bacteriology*, vol. 196, no. 8, pp. 1471–1483, Apr. 2014, doi: 10.1128/JB.01293-13.

[67] Z. T. Pimentel and Y. Zhang, “Evolution of the natural transformation protein, ComEC, in Bacteria,” *Frontiers in Microbiology*, vol. 9, no. DEC, Dec. 2018, doi: 10.3389/fmicb.2018.02980.

[68] S. P. Otto and T. Lenormand, “Resolving the paradox of sex and recombination,” *Nat Rev Genet*, vol. 3, no. 4, pp. 252–261, Apr. 2002, doi: 10.1038/nrg761.

[69] Fisher RA, *The genetical theory of natural selection*. Oxford: Clarendon Press., 1930.

[70] H. J. Muller, “Some Genetic Aspects of Sex,” *The American Naturalist*, vol. 66, no. 703, pp. 118–138, Sep. 1932, doi: 10.1086/280418.

[71] W. G. Hill and A. Robertson, “The effect of linkage on limits to artificial selection,” *Genetical Research*, vol. 8, no. 3, pp. 269–294, 1966, doi: 10.1017/S0016672300010156.

[72] Y. Kim and H. A. Orr, “Adaptation in sexuals vs. asexuals: Clonal interference and the Fisher-Muller model,” *Genetics*, vol. 171, no. 3, pp. 1377–1386, Nov. 2005, doi: 10.1534/genetics.105.045252.

[73] J. R. Peck, “A ruby in the rubbish: Beneficial mutations, deleterious mutations and the evolution of sex,” *Genetics*, vol. 137, no. 2, pp. 597–606, 1994, doi: 10.1093/genetics/137.2.597.

[74] B. J. Shapiro *et al.*, “Population genomics of early events in the ecological differentiation of bacteria,” *Science*, vol. 335, no. 6077, pp. 48–51, Apr. 2012, doi: 10.1126/science.1218198.

[75] H. Cadillo-Quiroz *et al.*, “Patterns of gene flow define species of thermophilic Archaea,” *PLoS Biology*, vol. 10, no. 2, Feb. 2012, doi: 10.1371/journal.pbio.1001265.

[76] R. J. Redfield, M. R. Schrag, and A. M. Dean, “The Evolution of Bacterial Transformation: Sex With Poor Relations,” *Genetics*, vol. 146, no. 1, pp. 27–38, May 1997, doi: 10.1093/genetics/146.1.27.

[77] A. L. Utnes *et al.*, “Growth phase-specific evolutionary benefits of natural transformation in Acinetobacter baylyi,” *ISME Journal*, vol. 9, no. 10, pp. 2221–2231, 2015, doi: 10.1038/ismej.2015.35.

[78] D. Dubnau, “DNA uptake in bacteria,” *Annual Review of Microbiology*, vol. 53, pp. 217–244, 1999, doi: 10.1146/annurev.micro.53.1.217.

[79] T. F. Cooper, “Recombination speeds adaptation by reducing competition between beneficial mutations in populations of Escherichia coli,” *PLoS Biology*, vol. 5, no. 9, pp. 1899–1905, Sep. 2007, doi: 10.1371/journal.pbio.0050225.

[80] D. J. P. Engelmoer, I. Donaldson, and D. E. Rozen, “Conservative Sex and the Benefits of Transformation in Streptococcus pneumoniae,” *PLoS Pathogens*, vol. 9, no. 11, Nov. 2013, doi: 10.1371/journal.ppat.1003758.

[81] D. A. Baltrus, K. Guillemin, and P. C. Phillips, “Natural transformation increases the rate of adaptation in the human pathogen Helicobacter pylori,” *Evolution*, vol. 62, no. 1, pp. 39–49, Jan. 2008, doi: 10.1111/j.1558-5646.2007.00271.x.

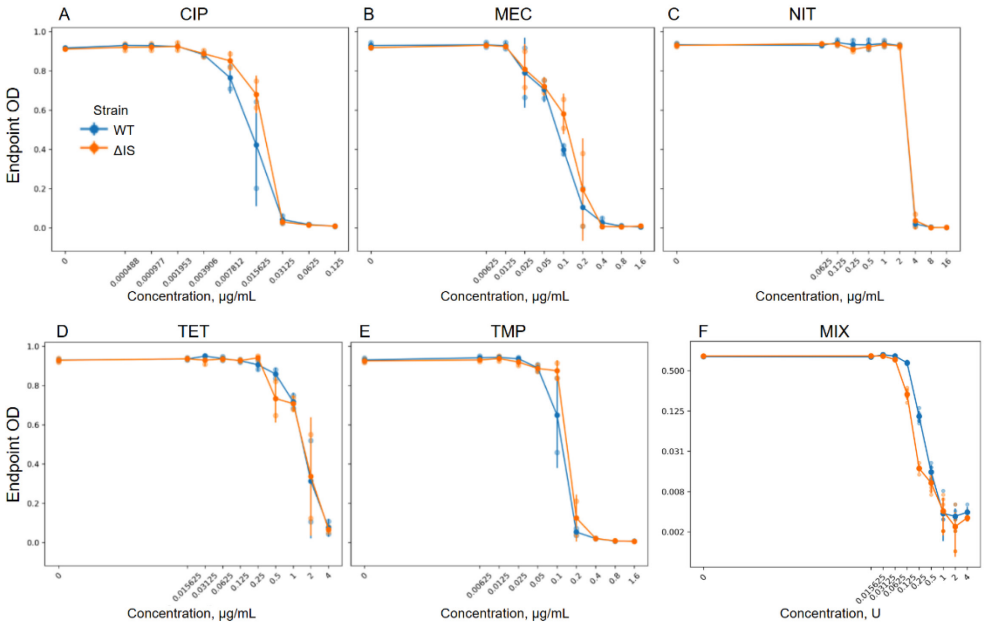
[82] J. M. Bacher, D. Metzgar, and V. De Crécy-Lagard, “Rapid evolution of diminished transformability in Acinetobacter baylyi,” *Journal of Bacteriology*, vol. 188, no. 24, pp. 8534–8542, Dec. 2006, doi: 10.1128/JB.00846-06.

[83] M. J. McDonald, D. P. Rice, and M. M. Desai, “Sex speeds adaptation by altering the dynamics of molecular evolution,” *Nature*, vol. 531, no. 7593, Art. no. 7593, Mar. 2016, doi: 10.1038/nature17143.

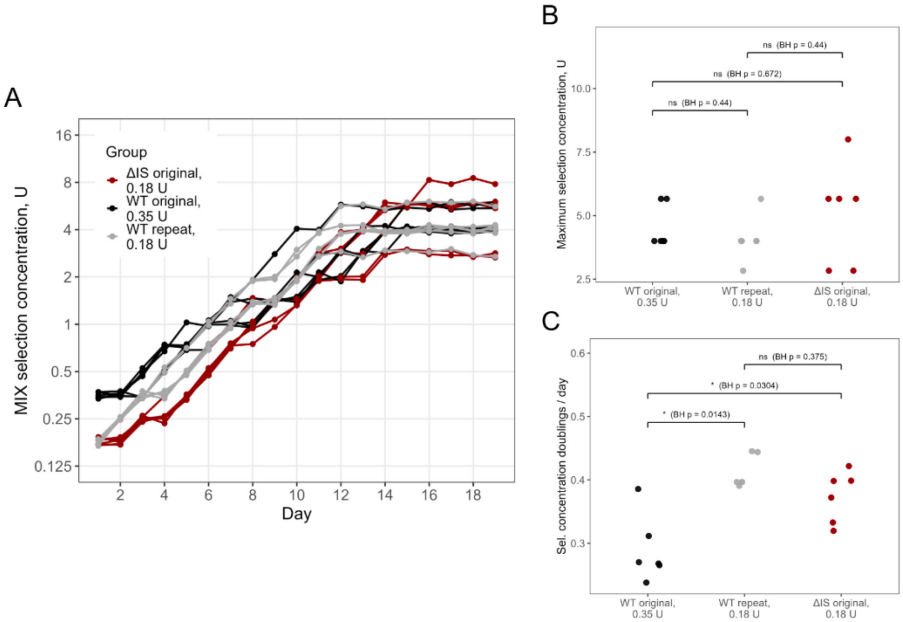
[84] C. R. Harwood and S. M. Cutting, Eds., *Molecular biological methods for Bacillus*. in Modern microbiological methods. Chichester ; New York: Wiley, 1990.

[85] J. Radeck *et al.*, “The Bacillus BioBrick Box: Generation and evaluation of essential genetic building blocks for standardized work with Bacillus subtilis,” *Journal of Biological Engineering*, vol. 7, no. 1, p. 29, Dec. 2013, doi: 10.1186/1754-1611-7-29.

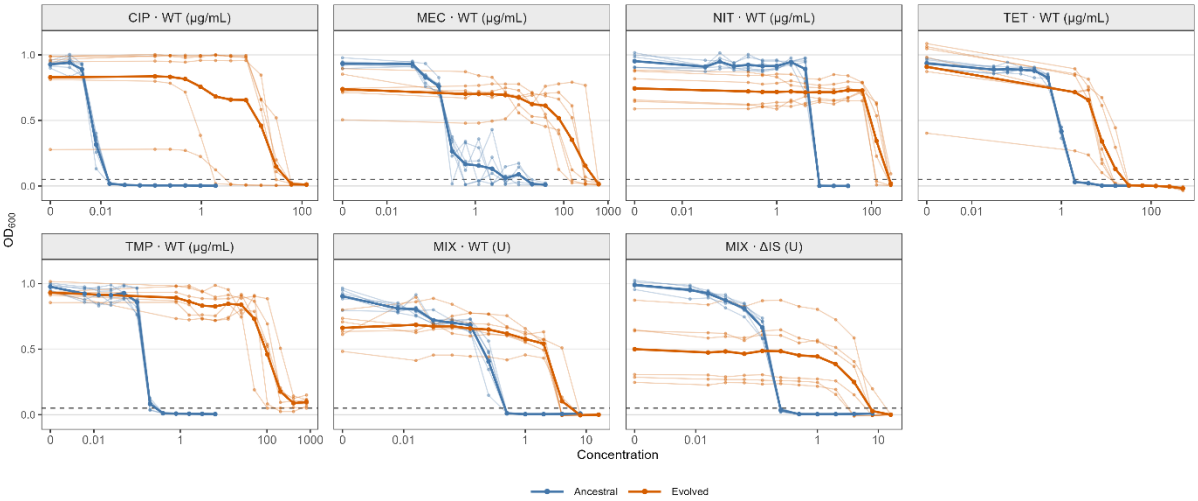
# A. Appendix 1 - Supplementary Figures



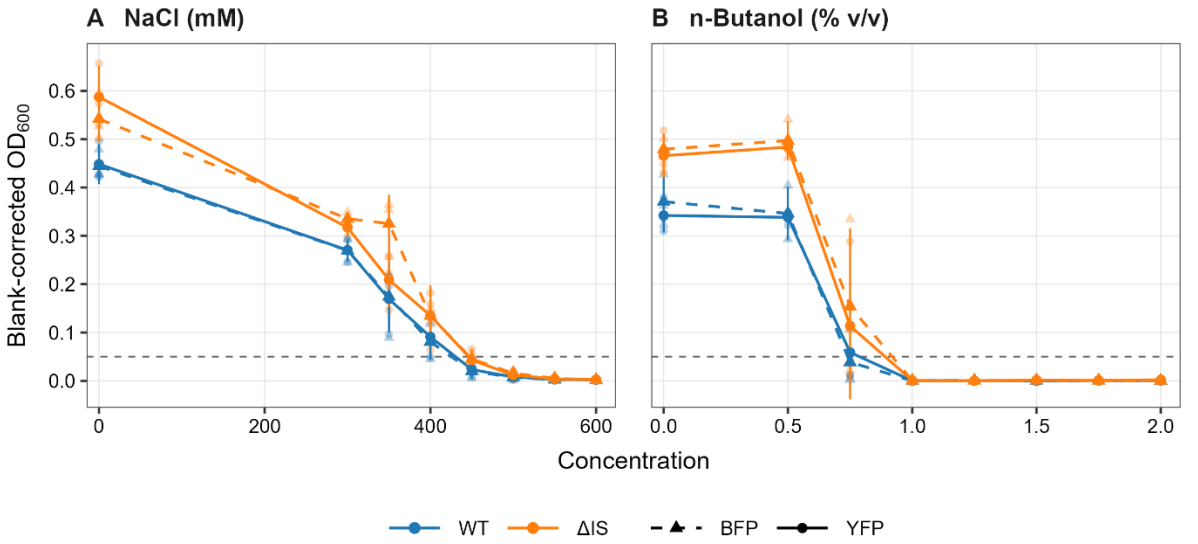

***Supplementary Figure 1. Preliminary dose-response curves of ancestral WT and ΔIS strains to individual antibiotics and MIX.*** *Endpoint optical density after 24 h was measured using a Bioscreen C MBR. (A-E) Responses to CIP, MEC, NIT, TET, and TMP, respectively. (F) Response to MIX. Small transparent points show individual biological replicates; larger points and error bars show means ± SD. Single-antibiotic assays included two biological replicates per strain, and MIX assays included six. The y-axis is linear in A-E and logarithmic in F.*



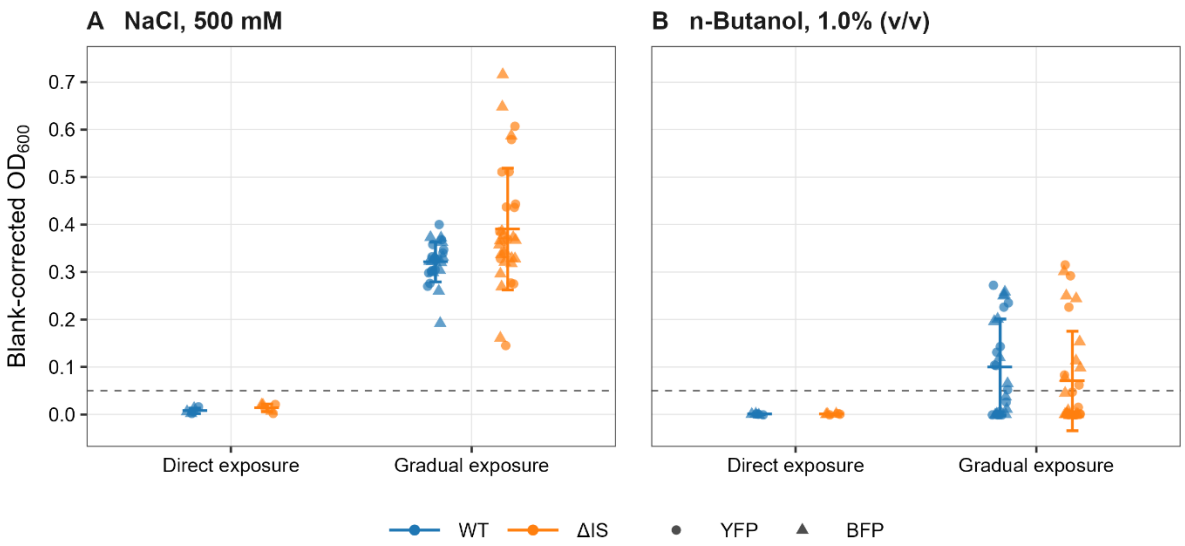

***Supplementary Figure 2. Adaptation of original WT, repeated WT, and original ΔIS E. coli populations under MIX selection.*** *(A) Selection-concentration trajectories over 19 days. (B) Maximum MIX selection concentration reached. (C) Adaptation rate, expressed as concentration doublings per day. Original WT populations began selection at 0.35 U, whereas repeated WT and original ΔIS populations began at 0.18 U. ΔIS was not evolved again; its data were taken from the original experiment. Six independently evolving populations were analyzed per group. Pairwise comparisons used two-sided Wilcoxon rank-sum tests; BH-adjusted p values are shown.*




***Supplementary Figure 3. Dose-response curves of ancestral and evolved WT and ΔIS E. coli.*** *Panels show background-corrected endpoint OD600 across concentrations of the indicated antibiotic (µg/mL) or MIX (U), with evolved isolates tested against their adaptation treatment. Thin lines show individual cultures (n = 6 per group), and thick lines show means. The dashed line marks the MIC threshold of OD600 = 0.05. Concentrations are displayed on a pseudo-logarithmic scale to include antibiotic-free controls.*




***Supplementary Figure 4. Ancestral dose-response curves for NaCl and n-butanol.*** *Endpoint OD of ancestral WT and ΔIS strains carrying YFP or BFP was measured across the indicated concentrations of (A) NaCl and (B) n-butanol. Small transparent points show individual biological replicates; larger points and error bars show mean ± SD (n = 3 per strain). The dashed line marks the MIC threshold of OD600 = 0.05.*




***Supplementary Figure 5. Endpoint OD at the estimated ancestral MIC after direct or gradual exposure.*** *Ancestral cultures exposed directly from inoculation were compared with cultures propagated under gradually increasing concentrations of (A) NaCl, at 500 mM on day 5, and (B) n-butanol, at 1.0% (v/v) on day 8. Points represent individual observations; Direct-exposure assays included three biological replicates per labelled strain. Gradual-exposure groups contained 30 WT and ΔIS cultures each. Mean ± SD across each background and exposure is shown as a summary. The dashed line marks the MIC threshold of OD600 = 0.05.*

## B. Appendix 2 - Declaration of the use of Generative AI and AI tools

In this thesis, the generative AI tool ChatGPT was employed to assist with specific tasks described below.

In Chapter 2, GenAI was used to assist with writing R code for data analysis and visualization. Specifically, it was used for debugging code for annotation assignment to overlapping multi-gene mutations, suggesting data visualization code examples, and refining the visual style of figures generated by R scripts.

In Chapter 4, GenAI assisted with preparing the introduction subsection by analyzing the author's thesis proposal document to identify and retain only the content appropriate for the scope of the project described in that chapter.

Across Chapters 1, 2, 3, and 4, GenAI was used to support writing style refinement to improve clarity and readability.

GenAI was used as a complementary tool to improve clarity and efficiency, and did not substitute for traditional research methodologies. All AI-generated suggestions were thoroughly reviewed and adapted to the needs of the thesis, and all AI-assisted code was validated for accuracy and adapted accordingly. The author takes full responsibility and ownership of all content submitted in this thesis and confirms that it meets the established academic standards.